Gernot Paul WEINBERGER, BSc

Synthesis and characterization of sterically protected 1,3 – functionalized trisilanes

MASTER'S THESIS

to achieve the university degree of

Diplom-Ingenieur

Master's degree programme: Technical Chemistry

submitted to

Graz University of Technology

Supervisor

Assoc.Prof. Dipl.-Ing. Dr.techn. Michaela Flock

Institute of Inorganic chemistry

Graz, 2018

Affidavit

I declare that I have authored this thesis independently, that I have not used other than the declared sources/resources, and that I have explicitly indicated all material which has been quoted either literally or by content from the sources used. The text document uploaded to TUGRAZonline is identical to the present master's thesis.

Date Signature

Danksagung

Hiermit möchte ich mich bei all jenen bedanken, die mich während meiner Studienzeit begleitet, unterstützt und aufgebaut haben.

Ein besonderer Dank gilt Assoc.Prof. Dipl.-Ing. Dr.techn. Michaela Flock, die die Betreuung meiner Masterarbeit übernommen hat, mir stets mit Feedback und Ratschlägen zur Seite stand und immer ein offenes Ohr für neue Synthese Strategien hatte. Außerdem möchte ich mich dafür bedanken liebe Michi, dass du mir sehr viel Freiraum beim Ausarbeiten von Syntheserouten und Ansätzen gelassen hast und doch immer, wenn ich irgendwo nicht weitergekommen bin, so manch unerwartetes Problem zu erklären und zu lösen versucht hast. Bis ich die ganzen Kniffe der theoretischen Molekülberechnungen ganz verstanden habe wird es wohl noch etwas dauern, aber die bereits angewendeten Rechnungen, sei es um Vergleichsspektren zu erhalten oder Abschirmungen besser zu verstehen, haben mir bereits sehr geholfen.

Weiterer Dank gilt auch Univ.-Prof. Dipl.-Chem. Dr.rer.nat. Frank Uhlig für die Finanzierung dieser Arbeit und der Ratschläge trotz eines immer sehr vollen Terminkalenders. Ein Dankeschön möchte ich auch an Assoc.Prof. Dipl.-Ing. Dr.techn. Roland Fischer für die Weitergabe seines vielfältigen Wissens in der Silan-Synthese und die durchgeführten Kristallstruktur Analysen richten. I would also like to thank our crystallographer Dr. Ana Torvisco Gomez for her patience with me and for supporting me with hints about crystallisation methods.

Ein großes Dankeschön gilt natürlich unseren Problemlösern, Babsi, Moni, Astrid und Resi, die ich einiges an Nerven gekostet habe und die trotzdem immer alles unternommen haben, damit ich alle erdenklichen Synthesen durchführen konnte.

Danken möchte ich außerdem all meinen Institutskollegen für die gute Zusammenarbeit, Unterstützung, Motivation und die schöne Zeit. Leute ihr seid die Besten.

Ein besonderes Dankeschön geht jedoch an diejenigen, die mich nicht nur während des Studiums, sondern auch in allen anderen Bereichen meines Lebens ständig unterstützen, aufbauen und motivieren. Lieber Peter, lieber Jürgen, lieber Bernd, lieber Stefan, wenn man solche Freunde hat kann man alles schaffen.

Tamara, was würde ich nur ohne dich machen. Du bist mein Fels in der Brandung, meine Entspannungszone, mein besseres Ich. Immer wenn ich am Boden bin oder grummelig, holst du mich wieder auf den Boden zurück, du magst mich wie ich bin und dafür liebe ich dich.

Abschließend möchte ich einen besonderen Dank an meine Familie richten. Ich möchte mich bei meinen Eltern für die Unterstützung und den Rückhalt während meiner gesamten Studienzeit bedanken. Ihr habt auch dann zu mir gehalten, wenn es nicht ganz einfach war und immer an mich geglaubt.

Zu guter Letzt möchte ich noch meinem werten Bruderherz danken, dafür, dass er mich auf die Palme bringt und wir miteinander streiten können und trotzdem immer für einander da sind. Wenn man so einen Bruder hat kann einen nichts umhauen, zu zweit haben wir noch alles gepackt.

Zusammenfassung

In dieser Arbeit wird die Herstellung von sterisch abgeschirmten Trisilanen und deren 1,3-Funktionalisierung beschrieben. Ausgehend von Tetrakis(trimethylsilyl)silan wurden verschiedene Routen getestet, um zur gewünschten Silankette (1,1,1,3,3,5,5,5-Octamethyl-2,2,4,4-tetrakis(trimethylsilyl)pentasilan) zu kommen und die am besten funktionierende Route wurde optimiert. Die Funktionalisierungen des Pentasilans hin zum 1,3-funktionalisierten Trisilandihydrid, -dichlorid und -diphosphan, wurden erstmals durchgeführt und die Produkte vollständig charakterisiert.

Weiters wird in dieser Arbeit die Umsetzung der synthetisierten Silankette zum bisher unbekannten 1,3-Dihydrid des Trisilans, unter Abspaltung von zwei Trimethylsilyl Gruppen, beschrieben. Das bisher unbekannte Dihydrid konnte ebenfalls vollständig charakterisiert werden. Verschiedene Ansätze, um zum 1,3-Diphosphan zu gelangen, wurden untersucht. Nachdem sich die Synthesewege ohne Verwendung von Chlorsilanen als nicht zweckdienlich herausstellten, wurden unterschiedlichste Chlorierungsmethoden getestet. Standardmethoden für Silane konnten keine vollständigen Umsätze liefern und auch neue Methoden, welche $P(C_6F_5)_3$ als Katalysator verwenden, wurden auf Grund niedriger Ausbeuten verworfen. Die besten Ergebnisse wurden mittels Phosphorpentachlorid Methode erzielt. Das bisher unbekannte 1,3-Dichlorotrisilan konnte vollständig charakterisiert werden.

Für die Kopplung des Dichlorsilans zum Diphosphan wird Alkali-Phosphanid benötigt. [1] Die Möglichkeiten Natriumphosphid ohne Verwendung von weißem Phosphor und kommerziell erhältlichem Phosphingas zu synthetisieren, wurden untersucht. Hierfür wurden Vorschriften von der ETH Zürich adaptiert, um zu einem reinen Produkt zu gelangen [2].

Das 1,3-Diphosphatrisilan konnte hergestellt und mittels ^{31}P NMR charakterisiert werden.

Die durchgeführten Synthesen wurden durch DFT-Rechnungen unterstützt, die sowohl Aufschluss über die zu erwartenden NMR Verschiebungen als auch über die verschiedenen möglichen Konformationen der erstmals synthetisierten Verbindungen gaben.

Abstract

In this thesis the synthesis of sterically highly protected trisilanes and their 1,3-functionalisation is described. Starting from tetrakis(trimethylsilyl)silane different routes were tested, which led to the desired silane chain (1,1,1,3,3,5,5,5-octamethyl-2,2,4,4-tetrakis(trimethylsilyl)-pentasilane). New synthesis routes used for the functionalisation of the pentasilane to the trisilane dihydride, dichloride and diphosphane were invented and the products fully characterized.

The conversion of the pentasilane to the former unknown 1,3-dihydridotrisilane, by elimination of two trimethylsilyl groups, is explained. The yet unknown dihydride was also fully characterized. Different approaches to convert the silane chain to the diphospha derivative were investigated. Synthesis routes without using chlorosilanes could be discarded, due to low yields and inseparable side products. Therefore, different chlorination routes have been tested. Standard procedures for silanes did not result in high yields and also newly established methods using $P(C_6F_5)_3$ as a catalyst did not work properly, due to steric protection. The best results could be obtained using phosphorus pentachloride as chlorination reagent. The yet unknown dichloride could be fully characterized.

To produce the 1,3-diphosphatrisilane coupling of chloro silane with alkali phosphanes was identified as the best way. [1] Therefore, the possibilities to synthesize sodium phosphide without using white phosphorus and commercially available phosphine gas were investigated. To achieve this, syntheses routes established at ETH Zurich [2] were adapted to cope our needs. This process worked out well and the produced sodium phosphide could be fully characterized.

The produced diphosphasilane was characterized by ^{31}P NMR. Due to the small amount of product available further characterization was not possible.

The performed syntheses were supported by DFT calculations, which gave information about the expected regions of the NMR shifts and also about the different conformations of the formerly unknown compounds.

Table of contents

I. List of figures

II. List of tables

1 Introduction

The first sterically highly protected pentasilane species shown in figure 1 was synthesized by Marschner in 1998 [3].

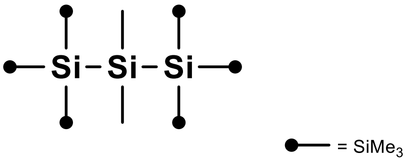

Figure 1: 1,1,1,3,3,5,5,5-octamethyl-2,2,4,4-tetrakis(trimethylsilyl)-pentasilane

Since then it was mostly used as starting material for ring closure reactions [4, 5, 6, 7, 8, 9] mainly due to the highly protective trimethylsilyl (TMS) groups.

In addition, several derivatives containing different halides on the central silicon were synthesized [10]. The derivative containing only one methyl group and one hydrogen on the central silicon was investigated by Stüger *et al.* [11] in terms of the ability of stabilisation of ring closure reactions.

Other known modifications include the metalation with potassium to the dianion [12] and the mono-substitution of one TMS-group by hydrogen [13] of the pentasilane. Both compounds could be crystallized. The 1,3-dihydrogenated and 1,3-dihalogenated species of the trisilane, which could be of interest for further syntheses, remained unexplored so far.

Other protected trisilanes have been investigated by Hassler *et al.*, especially 1,3-methyl substituted derivatives were functionalized using different halides as substituents on the central silicon atom [14, 4].

A very interesting derivative would be the diphosphasilane, due to its special donor properties known from its carbon analogue. α,ω-phosphorus substituted diphosphanes are literature known for many years. They are most commonly used as ligands to transition metals like their monophosphane counterparts [15, 4]. Due to the good electron donating properties of phosphorus, two different sorts of ligands, shown in Figure 2, can be formed.

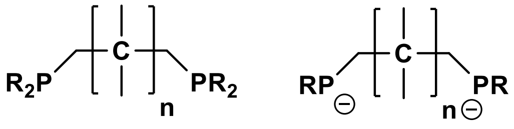

1 **2** n = 0,1,2,3...

Figure 2: Types of diphosphane and diphosphanide ligands used for transition metal complexes

For the ligand type **1** (see figure 2) the substituents on the phosphorus include methyl- and phenyl groups. They form complexes with large metal centers (M = Ru, W, Mo). The stabilisation in these compounds is purely afforded by the interaction of the lone pair of the phosphorus [7, 8]. The other known ligand type **2** has a covalent P-M bond and is by far less often formed [9].

While both ligand types featuring a carbon-based backbone are quite common, the silicon derivatives are relatively unexplored. The known type **1** derivatives nearly all feature a $[RPH\text{-}SiMe_2\text{-}]_2$ core with R = Me, *i*Pr, Ph [16, 17, 18]. One exception is the $[Me_2P\text{-}SiMe_2\text{-}]_2$ core which could be used as a ligand to a molybdenum center [19]. There is also one tetraphenylated diphosphasilane known $[Ph_2P\text{-}SiMe_2\text{-}]_2$, which has been synthesized by Hassler [20]. The addition of boron species as substituents on the phosphorus led to an additional type **1** silicon ligand $\{[(i\text{Pr}_2N)_2B]PH\text{-}SiMe_2\text{-}\}_2$ [21], which is suitable for coordination to a molybdenum tetracarbonyl complex $\{[(i\text{Pr}_2N)_2B]PH\text{-}SiMe_2\text{-}\}_2Mo(CO)_4$ [22].

The type **2** silicon derivatives are even less explored; cleavage of the hydrogen of $[PhPH\text{-}SiMe_2\text{-}]_2$ and subsequent reaction with transition metals led to such compounds [23, 24].

Due to the steric shielding and stabilizing abilities of the TMS group, it has been widely applied in main group 4 chemistry [25, 26, 27]. Until 2006 no diphosphane with the bulky TMS group as phosphorus substituent was reported. Since the first species were reported by Hassler *et al.* [1] a lot of research in this field was performed. Through coupling of two hypersilylphosphanes (tris(trimethylsilyl)silylphosphine) with tetramethyl-1,2-dichlorosilane new diphosphanes could be obtained by Flock *et al.* [28].

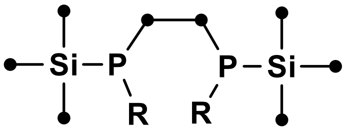

Figure 3: Diphosphasilanes synthesized by hypersilylphosphane coupling (R = H, Li, TMS) *[28]*

A huge discrepancy can be seen between the amount of known α,ω-diphosphanes with carbon backbone and those containing a silicon backbone (figure 4). Even with a very short backbone length of two Si atoms only 27 diphosphanes are characterized. With a higher backbone length only one diphosphasilane is known (see figure 5). [20]

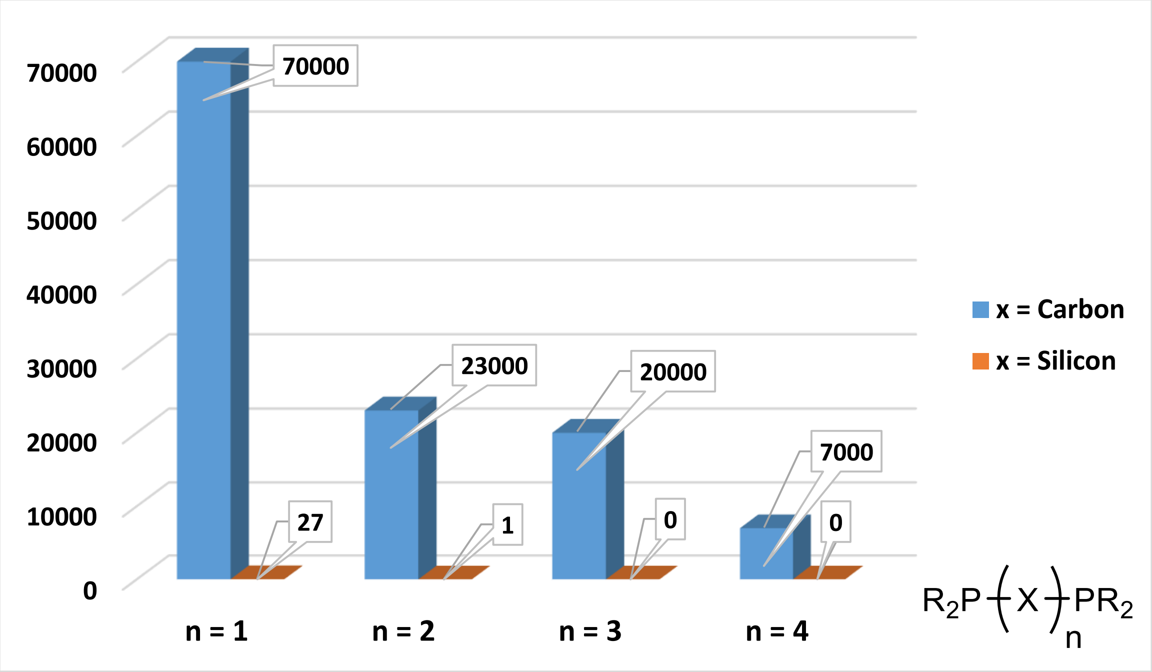

Figure 4: Comparison of the amount of silicon backboned to carbon backboned α,ω-diphosphanes

This small number of diphospha silanes may be explained with the weaker Si-Si and Si-P bonds as compared to the carbon bonds. Bonding energies are shown in Table 1.

Table 1: Comparison of bonding energies within silicon and carbon species ([a] *[29]*,[b] *[30]*,[c] *[31]*)

X-Y	E(X-Y) [kcal/mol, 298.15 K]	Π-bond energies [kcal/mol, 298.15 K]
Si - P	49.22	22.8[a]
C - P	64.86	42.2[b]
Si - Si	53.74	8.6[a]
C - C	85.33	53.0[c]

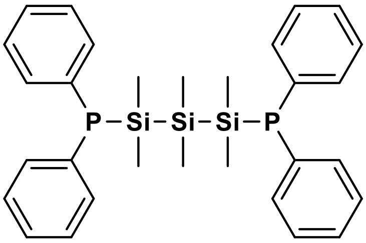

Figure 5: The only stable diphosphatrisilane synthesized by Hassler *[20]*

The goal of this thesis was to investigate the possibilities of the synthesis of novel 1,3-difunctionalized trisilanes, the optimisation of the synthesis and the characterization of these compounds.

2 Results and discussion

2.1 Density Functional Theory (DFT) Study

DFT calculations open up a way of forecasting the most stable structures and can give a prediction of the expected NMR spectra. This method is helping greatly in the assignment of NMR shifts of formerly unknown compounds. Even though the NMR shifts don't fit perfectly.

The calculations of the optimized structures of the dihydride, the dichloride and the diphosphasilane of the trisilane were performed at the mPW1PW91/6-31+G* [32, 33] level. The geometries of the molecules were calculated in the gas phase, without the influence of a solvent. These calculations led to several minimum configurations verified by vibrational frequency calculation which are displayed in Table 2.

Table 2: Dihedral angles and total energies of the mPW1PW91/6-31+G* calculated dihydrides, dichlorides and diphosphanes

R	R_1-Si_1-Si_2-Si_3 [°]	Si_1-Si_2-Si_3-R_2 [°]	ΔE rel. [kJ/mol]
H_1	-38.4	-38.4	0.0
H_2	149.5	-37.3	7.0
H_3	138.2	-31.5	8.8
H_4	61.0	-160.1	11.3
H_5	58.8	-161.1	11.6
H_6	175.8	175.8	16.2
Cl_1	71.6	-171.3	0.0
Cl_2	-35.9	-35.9	0.2
Cl_3	165.6	-52.7	0.9
Cl_4	163.2	-55.2	2.7
Cl_5	175.9	175.9	5.8
Cl_6	22.9	-63.9	11.0
$[PH_2]_1$	-38.6	-28.3	0.0
$[PH_2]_2$	-31.5	-31.4	0.8
$[PH_2]_3$	-179.5	-27.2	2.6
$[PH_2]_4$	74.4	-171.6	5.0
$[PH_2]_5$*	75.5	-167.9	6.6
$[PH_2]_6$	168.0	-77.8	6.7
$[PH_2]_7$	22.5	-59.4	6.7
$[PH_2]_8$	161.1	-58.3	9.3
$[PH_2]_9$	-178.1	151.0	101.6

*dihedral angles are equal, the hydrogens connected to the phosphorus occupy different positions

The global minima of the three-different species were marked bold and were further used for the calculation of NMR spectra. Figure 6 showed the global minima and the structure with the next higher energetically stable minimum of the three silanes.

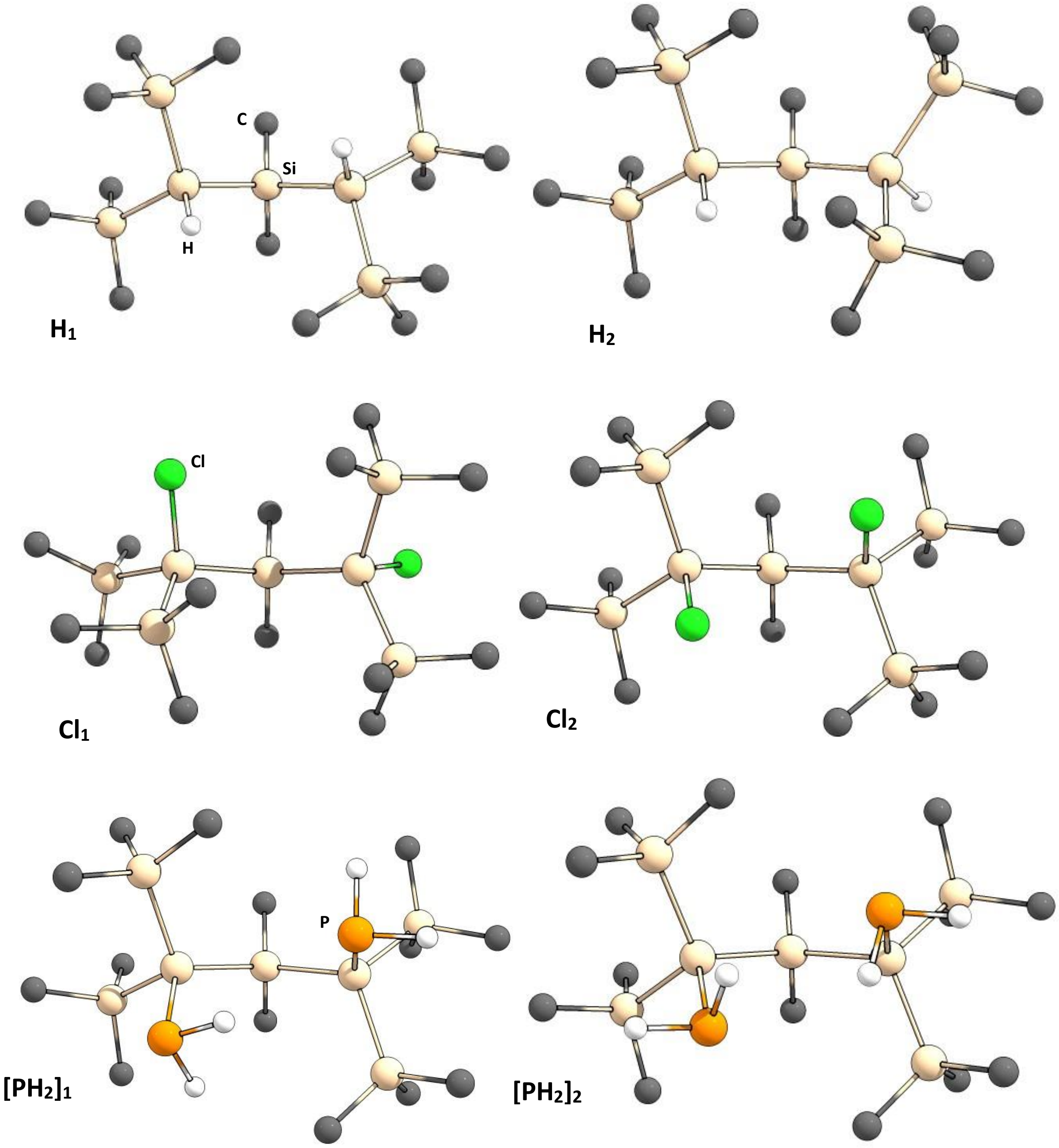

Figure 6: Calculated structures of the two energetically lowest conformations of each silane

The most interesting aspect of these figures were the different global minima conformations. While the global minimum of the dihydride (**H_1**) and the diphosphane (**$[PH_2]_1$**) showed trans configuration, the global minimum of the dichloride (**Cl_1**) showed ci*s* configuration. The obtained crystal structure of the dihydride showed *trans* configuration, which matches the calculated structure. The orientation of the shown phosphane groups (**$[PH_2]_1$**, **$[PH_2]_2$**) indicate that ring closure reactions leading for instance to diphosphatetrylenes should be considered and are therefore interesting for further investigations.

The two energetically most stable conformations of the dichloride (Cl_1 and Cl_2) and diphosphane ($[PH_2]_1$ and $[PH_2]_2$) show very little energy difference. Therefore, no exact prediction on the conformation of the crystals was possible.

Due to the additional hydrogens on the phosphorus atom of the diphosphanes, the amount of possible conformations rose enormously, this could be seen at conformation **$[PH_2]_5$**. The dihedral angles matched the ones of **$[PH_2]_4$**, but because of the different hydrogen positions the energy of the conformations differed.

The calculations of the NMR magnetic shieldings were performed using the all electron IGLO-II basis set [34].

Table 3: Comparison of mPW1PW91/IGLO-II calculated and measured NMR shifts

Compound	^{29}Si NMR exp.	^{29}Si NMR calc.	^{31}P NMR exp.	^{31}P NMR calc.
H_1	-11.2 ppm -36.0 ppm -109.4 ppm	-10.9 ppm -29.5 ppm -107.7 ppm	x	x
Cl_1	-8.7 ppm -10.4 ppm -27.2 ppm	4.6 ppm -8.9 ppm -24.2 ppm	x	x
$[PH_2]_1$	x x -107.2 ppm	-9.4 ppm -25.4 ppm -97.3 ppm	-265.4 ppm	-265.3 ppm

The differences between the calculated and the measured values are shown in Table 3. The values differ from 0.3 to 13.2 ppm depending on the substituents. The highest difference could be observed at the dichloride as expected, due to the larger error of the calculations [35]. Even with this derivation the calculations gave a good idea in which range the shifts of the compounds had to be expected.

2.2 Synthesis of the nonasilane F

Different routes to linear silanes are known in literature, but only one is published for the nonasilane [3]. Therefore, several routes were investigated and the best one optimized.

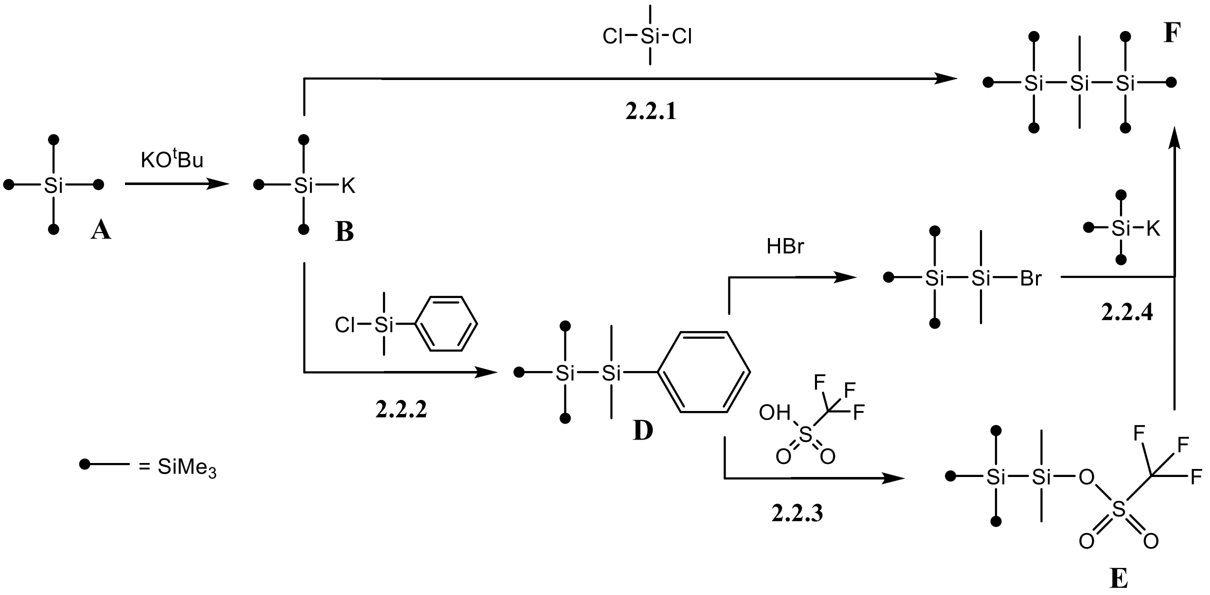

Figure 7: Possible routes towards nonasilanes

2.2.1 Coupling with dimethyldichlorosilane

The first approach towards the nonasilane followed the example of Pannell and co-workers [36] who synthesized an equivalent decasilane. Starting from tetrakis(trimethylsilyl)silane an anion was produced following the potassium-*tert*-butoxide route first reported by Marschner [3]. Thereafter, the anion was coupled with dimethyldichlorosilane (figure 7, 2.2.1) and the product formation controlled *via* NMR-spectroscopy. The NMR showed that rather than a coupling reaction a transmetallation took place resulting in the starting material tetrakis(trimethylsilyl)silane.

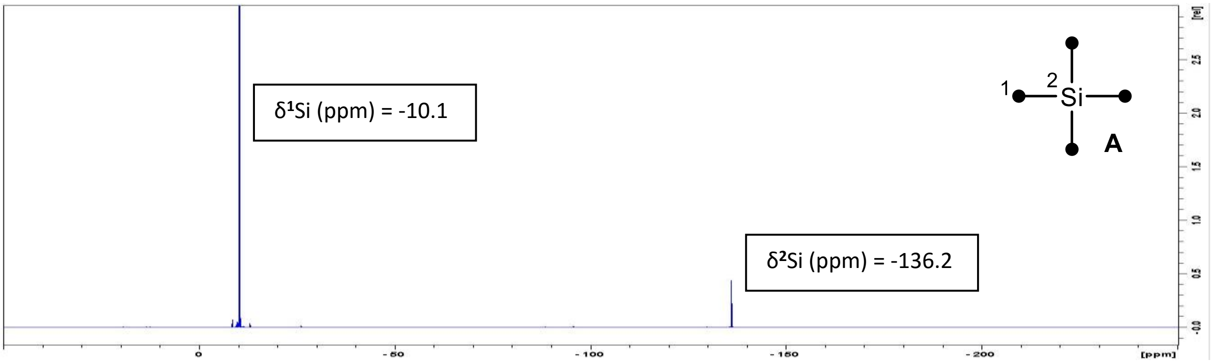

Figure 8: ^{29}Si NMR of the reaction solution showing tetrakis(trimethylsilyl)silane A

The reason for this behaviour is the monosilane bridge, which is too short for the coupling of the two sterically protected hypersilyl-anions.

2.2.2 Coupling with dimethylphenylchlorosilane

Due to the impossibility of the direct synthesis route, the known route from Marschner [3] was investigated. The first step is the same as in the direct route, generating a hypersilyl-anion in DME. The produced silylether side product was evaporated together with the solvent and the anion dissolved in toluene. Unlike the original route we cooled the anion solution to -70 °C and added the dimethylphenylchlorosilane directly *via* a syringe to the reaction solution. This resulted in an increased yield of the desired phenylated pentasilane from 60% up to almost full conversion. The NMR showed that only one silicon species is left in the reaction. The shifts differ only around 1 ppm from the literature values, due to DME as solvent instead of toluene (^{29}Si Toluene| δ (ppm) = -8.9, -12.5, -133.2). Crystals suitable for X-ray diffraction were obtained by recrystallization in acetone at -30 °C.

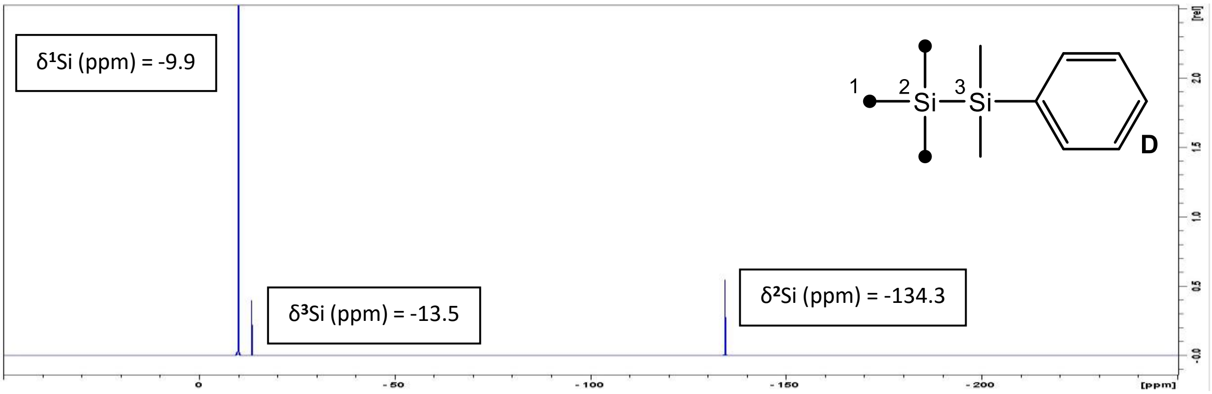

Figure 9: ^{29}Si NMR of 1,1,1,3,3-pentamethyl-3-phenyl-2,2-bis-(trimethylsilyl)-pentasilane D

2.2.3 Trifluoromethanesulfonic pathway

The literature known route [3] continues with a bromination of the phenylated silane using gaseous hydrogen bromide to get a reactive intermediate, which can perform a coupling reaction with another hypersilyl anion. Instead of continuing with the bromination route we looked to a different pathway, the reaction with trifluormethanesulfonic acid.

Cleavage of phenylated silanes with trifluoromethanesulfonic acid (triflate) was first reported by Joyce and co-workers [37] and since became a routine method in silicon chemistry. The phenylated pentasilane was reacted with triflate at 0 °C, was allowed to warm to room temperature and was stirred for another 20 h. The NMR showed an expected shift of the terminal silicon from -13.4 ppm onto the positive side to 56.4 due the strong electron withdrawing silicon - oxygen bond. The other two silicon shifts underwent just minor changes.

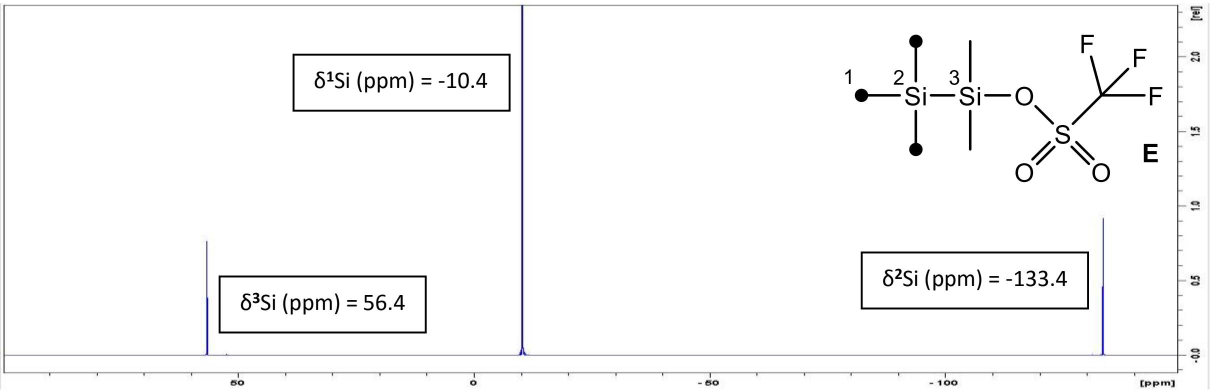

Figure 10: ^{29}Si NMR of 1,1,1,3,3-pentamethyl-2,2-bis-(trimethylsilyl)-pentasilyl- trifluoromethanesulfonate E

2.2.4 Hypersilyl coupling

The reactions of silicon triflates with alkaline-silanides were first described by Uhlig and co-workers [38]. The synthesized silicon triflate was cooled to -78 °C and 1.1 equivalents of the hypersilyl-anion were added *via* cannula. Immediately a white precipitate (potassium triflate) formed. The product had to be separated from the salt before the quenching step, to avoid the formation of a highly viscous phase during extraction. The latter resulted in a difficult work-up and very low yields. Recrystallization from an ethanol/ethyl acetate mixture yielded white crystals. After drying the product at 140 °C for at least 2 hours the attached solvent molecules were removed and stochiometrical use was possible. The NMR peaks at -26.2 and -118.9 ppm as well as the melting point of 172 °C and GC-MS confirmed the formation of the desired product. The elemental analysis gave values of 35.8 % carbon 9.7 % hydrogen which differed to the calculated 41.1 % carbon and 10.8 % hydrogen. This may be caused due to silane decomposition under oxygen atmosphere.

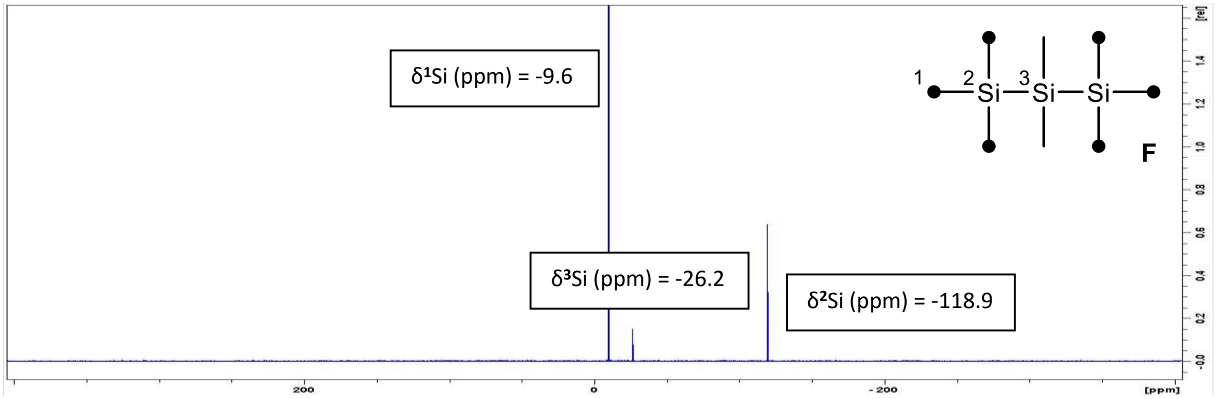

Figure 11: ^{29}Si NMR of 1,1,1,3,3,5,5,5-octamethyl-2,2,4,4-tetrakis(trimethylsilyl)-pentasilane F

2.3 Synthesis of the dichlorinated heptasilane J

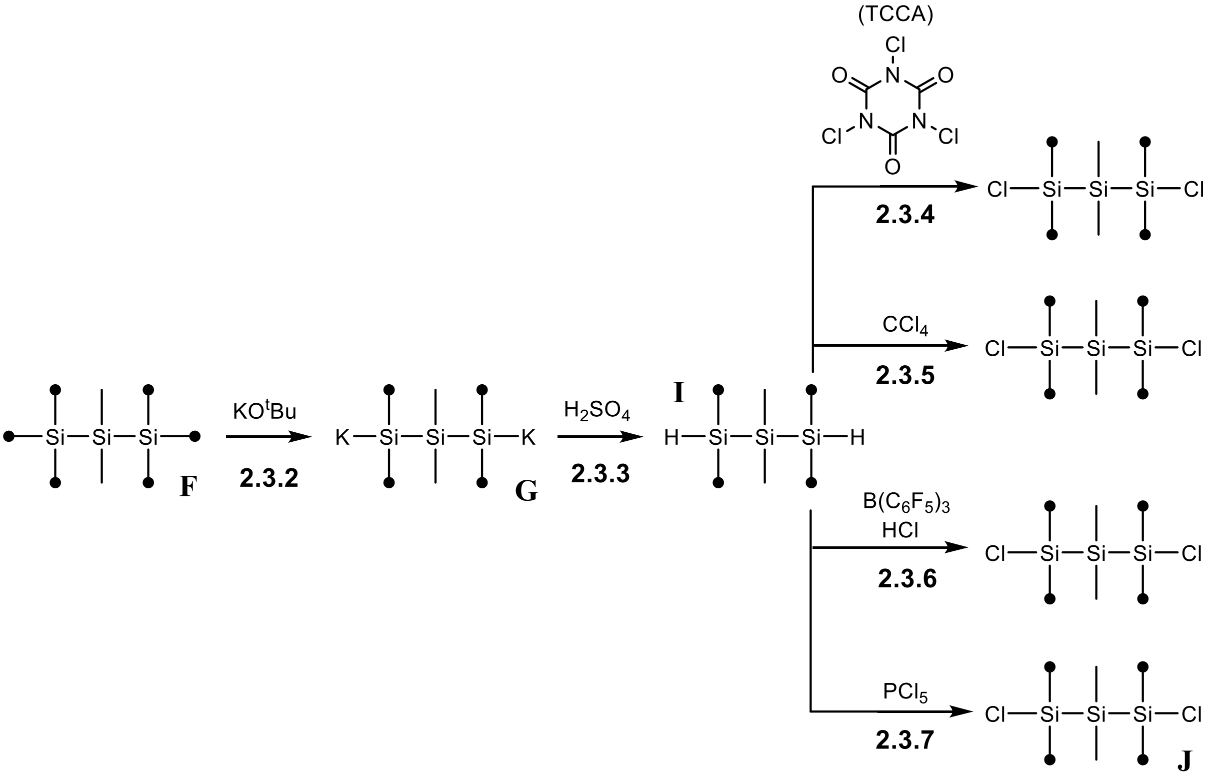

Figure 12: Synthesis routes towards dichlorides

Due to the relatively unexplored properties of TMS-protected pentasilane chains, it was not certain if known mechanisms for smaller silianes could be used for the chlorination of the sterically protected chain. Therefore, several approaches were investigated.

2.3.1 First steps

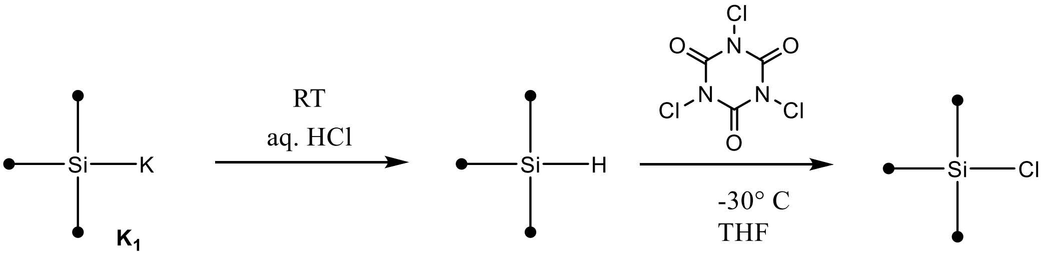

Figure 13: Synthesis of hypersilylchloride

As reported first by Varaprath and Stutts [39] trichloroisocyanuric acid (**TCCA**) is a viable chlorination agent for several silanes producing high yields. To test the application of the method with the sterically highly protected chain, a chlorination test of the easily available tris(trimethylsilyl)silane **K_1** was performed. Due to the high similarity of this silane with our pentasilane the reaction was expected to work similarly well for both silanes. A hypersilyl anion was reacted with aqueous hydrochloric acid and extracted with diethyl ether. The hydride species was then dissolved in THF, cooled to -30 °C and 1.5 equivalents of TCCA were added to the solution. After evaporation of the solvent, the remaining colorless oil was dissolved in pentane while TCCA and cyanuric acid residues precipitate as a white solid. The NMR of the solution showed the same shifts as the literature known values for hypersilyl chloride (^{29}Si | δ (ppm) = -11.7, -14.7) with almost quantitative yield.

2.3.2 Synthesis of the dianion G

The conversion of the chain with potassium-*tert*-butoxide, which was first described by Marschner, Kayser and Kickelbick [12], was slightly optimized by using dimethoxyethane instead of THF: this led to a reduced reaction temperature from 60 °C to room temperature and almost full conversion within 48 hours. The NMR shifts matched the literature of ^{29}Si | δ (ppm) = -5.3, -16.5, -172.0. [12]

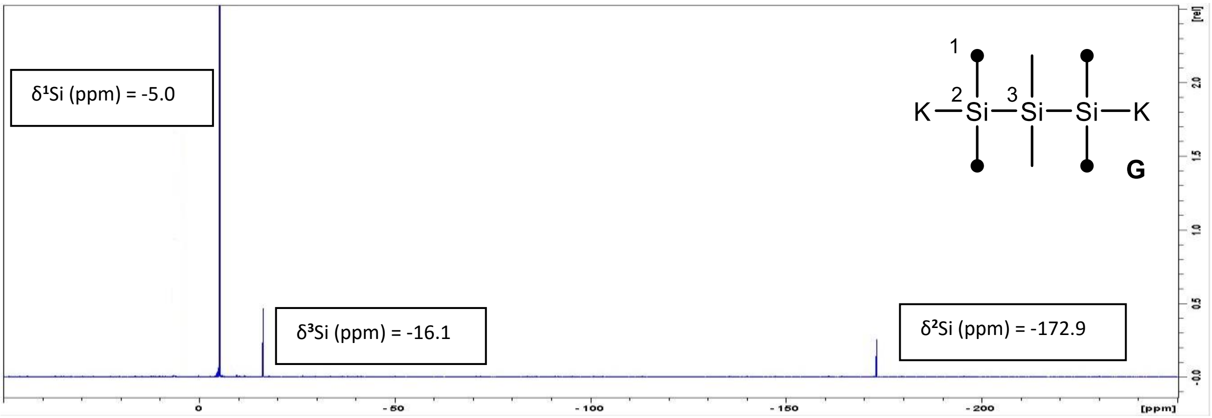

Figure 14: ^{29}Si NMR of Synthesis of 1,1,1,3,3,5,5,5-octamethyl-2,4-bis(trimethylsilyl)-pentasilyl-2,4-dipotassium G

Stopping the reaction earlier resulted in a main portion of the chain being converted to the monosilanide. The separation of these two species was nearly impossible due to the high similarities, therefore full conversion was very important.

2.3.3 Synthesis of the dihydride I

While the monohydrated species is already known in literature [13] the dihydrated species remained so far unexplored. The first approach was the reaction of the pentasilane treated with potassium *tert*-butoxide and stirred for 20 h, with degassed aqueous sulphuric acid. After extraction with diethyl ether the completion was controlled with NMR spectroscopy.

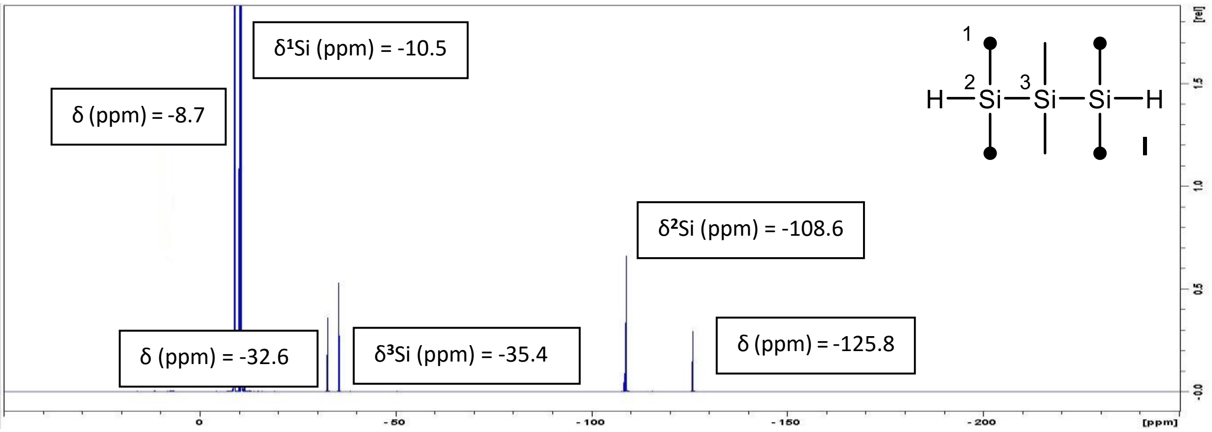

Figure 15: ^{29}Si NMR of the mixture of mono and dihydride

The NMR of this reaction (Figure 15) showed an incomplete conversion to the dianion **G** resulting in a mixture of the mono- and dihydrated silane. (^{29}Si | δ (ppm) mono: -8.7, -32.6, -125.8 | di: -10.5, -35.4, -108.6)

Just the monohydride crystal could be isolated and measured by X-ray diffraction. The crystal matches the literature values described by Baumgartner et al. [13], but exhibits a different space group ($P2_1/n$ instead of $C2/c$).

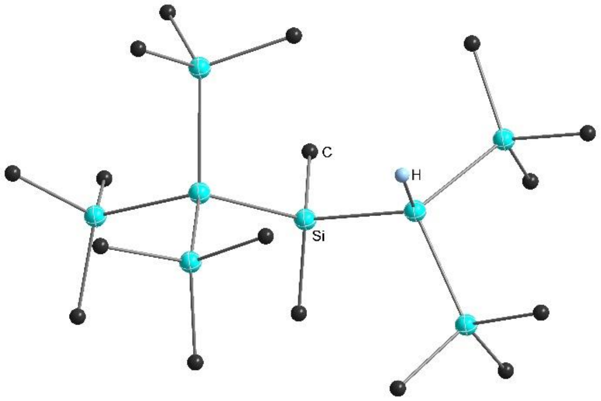

Figure 16: Crystal structure of 1,1,1,3,3,5,5,5-octamethyl-2,2,4-tris(trimethylsilyl)-pentasilyl-4-hydride

In the second approach the nonasilane **F** solution was stirred with potassium-*tert*-butoxide and DME for at least 48 h. A color change from yellow to green took place and the solvent was evaporated together with the formed silyl ether. The remaining green oil was then added to toluene and transferred to a vessel containing degassed aqueous sulphuric acid. After extraction with diethyl ether and removal of the solvent a colorless oil remained. Formation of white crystals could be observed after one week of product storage in acetone at -30 °C. The crystals have a melting point between 42 °C and 45 °C and could be measured on the X-ray diffractometer. The solid state structure and the NMR-measurement proved the formation of the dihydride.

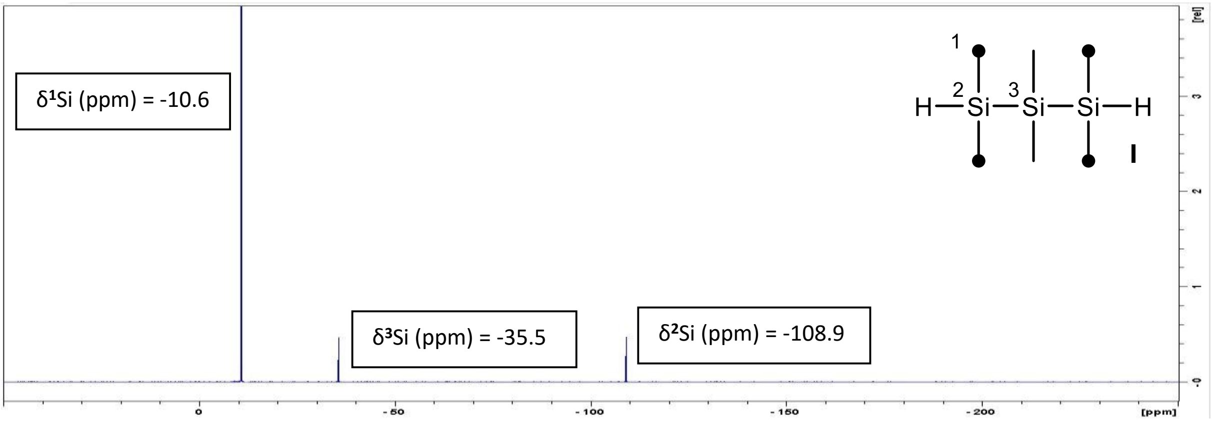

Figure 17: ^{29}Si NMR of 1,1,1,3,3,5,5,5-octamethyl-2,4-bis-(trimethylsilyl)-pentasilyl-2,4-dihydride I

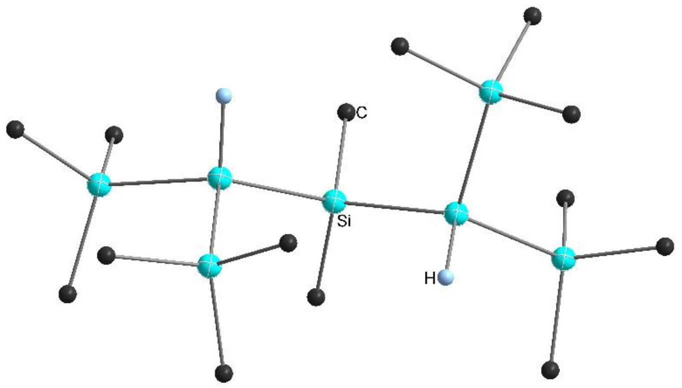

Figure 18: Crystal structure of 1,1,1,3,3,5,5,5-octamethyl-2,4-bis-(trimethylsilyl)-pentasilyl-2,4-dihydride I

Table 4: Comparison of the crystal values

	Baumgartner et al.	**Monohydride**	**Dihydride I**
Formula	$Si_8C_{17}H_{52}$	$C_{17}H_{52}Si_8$	$C_{14}H_{44}Si_7$
Fw (g mol^{-1})	481.31	481.30	409.12
a (Å)	31.743(6)	9.3283(8)	17.8251(15)
b (Å)	9.759(2)	27.751(3)	25.516(3)
c (Å)	23.294(9)	12.9844(11)	13.0523(12)
α (°)	90	90	90
β (°)	111.56	108.707(3)	109.476(3)
γ (°)	90	90	90
V (Å^3)	6711(2)	3183.7(5)	5596.8(9)
Z	8	4	8
Crystal size (mm)	0.35 × 0.15 × 0.10	0.20 × 0.15 × 0.12	0.08 × 0.07 × 0.06
Crystal habit	Plate, colorless	Block, colorless	Plate, colorless
Crystal system	Monoclinic	Monoclinic	Monoclinic
Space group	C2/c	$P2_1/n$	$P2_1/c$
d_{calc} (mg/m^3)	0.953	1.004	0.971
μ (mm^{-1})	0.32	0.34	0.34
T (K)	293(2)	100(2)	100(2)
2θ range (°)	1.38-23.31	2.2-32.6	2.3-29.6
F(000)	2128	1064	1808
R_{int}	-	0.043	0.054
independent reflns	4818	5577	10868
No. of params	247	434	423
R1, wR2 (all data)[a]	R1 = 0.055 wR2 = 0.134	R1 = 0.0240 wR2 = 0.0575	R1 = 0.0657 wR2 = 0.0941
R1, wR2 (>2σ)[b]	R1 = 0.090 wR2 = 0.148	R1 = 0.0218 wR2 = 0.0560	R1 = 0.0374 wR2 = 0.0809
Si-H (Å)	1.46(3)	1.39(2)	1.42(2) 1.40(2)
R_1-Si-Si-Si-R_2 (°)	114.8 (R_1=H R_2=$SiMe_3$)	113.9 (R_1=H R_2=$SiMe_3$)	112.9 (R_1=H R_2=H)

The comparison of the different crystals shows that the difference of the space group could be explained with the temperature difference of the measurement. The monohydride measured by Baumgartner et al. [13] is also more closely packed in the extended structure. The silicon-hydrogen bond lengths and the angle along the main axis do not differ a lot and fall within the normal range for silanes. The structure of the measured dihydride also shows, that the two hydrogen atoms are located trans to each other. This corresponds to the global minimum structure from the DFT calculations.

2.3.4 TCCA route

The first approach to generate a dichloride out of the dihydride consisted of the previously tested synthesis using TCCA as a chlorinating agent due to its high selectivity. Therefore, the dihydride was dissolved in THF and cooled to -70 °C. Then 3 equivalents of TCCA pellets were added to the reaction mixture. The reaction was then stirred for 20h, during which a white precipitate (TCCA and TCCH [isocyanuric acid] residues) formed and was controlled *via* NMR spectroscopy. When no hydride peak could be detected in the spectra the liquid phase was transferred *via* filter cannula into another Schlenk. After the solvent was evaporated, a waxy yellow substance remained. 20 ml of pentane were added to precipitate the remaining TCCA and TCCH from the solution. A clear yellow solution and a colorless solid remained in the vessel. After another filtration a pale yellow solution was obtained. The proton NMR confirmed that neither TCCA nor TCCH was left in the solution due to the missing peak at 10 ppm. The silicon NMR showed a mixture of the dichlorinated and other unidentified species. The corresponding peak confirming a Si-H bond could not be seen in the area around -100 ppm but due to many peaks in the area of 10 ppm it was not possible to assign the peaks to specific silanes. Separation *via* distillation was not possible due to the small batch of silanes.

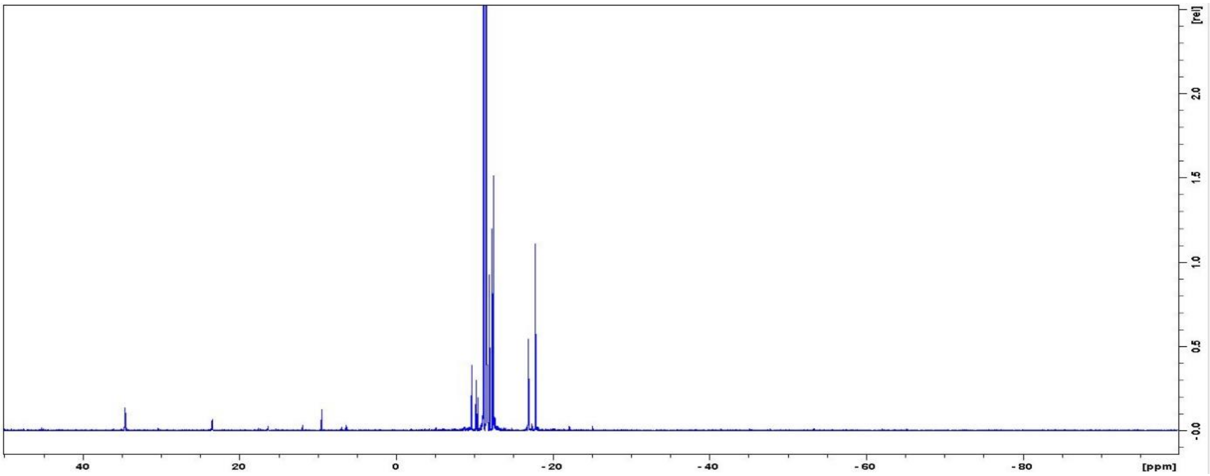

Figure 19: ^{29}Si NMR of 1,1,1,3,3,5,5,5-octamethyl-2,4-bis(trimethylsilyl)-pentasilyl-2,4-dichloride J and other chlorinated silanes

2.3.5 Carbon tetrachloride route

The next synthesis route that was tested is one of the standard chlorination routes for silanes. The dihydride is dissolved in dry carbon tetrachloride and stirred while heated to 60 °C with an oil bath for 48 h. The NMR measurement of the solution showed that no reaction took place and therefore the temperature was adjusted to 90 °C and the solution stirred for another 48 h. Instead of the desired dichloride the NMR showed that the bonds of both, the carbon tetrachloride and the dihydride, were cleaved resulting in hexachloro-ethane and a mixture of several silanes. This could be explained with the radical mechanism of the carbon tetrachloride route and the weak silicon-silicon bond which can also be attacked by the formed radical. This route is considered not useful for chlorination of sterically protected silanes.

2.3.6 Boron catalysed route

In addition to literature known chlorination routes involving transition metal catalysts, chlorine or chlorinated carbons, Dobrovetsky and Chulsky [40] recently reported a new route using tris(pentafluorophenyl)borane as catalyst and gaseous hydrogen chloride as chlorination agent. Therefore, 10 mole% of tris(pentafluorophenyl)borane were dissolved in toluene and added to a solution of dihydride in toluene. Then 10 equivalents of sodium chloride were added to another reaction vessel and dried in vacuum. The silane solution was cooled to -90 °C and concentrated sulphuric acid was added to the sodium chloride. The formed hydrogen chloride was bubbled through the silane solution until the gas formation ceased. The reaction solution was then measured *via* NMR-spectroscopy but no product formation could be observed. The mechanism stated in literature (Figure 20) could explain, why no reaction took place. Sterically accessible silanes were used, allowing the formation of the transition state (figure 20) needed for the product formation. The sterically demanding TMS group seems to hinder the formation of this transition state and therefore the chlorination reaction.

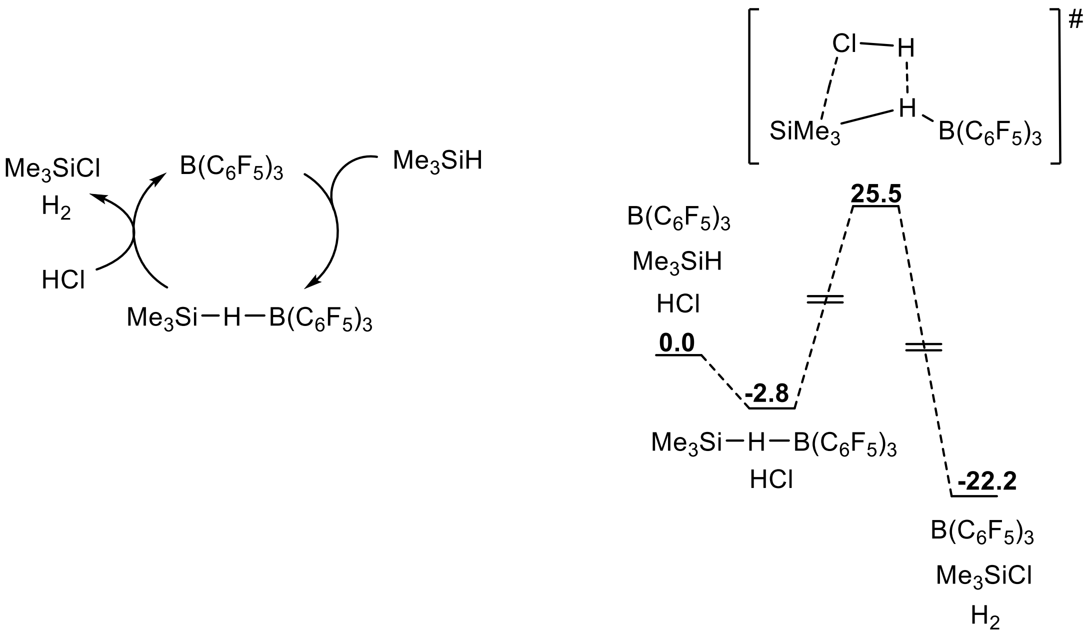

Figure 20: Boron catalysed mechanism and transition states *[40]*

2.3.7 Phosphorus pentachloride route

Another method most commonly used in organic synthesis, especially in chlorination of carbonic acids is the use of phosphorus pentachloride. This method was tested and approved working with the similar tris(trimethylsilyl)silane by Albert and Yamamoto [41]. Therefore, the dihydride was dissolved in DME and 1.1 equivalents of phosphorus pentachloride were added. The solution heated up and was stirred for 20 h at room temperature, where a color change from colorless to pale yellow occured. The NMR showed a mixture of the monochlorinated, dichlorinated and dihydride species.

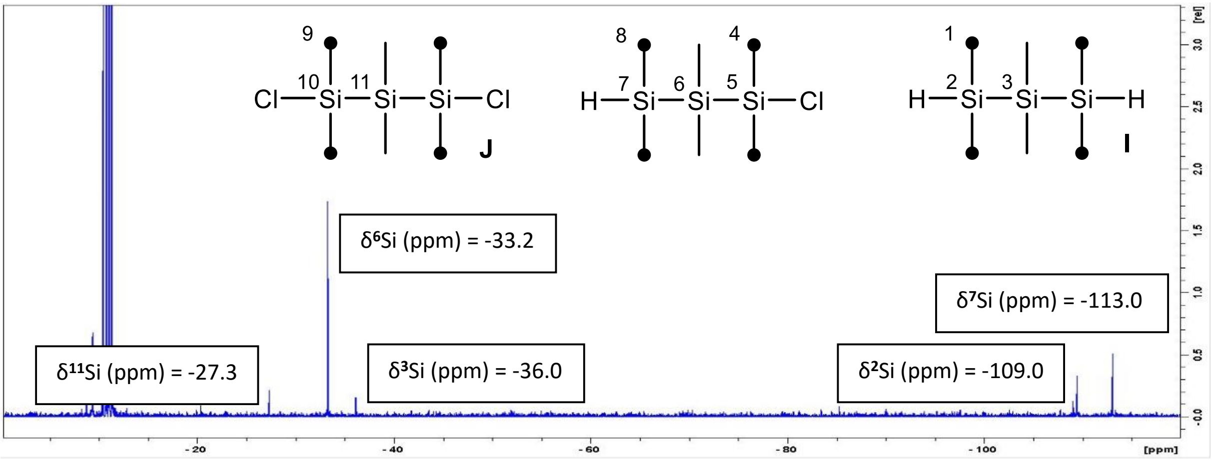

Figure 21: ^{29}Si NMR of 1,1,1,3,3,5,5,5-octamethyl-2,4-bis(trimethylsilyl)-pentasilyl-2,4-dichloride J, the monochloride and of 1,1,1,3,3,5,5,5-octamethyl-2,4-bis(trimethylsilyl)-pentasilyl-2,4-dihydride I

The very interesting part of the spectrum was the field from -8 to -12, where the TMS shifts of all three species and the shift of the silicon connected to chlorine, occur as shown in Figure 22.

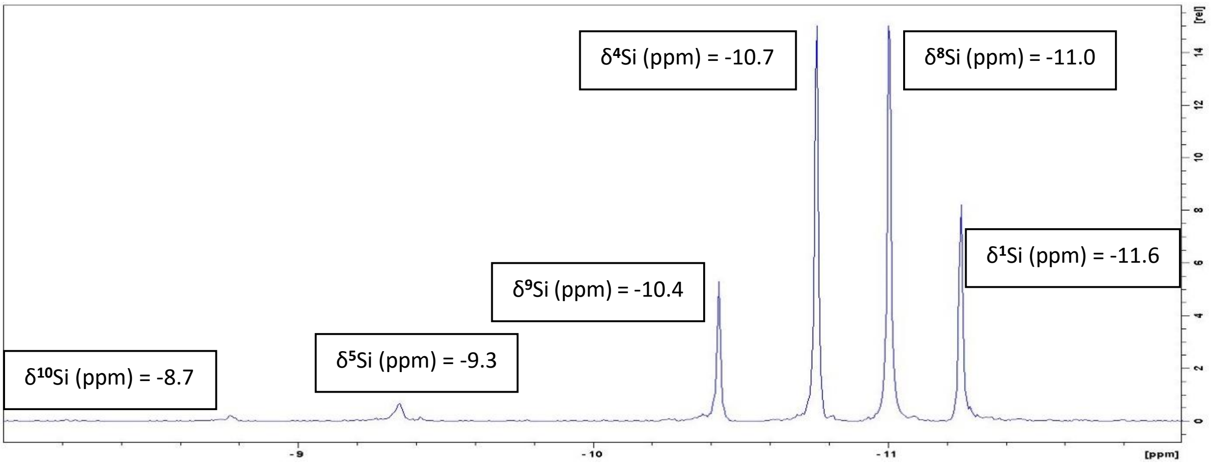

Figure 22: ^{29}Si NMR TMS shifts of the mono-, dichlorinated and dihydride species

To get full conversion to the dichlorinated species two additional equivalents of PCl_5 were added and the mixture was stirred for another 48 h at room temperature. The NMR confirmed that only the desired product formed.

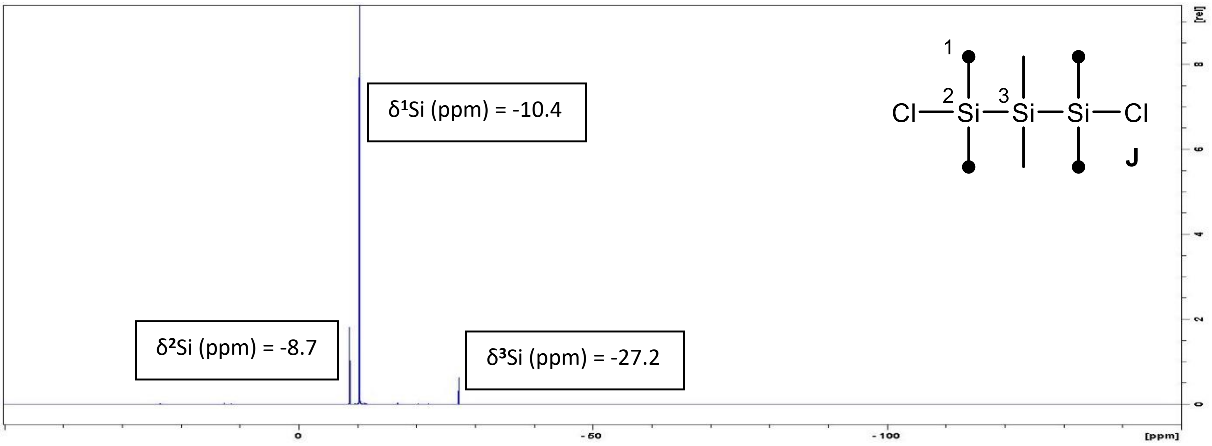

Figure 23: ^{29}Si NMR of 1,1,1,3,3,5,5,5-octamethyl-2,4-bis(trimethylsilyl)-pentasilyl-2,4-dichloride J

The ^{31}P NMR showed that additionally to the formed phosphorus trichloride and phosphoryl chloride, traces of phosphorus pentachloride remained in the mixture.

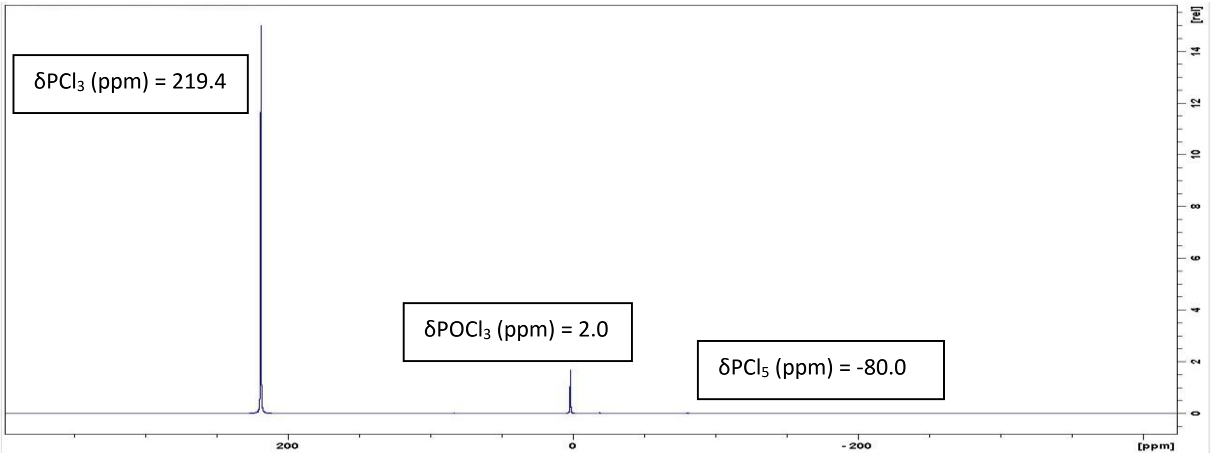

Figure 24: ^{31}P NMR of the reaction solution of the dichloride J

The formed phosphoryl chloride could be explained by the state of the used dihydride crystals. Due to the storage under air, they seemed to have reacted with the moisture and therefore, a part of the dihydride hydrolysed.

The PCl_3 residue could be removed together with the solvent under reduced pressure (1 mbar). This was also confirmed by ^{31}P NMR.

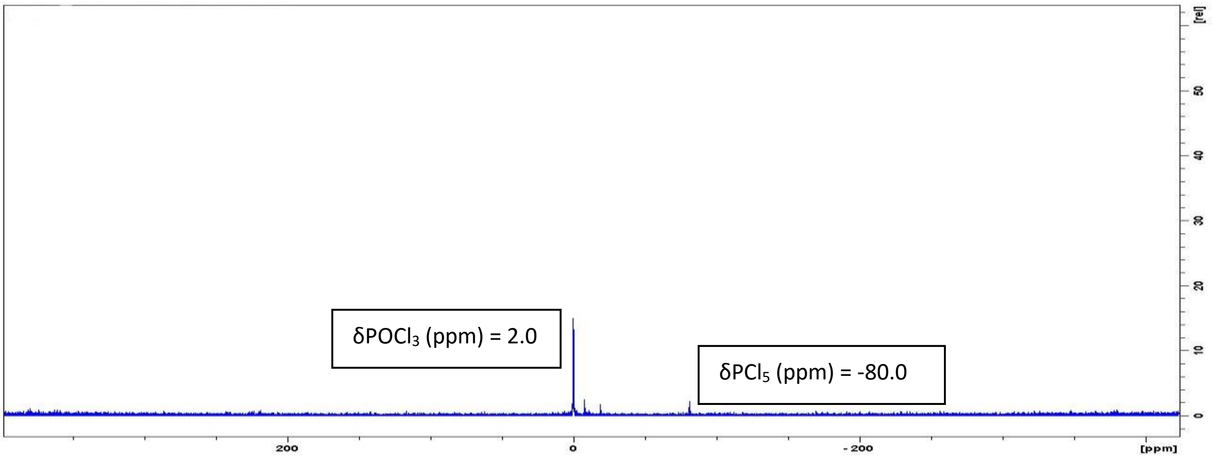

Figure 25: ^{31}P NMR of the reaction solution of the dichloride J after the first purification

The remaining phosphoryl chloride and PCl_5 could be removed with further evaporation over 3 h with a 50 °C water bath (supplying the needed temperature to get rid of the high boiling phosphoryl chloride (105.8 °C at 1 atm)). The product remained as a highly viscous grey liquid. Due to the high selectivity, easy workup and simple process, the phosphorus pentachloride route is considered the best route for the chlorination of highly protected silanes.

2.4 Synthesis of sodium phosphide P/Q

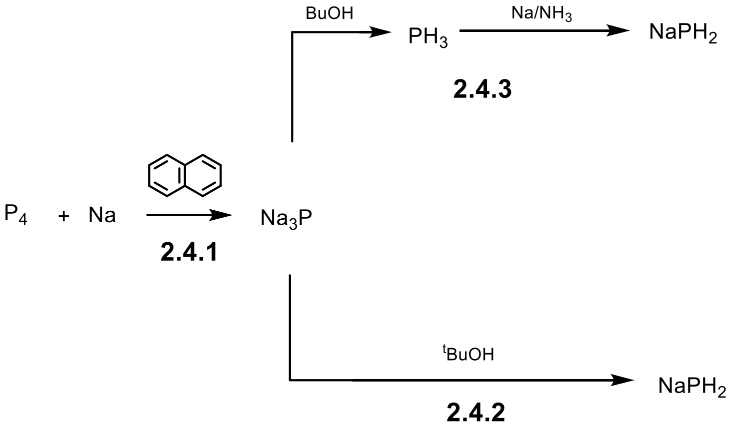

Figure 26: Sodium phosphide synthesis routes

One of the most challenging aspects of this thesis was the generation of sodium phosphide without the use of white phosphorus or commercially available phosphine gas. A lot of investigation was done at ETH Zurich by Grützmacher [42] and Hendriksen [2]. The existing synthesis schemes were adapted and modified to cope with our needs.

2.4.1 Synthesis of trisodium phosphide

Due to the high reactivity and toxicity of white phosphorus the relatively unreactive red phosphorus was used in all discussed reactions. While Hendriksen used only white phosphorus in his synthesis during his doctoral thesis, he also cited a reduction of red phosphorus in the presence of sodium and naphthalene [43] to the desired intermediate trisodium phosphide. The first reduction of red phosphorus using naphthalene was reported by Widhalm et al. [44].

Other than in the mentioned reactions we first added red phosphorus to a 500 ml three necked round bottom flask and evaporated the vessel three times under cautious heating. The phosphorus was then dispersed in DME and sublimated naphthalene dissolved in DME was added to the suspension. Sodium metal was cut into small pieces dabbed with DME and admixed to the reaction solution. The color changed from a light red to a black suspension. After 20 h of stirring at room temperature no sodium pieces were left in the reaction mixture. To dispose of the remaining naphthalene another 200 ml of DME were added. The solvent with the naphthalene was then separated *via* filter cannula from the product, which remained as a black solid. The remaining solvent residues were evaporated in vacuum.

The contaminated filter cannula was put carefully into aqueous potassium permanganate, which led to spontaneous ignition of the sodium triphosphide residues on the filter. Due to the very small particles of the sodium triphosphide, a small amount passed through the filter and remained with the naphthalene in the DME. To quench this suspension, it was cooled with an ice bath and connected to two safety wash bottles filled with a 5% aqueous potassium permanganate solution to convert the produced phosphine gas. Under nitrogen atmosphere aqueous potassium permanganate was then slowly added to the suspension, until no further reaction occured.

2.4.2 Direct synthesis of alkoxy packed sodium phosphide

The first approach leading to sodium phosphide is an adapted form of the synthesis route described in the doctoral thesis of Hendriksen, differing in the starting material red phosphorus compared to the white phosphorus used. The produced trisodium phosphide was dissolved in DME and two safety wash bottles with aqueous potassium permanganate were connected to the vessel. Afterwards *tert*-butanol was slowly added *via* a syringe through a septum. Immediately phosphine gas formation took place, the reaction solution started to warm up and the color of the solution changed from black to light brown. To accelerate the reaction, the vessel was heated with a 40 °C water bath and stirred for 20 h. The dissolved sodium phosphide was separated from the by-products *via* a filter cannula, which led to a clear yellow solution. The solvent was then evaporated with the help of an extra cooling trap, due to the formation of phosphine gas. Even then we could observe heavy reactions occurring in the safety vessel. The product remained as a pale yellow solid. The ^{31}P-NMR spectrum showed that only the alkoxy-packed sodium phosphide formed and the shifts and coupling constant match the literature values (^{31}P | δ (ppm) = -289.6 | $^{1}J_{PH}$ = 145.0 Hz).

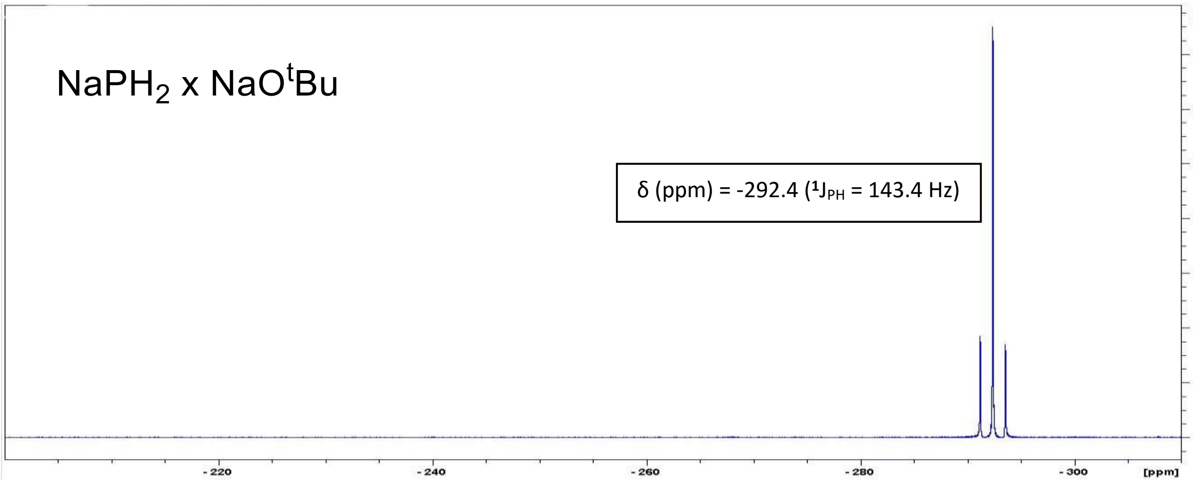

Figure 27: ^{31}P-NMR of sodium tert-butoxide packed sodium phosphide P

The problem with this route was the formation of sodium *tert*-butoxide as a side product, which is a strong base and, due to its high reactivity, is not suitable to be in a reaction with chloro silanes. The separation of the butoxide and the phosphide was not possible to achieve, due to the similar properties in terms of solubility and crystallization behavior.

2.4.3 Synthesis route using *in situ* generation of phosphine gas

The direct route yielded a product contaminated with sodium *tert*-butoxide. Because we can't use a product with a strong base in it, we had to think about other ways to get a pure product. The reaction of alcohol with trisodium phosphide led to a formation of phosphine gas, which could be very useful for the synthesis of a pure product. The literature known processes invented by Evers [45] and Brandsma [46] use a mixture of liquid ammonia and alkali metal combined with phosphine gas to synthesize alkaline metal phosphines.

Since no phosphine gas was available, an *in situ* production was considered. Therefore, trisodium phosphide was prepared as a starting material and dissolved it in DME. In a second vessel ammonia was condensed in a liquid nitrogen bath and small pieces of sodium metal were added to the liquid, which changed the color of the solution to deep blue. Due to the large amount of sodium metal needed, a mechanical stirrer was used. The trisodium phosphide flask was connected to the sodium/ammonia containing flask and a mixture of DME and butanol (2:1) was slowly added *via* dropping funnel to the trisodium phosphide. Immediately phosphine gas evolved from the solution, the temperature rose rapidly and white smears formed in the dark suspension. The evolving phosphine flowed through the sodium/ammonia and the exhaust gases had to be channelled through two safety wash bottles with aqueous potassium permanganate. After complete addition the trisodium phosphide solution had a grey color and cooled down. If enough phosphine evolved the sodium/ammonia solution should also change the color from deep blue to colorless, but in our case too little phosphine reacted and therefore some sodium metal remained unreacted in the solution. The reaction vessel was then warmed to room temperature to evaporate the ammonia and the product remained as yellow powder. To get rid of the metal residues the powder was dissolved in DME and separated from the metallic parts *via* filter cannula. The ^{31}P NMR-spectra matched the literature values for sodium phosphide, but, due to the treatment with DME after the reaction, the solvent was chelating onto the phosphide. Solvent exchange and evaporating with high vacuum could not clear the phosphide of the solvent. This meant we had to quantify the content of chelated DME, to use the sodium phosphide stoichiometrically. This turned out very difficult, due to the bad solubility of the phosphide in most deuterated solvents.

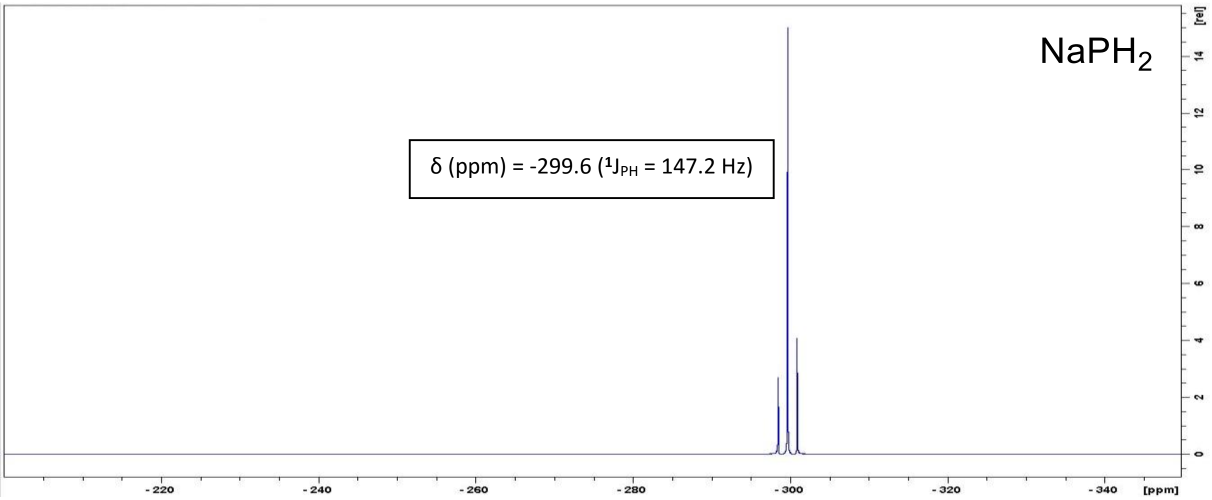

Figure 28: ^{31}P-NMR of sodium phosphide Q

With the help of THF-d8 the ^{1}H- NMR showed that one DME molecule bridged two sodium phosphide molecules (see figure 29). Therefore, the molar mass of the product rose to 101.04 g ($NaPH_2$ x 0.5 DME). This problem could be avoided by using a larger excess of phosphine in the synthesis and more stable cooling.

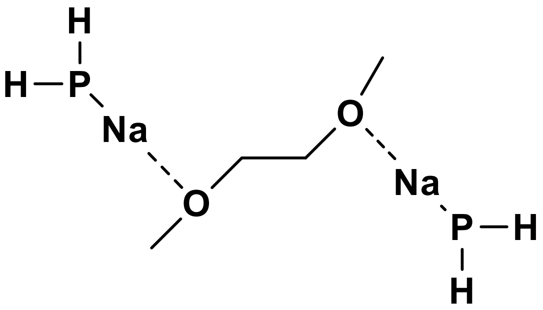

Figure 29: Structure of the sodium phosphide – DME product

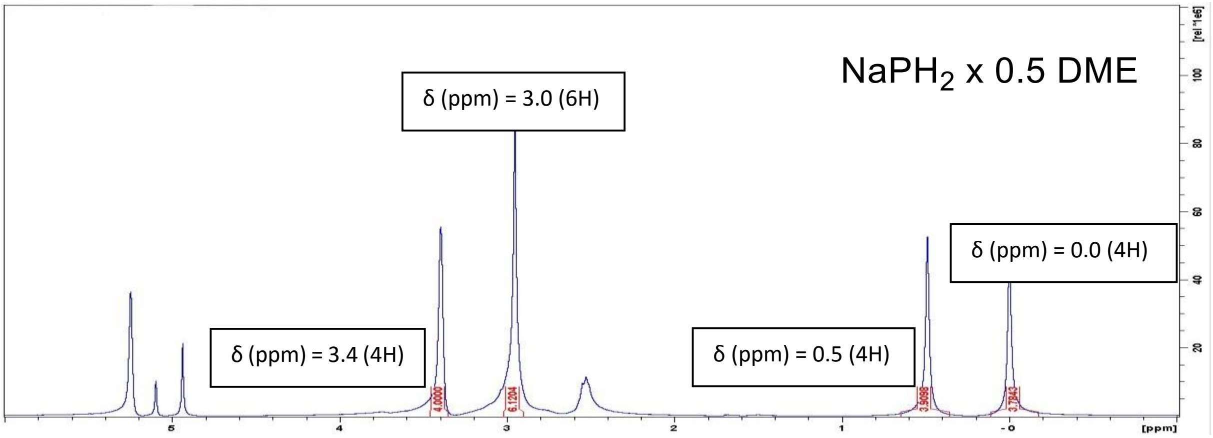

Figure 30: ^{1}H-NMR of sodium phosphide Q

2.5 Synthesis of the diphosphasilanes H/R/S

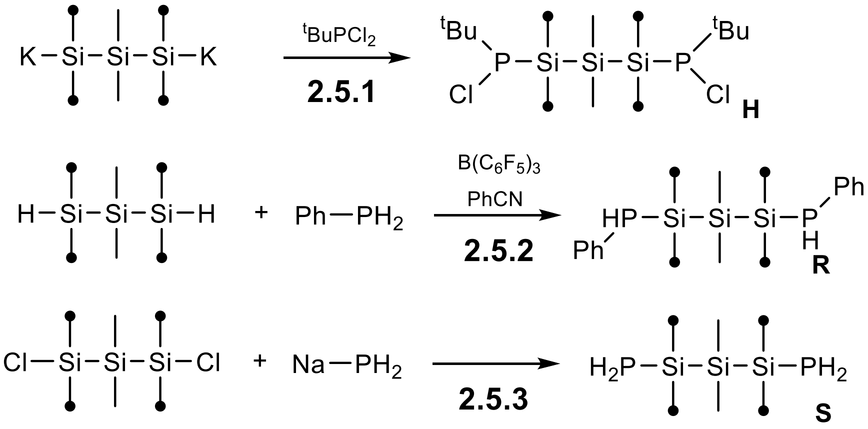

Figure 31: Synthesis routes towards diphosphasilane

Due to little knowledge on diphosphanes containing a trisilane backbone, several approaches to get a product have been investigated as displayed in figure 31.

2.5.1 Synthesis using phosphorus chloride

The most common and simple route started from a silane dianion and used a phosphorus chloride for the coupling. The dianion was weighed into a Schlenk, dissolved in toluene and cooled to -78 °C. $^tBuPCl_2$ was slowly added *via* a syringe to the solution and was kept at -78 °C and stirred for 20 h. During this time potassium chloride precipitated from the solution. The salt was separated from the colorless solution *via* filter cannula and the solution stored in the fridge at -30 °C. The NMR-measurements showed that no silicon-phosphorus, but phosphorus-phosphorus interaction occurred. Additionally, transmetallation to tetrakis-(trimethylsilyl)silane took place. It was also stated by Appel et al. [47] that the product in such reactions might form, but decompose to the thermodynamically stable diphosphanes. The kinetic phosphasilane product was not stable, especially with potassium in the reaction. This route was not considered useful for the synthesis of diphosphasilanes.

2.5.2 Boron catalysed heterogeneous dehydrocoupling

Recent research on the use of tris(pentafluorophenyl)borane in the direct silicon – phosphorus bond formation [48] showed good results with sterically less demanding substituents on the silicon. To adapt this procedure for our used silane, we weighed the silane into a Schlenk and evaporated it with cautious heating three times. Then the boron species was added in the glovebox, the mixture dissolved in deuterated benzene and benzonitrile, was added. Phenylphosphine was added and the mixture stirred for 20 h at room temperature. The NMR showed no product formation. This again could be explained with a failure to form the needed transition state described Figure 20 due to the sterically very demanding TMS groups. The good results stated in the literature could not be confirmed for sterically well shielded silanes and therefore this route was also not suitable for the synthesis of the desired product.

2.5.3 Synthesis using sodium phosphide

The coupling of the similar hypersilylchloride with sodium phosphide was first reported by Hassler *et al.* [1] and was expected to be working with our dichloride. Therefore, the sodium phosphide and the dichloride were dissolved in THF and the dichloride solution added to the phosphide solution. Immediately gas formation could be observed and a color change of the former yellow solution to orange took place. The measured ^{31}P NMR showed a very high phosphine concentration in the solution, which indicates that the used THF was not totally dry or it could be cleaved by the aggressive components.

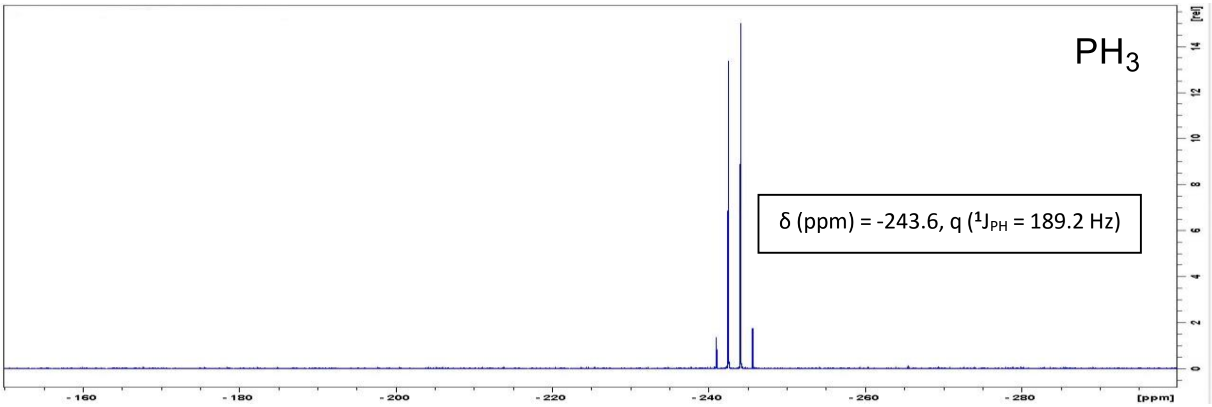

Figure 32: ^{31}P-NMR of the chloride-phosphide mixture

This led to hydrolysis of the product and formation of siloxanes. The solvent was then evaporated together with the formed phosphine and the remaining orange oil dissolved in diethyl ether. After 20 h a white solid (NaCl) dissipated from the light orange solution. The liquid phase was then transferred into a separate vessel *via* syringe filter which led to a clear orange solution. The solvent was evaporated and the product remained as an orange oil. The ^{31}P shows that not only the desired product, but also several side products formed.

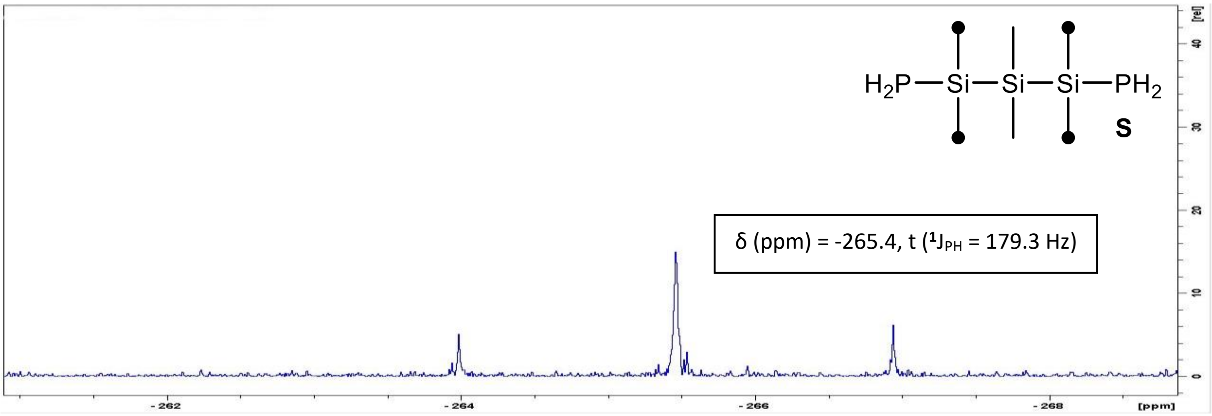

Figure 33: ^{31}P-NMR of 1,1,1,3,3,5,5,5-Octamethyl-2,4-bis(trimethylsilyl)-pentasilyl-2,4-diphosphine S

The phosphorus shifts matched the literature known ones for hypersilyl phosphane [1] [-265.4 ppm, t, ($^1J_{PH}$ = 178.7 Hz)].

The silicon NMR was hard to achieve, because of the small concentration of educts and the side reactions, due to the hydrolysis and cracking of the THF. The most promising shifts could be observed in the high field area, where a doublet at -107.2 ppm with a coupling of 46.4 Hz could be observed. This was comparable with the Si-P shift and coupling of the known hypersilyl phosphane [1] [-102.4 ppm, d, ($^1J_{PH}$ = 46.7 Hz)].

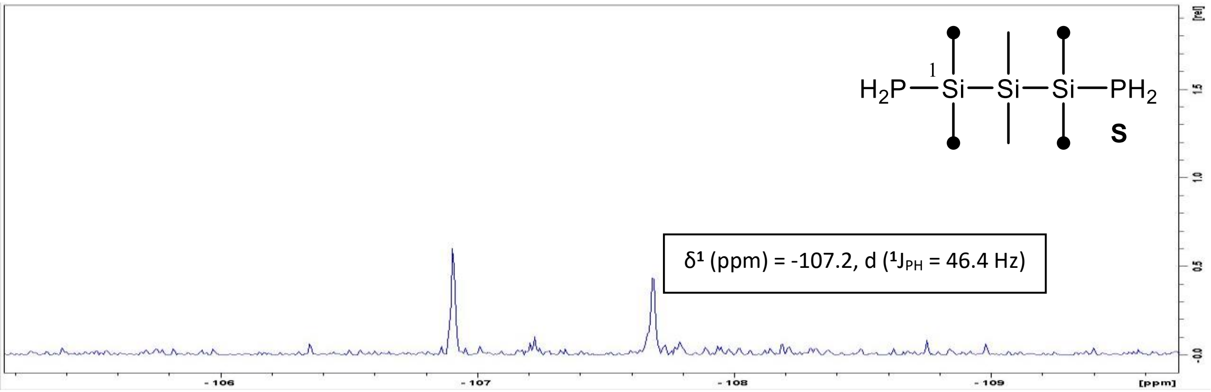

Figure 34: ^{29}Si-NMR of 1,1,1,3,3,5,5,5-Octamethyl-2,4-bis(trimethylsilyl)-pentasilyl-2,4-diphosphine S

Further workup was not possible due to the small amount of product (<0.2 g). Separation should be possible with fractionate sublimation and will be the aim of future work.

The synthesis route was considered the most promising one for the formation of short chain diphosphasilanes and the formation of a new diphosphasilane could be achieved. The coupling process has to be further optimized in terms of used solvent, reaction temperature and purification, which will also be continued in future work.

2.6 Conclusion and Outlook

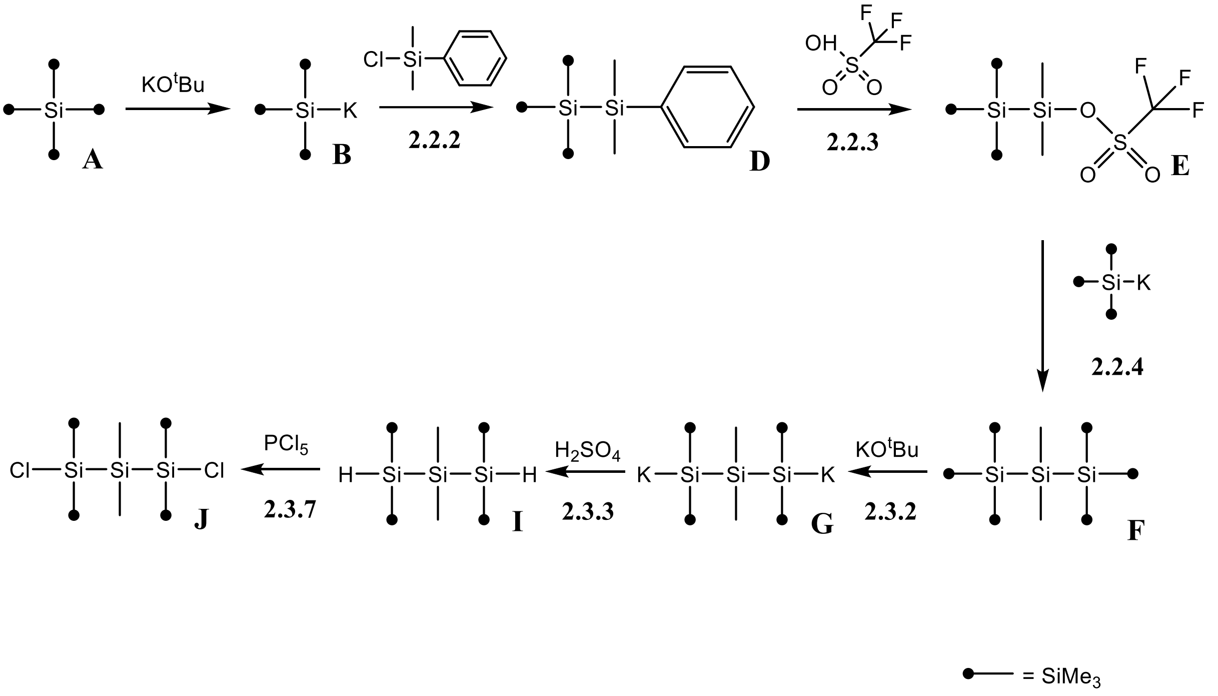

Figure 35: Scheme of the most efficient silane synthesis route

In summary, we were able to synthesize and characterize the literature known nonasilane chain *via* a novel synthesis route, without using gaseous hydrogen halide. This route was further optimized to improve the yields. The product purification was performed in the drying oven at 140 °C which led to solvent free crystals matching the literature known values.

It was not possible to obtain the diphosphane by the synthesis of the nonasilane potassium dianion directly with phosphorus chlorides due to the thermodynamically preferred side reaction yielding P-P bonding. Therefore, $NaPH_2$ needed to be synthesized first.

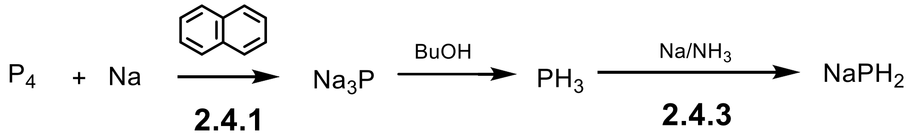

Figure 36: Scheme of the best sodium phosphide synthesis route

Most of the literature known aforementioned synthesis routes use either white phosphorus or phosphine gas for the formation of the phosphide. The next goal of this thesis was to avoid the use of both, the white phosphorus and commercial available phosphine gas in the synthesis. This led to a method established at ETH Zurich using trisodium phosphide as an intermediate. The literature method was adapted to cope with our needs. The direct approach, using *tert*-butanol led to alkoxide packed sodium phosphide which could not be separated from the sodium *tert*-butoxide side product and therefore was considered useless for further experiments.

To circumvent the formation of alkoxide side products we adapted a new route for the production of sodium phosphide using trisodium phosphide as starting material for *in situ* phosphine gas formation. The produced gas was then led into the literature known ammonia/sodium solution and sodium phosphide formed directly. The NMR-measurements showed that the desired product formed, but, due to cooling problems and too small amounts of phosphine during the synthesis an excess of sodium remained in the reaction vessel and had to be separated from the product. This was achieved through dissolution of the phosphide in DME and filtration *via* filter cannula. After the evaporation of the solvent, the DME was chelating onto the phosphide and it was not possible to remove it. With the help of deuterated THF it was possible to establish that one molecule of DME bridged two molecules of phosphide and therefore the exact molar mass of the product could be determined.

The synthesis of the yet unknown 1,3-dihydridotrisilane could be achieved *via* the literature known synthesis route described for the potassium dianion of the silane [3]. After aqueous workup with diluted sulphuric acid, the dihydride crystallized from acetone. The solid state structure could be determined *via* X-ray diffraction. In addition, monohydride crystals could be obtained, which differ in their space group to the literature known ones. The exact cause for the different space group could not be determined

The synthesis of the 1,3-dichloridotrisilane turned out to be very challenging and several routes have been tested. The recently discovered routes including tris(pentafluorophenyl)-borane as a catalyst and using either hydrogen chloride gas for the direct chlorination of the hydride or using phenyl phosphine for heterogeneous dehydrocoupling, were tested but turned out to be inapplicable. This could be explained by the high steric protection in our silane compared to the less protected silanes used in literature.

The most common chlorination route using carbon tetrachloride led to a decomposition of the silane chain and the formation of hexachloro ethane. Due to the radical mechanism of this reaction, the high reaction temperatures of 90 °C needed to start the reaction, seemed to boost the silicon-silicon bond cleavage.

The most promising route was the chlorination using TCCA as a chlorination agent. The prechlorination test with the similarly protected tris(trimethylsilyl)silane worked well. In the case of the trisilane the NMR-spectra indicate, that a mixture of mono- and dichlorinated silane were formed together with another silane by-product. Due to the small batch, it was not possible to separate the mixture *via* distillation. The difficult separation and the occurrence of a lot of side products made the TCCA route considered not useful for sterically well protected silanes.

The approach leading to the best results and therefore the method to go, was the chlorination using phosphorus pentachloride as a chlorination agent. The dihydride was diluted in DME and 1.1 equivalents of phosphorus pentachloride were added to the reaction mixture. After 20 h the NMR showed, that no full chlorination took place. To accelerate the process another 2 equivalents of phosphorus pentachloride were added and the mixture stirred for another 40 h. The NMR showed that full conversion to the dichlorinated silane could be obtained. Due to the state of the used dihydride crystals, additional to the normal formed PCl_3, phosphoryl chloride formed as a by-product. The by-products could be separated from the highly viscous product *via* evaporation under reduced pressure at 50 °C. The formation of dichloride crystals could not be achieved yet and is a goal of further investigations.

The coupling reaction of the dichloride with the sodium phosphide yielded the desired diphosphasilane, but several steps have to be further optimized. The quantification of the product could only be obtained *via* ^{31}P and ^{29}Si NMR, due to the small amount of the product.

The reproduction and crystallisation of the diphosphasilane is the aim of future work. The used THF seemed to be not totally dry or was cleaved during the coupling process and led to hydrolysis and siloxane side product formation. Therefore, it has to be investigated which solvent and reaction temperature gives the highest yields and the least side products. In addition, the small amount of product did not allow the purification *via* fractionated sublimation, which will also be tested in future work.

3 Experimental Part

3.1 Materials and Methods

All reactions, unless otherwise stated, were carried out using standard Schlenk line techniques under nitrogen atmosphere. All dried and deoxygenated solvents were obtained from a solvent drying system (Innovative Technology, Inc.). All other chemicals from commercial sources were utilized without further purification. Melting point measurements were carried out by threefold determination with a Stuart Scientific SMP 50 (up to 400 °C). Elemental analysis was performed with an Elementar Vario Micro Cube.

The •— symbol in the chemical formulas is substituting a trimethylsilyl group (TMS) and Hyp- is substituting a hypersilyl- or tris(trimethylsilyl)silane group.

3.1.1 NMR Spectroscopy

^{1}H (300.22 MHz), ^{13}C (75.5 MHz), ^{29}Si (59.6 MHz) and ^{31}P (121.5 MHz) NMR spectra were recorded on a Mercury 300 MHz spectrometer from Varian at 25 °C if not otherwise stated. Chemical shifts are given in parts per million (ppm) relative to TMS ($\delta = 0$ ppm) regarding ^{1}H, ^{13}C and ^{29}Si and relative to 85% H_3PO_4 in the case of ^{31}P. Coupling constants (J) are reported in Hertz (Hz). The letters s, d, t, q and m are used to indicate singlet, doublet, triplet, quadruplet and multiplet.

3.1.2 GC-MS Measurements

GC-MS measurements were carried out on an Agilent Technologies 7890A GC system coupled with an Agilent Technologies 5975C VLMSD mass spectrometer using a HP5 column (30m×0.250mm×0.025 µm) and a carrier helium gas flow of 0.92726 ml/min. A „hot-needle“, manual injection method at an injector temperature of 280 °C was performed. After 2 min the temperature was increased in 12 °C/min steps up to 300 °C and kept at 300 °C for 10 min. The MS conditions included positive EI ionization at an ionization energy of 70 eV and a full scan mode (50-500 m/z).

3.1.3 DFT Calculations

All calculations have been carried out using the GAUSSIAN09 program package [49] on a computing cluster with blade architecture. For all calculations the mPW1PW91 [32] hybrid functional was used. For optimisation and calculations of frequencies the 6-31+G* [33] basis set was applied. For calculation of the NMR magnetic shieldings the all electron IGLO-II [34] basis set was used (σ ^{1}H = 32.8, σ ^{13}C = 186.6, σ ^{29}Si = 360.6 (TMS), σ ^{31}P = 624.7 (PH_3)). The geometries of the molecules were calculated in the gas phase, without the influence of a solvent. The optimised geometries of all discussed molecules are collected in Appendix A.

3.1.4 X-ray Diffraction

All crystals suitable for single crystal X-ray diffractometry were removed from a Schlenk under inert conditions and immediately covered with a layer of silicone oil. A single crystal was selected, mounted on a glass rod on a copper pin, and placed in the cold N_2 stream provided by a Bruker APEX2. For the solving the structure SHELXS97 (Sheldrick 2008) was used, to refine the structure SHELXL2014 (Sheldrick 2014) was used.

3.2 Synthesis of tetrakis(trimethylsilyl)silane A

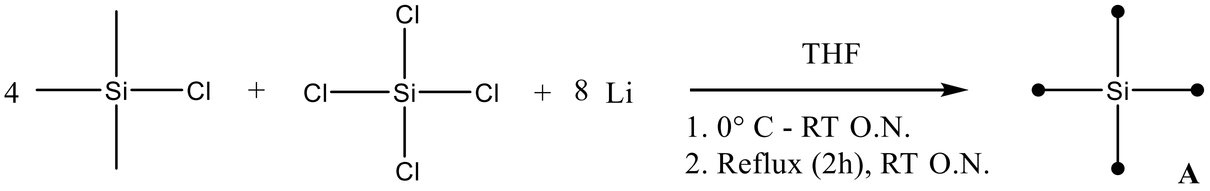

Figure 37: Synthesis of tetrakis(trimethylsilyl)silane A

Table 5: Synthesis of tetrakis(trimethylsilyl)silane A

Substance	Molar Weight [g/mol]	Density [g/cm³]	Mass [g]	Mole	Volume [ml]
TMS-Cl	108.5	0.854	320.05	2.95 mol	374.77
$SiCl_4$	169.9	1.48	80.82	0.475 mol	54.61
Li	6.94	x	35	5.04 mol	x
THF	72.11	0.899	x	x	2500

A 4 l three-necked round-bottom flask, equipped with a 1 l dropping funnel, a reflux condenser with a bubbler and a mechanical stirrer, was filled with 2.5 l of dry tetrahydrofuran (**THF**). Into a storage vessel equipped with an argon supply, 35 grams of lithium were weighed in fingertip sized strips and afterwards transferred into the three-necked flask. The dropping funnel was then filled with the trimethylchlorosilane (**TMS-Cl**) and the tetrachlorosilane (**$SiCl_4$**) and the mixture added under the use of a silicon oil cooling bath at -35 °C over the course of 6 hours. The reaction mixture changed from colorless liquid to a brown suspension. Upon complete addition the suspension was allowed to warm to room temperature and was stirred for another 24 hours. Then the reaction mixture was heated to reflux and another 10 ml of $SiCl_4$ were added to further react the remaining lithium. Afterwards the reaction mixture was stirred at room temperature for another 24 hours, then poured onto 1 l of a 1 M sulphuric acid/ice mixture and extracted three times with diethyl ether. Thereafter the combined organic phases were dried over sodium sulphate, filtered and the solvent evaporated. The remaining orange residue was further purified *via* sublimation, which led to a white solid.

Yield: 120.35 g | 79%

^{29}Si NMR ($CDCl_3$, 293K): δ -135.5 ppm, -9.8ppm | **^{1}H NMR ($CDCl_3$, 293K):** δ 0.2 ppm | **^{13}C NMR ($CDCl_3$, 293K):** δ 2 ppm | **SMP:** 263.5 °C

3.2.1 Synthesis of tris(trimethylsilyl)silylpotassium B

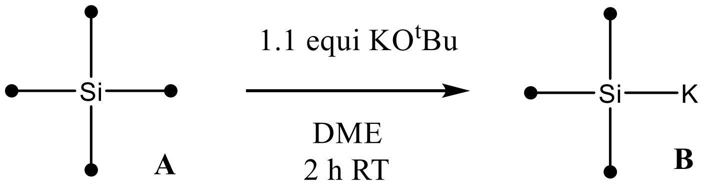

Figure 38: Synthesis of tris(trimethylsilyl)silylpotassium B

Table 6: Synthesis of tris(trimethylsilyl)silylpotassium B

Substance	**Molar Weight [g/mol]**	**Density [g/cm³]**	**Mass [g]**	**Mole**	**Volume [ml]**
Tetrakis(trimethylsilyl)-silane (A)	320.84	x	10.3	32.1 mmol	x
KOtBu	112.21	x	3.96	35.3 mmol	x
DME	90.12	0.87	x	x	30

Into a 100 ml Schlenk, with a magnetic stir bar, 10.3 g of tetrakis(trimethylsilyl)silane (**A**) were weighed and afterwards evaporated with cautious heating three times. Then the Schlenk was transferred into the glovebox and 3.96 g potassium-*tert*-butoxide (**KO^{t}Bu**) were added. After 30 ml of 1,2-dimethoxyethane (**DME**) were added with a syringe, the yellow solution was stirred for 2 hours. The formed silylether was then evaporated and the residue diluted in 30 ml of toluene.

Yield: ~99%

^{29}Si NMR (D_2O, 293K): δ -195.0 ppm, -4.6 ppm

3.2.2 Synthesis of 1,1,1,3,3,5,5,5-octamethyl-2,2,4,4-tetrakis-(trimethylsilyl)-pentasilane C

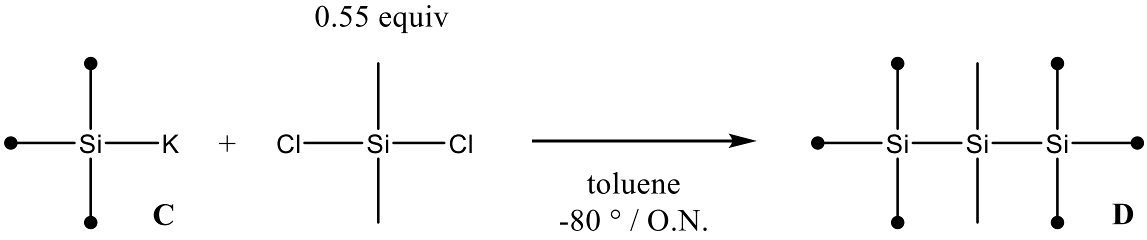

Figure 39: Synthesis of 1,1,1,3,3,5,5,5-octamethyl-2,2,4,4-tetrakis-(trimethylsilyl)-pentasilane C

Table 7: Synthesis of 1,1,1,3,3,5,5,5-octamethyl-2,2,4,4-tetrakis-(trimethylsilyl)-pentasilane C

Substance	Molar Weight [g/mol]	Density [g/cm³]	Mass [g]	Mole	Volume [ml]
Hyp-K (B)	286.66	x	4.47	15.6 mmol	x
Dichlorodimethylsilane	129.06	1.06	1.06	8.58 mmol	1.04
Toluene	92.14	0.867	x	x	10

Into a 100 ml Schlenk, with a magnetic stir bar, 10 ml of toluene were transferred and 1.04 ml of dichlorodimethylsilane were added. The solution was cooled to -80 °C with an EtOH/N_2 bath and **B** dissolved in toluene transferred slowly to the reaction vessel with a filter cannula. After the addition was finished the reaction was stirred for 2 h at -80 °C and afterwards allowed to warm up to room temperature and stirred for another 20 h. No product could be obtained due to transmetalation, the NMR-spectra just showed a mixture of **A** and **B**.

3.3 Synthesis of 1,1,1,3,3-pentamethyl-3-phenyl-2,2-bis-(trimethylsilyl)-pentasilane D

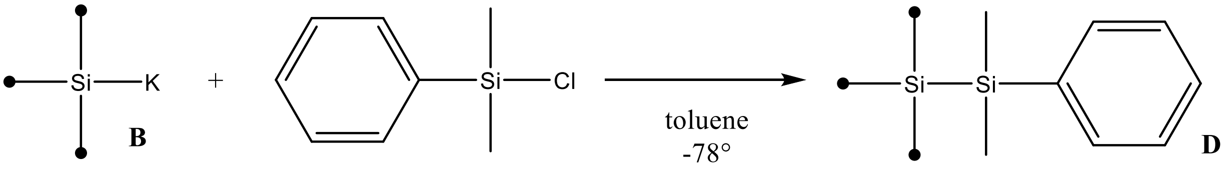

Figure 40: Synthesis of 1,1,1,3,3-pentamethyl-3-phenyl-2,2-bis-(trimethylsilyl)-pentasilane D

Table 8: Synthesis of 1,1,1,3,3-pentamethyl-3-phenyl-2,2-bis-(trimethylsilyl)-pentasilane D

Substance	**Molar Weight [g/mol]**	**Density [g/cm³]**	**Mass [g]**	**Mole**	**Volume [ml]**
Hyp-K (B)	286.66	x	9.20	32.1 mmol	x
Dimethylphenyl-chlorosilane	170.71	1.017	6.03	35.3	5.93
Toluene	92.14	0.867	x	x	25

a.) Into a 100 ml Schlenk, with a magnetic stir bar, 30 ml of toluene were transferred and 5.93 ml of dimethylphenylchlorosilane were added. The solution was cooled to -78 °C with an ethanol/nitrogen bath and 9.2 g **B** dissolved in toluene transferred slowly to the reaction vessel with a filter cannula.

b.) A 100 ml Schlenk, with a magnetic stir bar, with 9.2 g **B** dissolved in 30 ml of toluene was cooled to -78 °C with an ethanol/nitrogen bath and 5.93 ml of dimethylphenylchlorosilane were added dropwise *via* a syringe.

The colorless liquid turned yellowish and a fine precipitate (potassium chloride) formed. After the addition was finished the reaction was allowed to warm to room temperature and stirred for 24 h. In a 200 ml two-necked flask 100 ml 1 M sulphuric acid was degassed with nitrogen for at least 1 h, then the acidic solution was cooled to 0 °C with an ice bath and the reaction mixture added with a cannula. The mixture was extracted three times with diethylether and the combined organic phases were dried over sodium sulphate. The solvent was evaporated and a colorless oil remained.

Yield: a. 7.60 g | 60% | b. 12.30 g | 99%

^{29}Si NMR ($CDCl_3$, 293K): δ -134.1 ppm, -13.4 ppm, -9.8 ppm | **^{1}H NMR ($CDCl_3$, 293K):** δ 7.52 ppm (m, 2 H), 7.17 ppm (m, 3 H), 0.51 ppm (s, 6 H), 0.21 ppm (s, 27 H)

3.3.1 Synthesis of 1,1,1,3,3-pentamethyl-2,2-bis-(trimethylsilyl)-pentasilyl-trifluoromethanesulfonate E

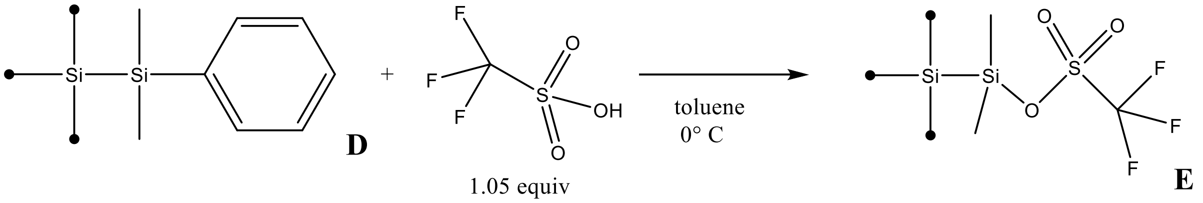

Figure 41: Synthesis of 1,1,1,3,3-pentamethyl-2,2-bis-(trimethylsilyl)-pentasilyl- trifluoromethanesulfonate E

Table 9: Synthesis of 1,1,1,3,3-pentamethyl-2,2-bis-(trimethylsilyl)-pentasilyl- trifluoromethanesulfonate E

Substance	Molar Weight [g/mol]	Density [g/cm³]	Mass [g]	Mole	Volume [ml]
$C_{17}H_{38}Si_5$ (D)	382.91	x	12.3	32 mmol	x
Trifluoromethanesulfonic acid	150.08	1.71	5.08	33.9 mmol	2.97
Toluene	92.14	0.867	x	X	30

Into a 100 ml Schlenk with a magnetic stir bar, 12.3 g of **D** dissolved in 30 ml of toluene were transferred. The solution was cooled to 0 °C with an ice bath and 2.97 ml trifluoromethanesulfonic acid (**triflat**) slowly added with syringes. A maximum of 0.5 ml of triflat should be used per syringe, since the acid destroys the syringes otherwise. Upon complete addition the reaction was allowed to warm to room temperature and stirred for another 20 h. The product formation was controlled by NMR-spectroscopy. The reaction solution was used without further purification for the next reaction step.

Yield: ~ 99%

^{29}Si NMR (C6D6, 293K): δ -134.4 ppm, -10.4 ppm, 56.4 ppm

3.3.2 Synthesis of 1,1,1,3,3,5,5,5-octamethyl-2,2,4,4-tetrakis(trimethylsilyl)-pentasilane F

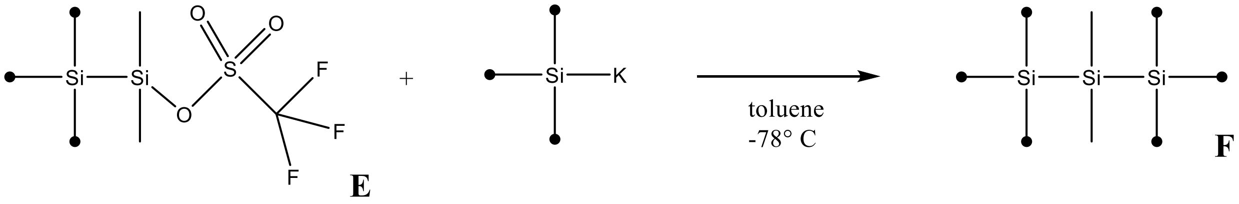

Figure 42: Synthesis of 1,1,1,3,3,5,5,5-octamethyl-2,2,4,4-tetrakis(trimethylsilyl)-pentasilane F

Table 10: Synthesis of 1,1,1,3,3,5,5,5-octamethyl-2,2,4,4-tetrakis(trimethylsilyl)-pentasilane F

Substance	Molar Weight [g/mol]	Density [g/cm³]	Mass [g]	Mole	Volume [ml]
$C_{12}H_{33}O_3F_3SSi_5$ (E)	454.88	x	14.68	32 mmol	x
Hyp-K (B)	286.66	x	10.18	35.2 mmol	x
Toluene	92.14	0.867	x	x	30

Into a 100 ml Schlenk, with a magnetic stir bar, 14.68 g of **E** dissolved in 30 ml of toluene were transferred. The solution was cooled to -78 °C with an ethanol/nitrogen bath and 10.18 g of freshly synthesized **B** dissolved in 30 ml of toluene were slowly added *via* cannula transfer. After the addition was finished, the reaction was allowed to warm to room temperature and stirred for another 20 h. During this time a white precipitate (potassium-triflate) was formed. In a 200 ml two-necked flask 100 ml of aqueous 1 M H_2SO_4 was degassed with nitrogen for at least 1 h, then the acidic solution was cooled to 0 °C with an ice bath and the reaction mixture added with a filter cannula. The mixture was extracted three times with diethylether and the combined organic phases dried over sodium sulphate. The solvent was evaporated and a colorless oil remained. After recrystallisation from ethanol/ethyl acetate white crystals formed.

Yield: 7.6 g | 43 %

^{29}Si NMR (C6D6, 293K): δ -118.9 ppm, -26.2 ppm, -9.6 ppm | **^{1}H NMR ($CDCl_3$, 293K):** δ 0.47 (s, 6 H), 0.21 (s, 54 H) | **^{13}C NMR ($CDCl_3$, 293K):** δ 5.72 ppm, 4.05 ppm | **mp:** 171-172 °C

3.4 Synthesis of 1,1,1,3,3,5,5,5-octamethyl-2,4-bis(trimethylsilyl)-pentasilyl-2,4-dipotassium G

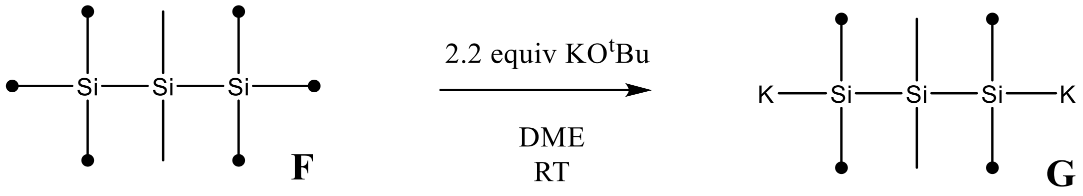

Figure 43: Synthesis of 1,1,1,3,3,5,5,5-octamethyl-2,4-bis(trimethylsilyl)-pentasilyl-2,4-dipotassium G

Table 11: Synthesis of 1,1,1,3,3,5,5,5-octamethyl-2,4-bis(trimethylsilyl)-pentasilyl-2,4-dipotassium G

Substance	Molar Weight [g/mol]	Density [g/cm³]	Mass [g]	Mole	Volume [ml]
$C_{20}H_{60}Si_9$ (F)	553.46	x	4	7 mmol	x
KO^{t}Bu	112.21	x	1.78	15.9 mmol	x
DME	90.12	0.87	x	x	30

Into a 50 ml Schlenk, with a magnetic stir bar, 4 g of **F** were weighed and afterwards evaporated with cautious heating three times. Then the Schlenk was transferred into the glovebox and 1.78 g **KO^{t}Bu** were added. After 30 ml of **DME** were added with a syringe, the yellow solution was stirred for 48 hours. During this time the color changed to dark green. To get rid of the formed silylether, the solution was then evaporated and the residue diluted in 30 ml of toluene. The conversion was then controlled by NMR-spectroscopy and the product was used directly for the next synthesis.

Yield: ~99%

^{29}Si NMR (D_2O, 293K): δ -172.2 ppm, -16.7 ppm, -4.6 ppm | **^{1}H NMR (C_6D_6, 293K):** δ 0.86 ppm (s, 6H), 0.46 ppm (s, 36H) | **^{13}C NMR (C_6D_6, 293K):** δ 8.45 ppm, 2.22 ppm

3.4.1 Synthesis of ((dimethylsilanediyl)bis(1,1,1,3,3,3-hexamethyl-trisilane-2,2-diyl))bis(tert-butylchlorophosphane) H

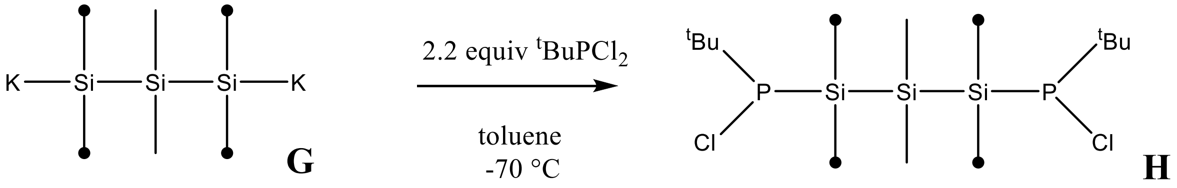

Figure 44: Synthesis of ((dimethylsilanediyl)bis(1,1,1,3,3,3-hexamethyl-trisilane-2,2-diyl))bis(tert-butylchlorophosphane) H

Table 12: Synthesis of ((dimethylsilanediyl)bis(1,1,1,3,3,3-hexamethyl-trisilane-2,2-diyl))bis(tert-butylchlorophosphane) H

Substance	**Molar Weight [g/mol]**	**Density [g/cm³]**	**Mass [g]**	**Mole**	**Volume [ml]**
$C_{14}H_{42}K_2Si_7$ [G]	484.09	x	0.218	0.45 mmol	x
$^tBuPCl_2$	157.98	x	0.156	0.99 mmol	x
Toluene	92.14	0.867	x	x	3

Into a 10 ml Schlenk, with a magnetic stir bar, 0.218 g of **G** were weighed evaporated with cautious heating three times and dissolved in 3 ml of toluene. The solution was cooled to -78 °C with an ethanol/nitrogen bath and 0.99 ml (1 mol/l solution) of *tert*-butyldichlorophosphine were slowly added *via* syringe. Upon complete addition the reaction was stirred for 2 h. During this time a white precipitate (potassium-chloride) was formed. Then the solution was separated from the chloride with a filter cannula and the colorless liquid was stored in the fridge at -30 °C. The reaction was controlled *via* NMR-spectroscopy but no formation of the desired product could be observed.

3.5 Synthesis of 1,1,1,3,3,5,5,5-octamethyl-2,4-bis-(trimethylsilyl)-pentasilyl-2,4-dihydride I

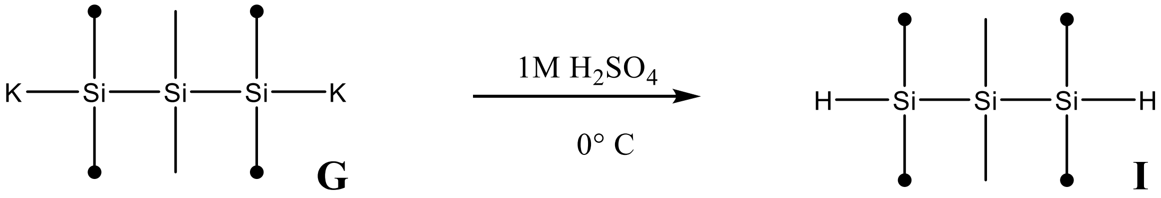

Figure 45: Synthesis of 1,1,1,3,3,5,5,5-octamethyl-2,4-bis-(trimethylsilyl)-pentasilyl-2,4-dihydride I

Table 13: Synthesis of 1,1,1,3,3,5,5,5-octamethyl-2,4-bis-(trimethylsilyl)-pentasilyl-2,4-dihydride I

Substance	Molar Weight [g/mol]	Density [g/cm³]	Mass [g]	Mole	Volume [ml]
$C_{14}H_{42}K_2Si_7$ [G]	484.09	x	3.39	7 mmol	x
Toluene	92.14	0.867	x	x	30

In a 100 ml two-necked flask 50 ml 1 M sulphuric acid was degassed with nitrogen for at least 1 h, then the acidic solution was cooled to 0 °C with an ice bath and 3.39 g **G** dissolved in 30 ml of toluene was added with a cannula. The mixture was extracted three times with diethylether and the combined organic phases dried over sodium sulphate. The solvent was evaporated and a yellowish oil remained. The product was crystallized from acetone and put into the fridge at -30 °C. White crystals precipitated.

Yield: 2.30 g | 80%

^{29}Si NMR ($CDCl_3$, 293K): δ -109.43 ppm, -36.0 ppm, -11.2 ppm | **^{1}H NMR (C_6D_6, 293K):** δ 2.66 (s, 2H), 0.45 (s, 6 H) 0.27 ppm (s, 36 H) | **^{13}C NMR (C_6D_6, 293K):** δ 2.46 ppm, 1.32 ppm | **mp:** 45-47 °C

3.5.1 Synthesis of 1,1,1,3,3,5,5,5-octamethyl-2,4-bis(trimethylsilyl)-pentasilyl-2,4-dichloride J

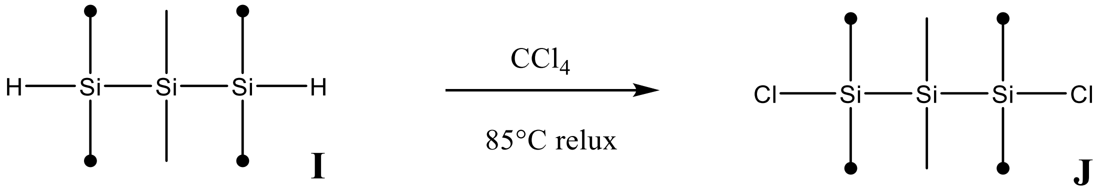

Figure 46: Synthesis of 1,1,1,3,3,5,5,5-octamethyl-2,4-bis(trimethylsilyl)-pentasilyl-2,4-dichloride J

Table 14: Synthesis of 1,1,1,3,3,5,5,5-octamethyl-2,4-bis(trimethylsilyl)-pentasilyl-2,4-dichloride J

Substance	Molar Weight [g/mol]	Density [g/cm³]	Mass [g]	Mole	Volume [ml]
$C_{14}H_{44}Si_7$ [I]	409.1	x	2.3	5.6 mmol	x
Carbontetrachloride	153.82	1.59	x	x	15

Into a 50 ml Schlenk, with a magnetic stir bar, 2.3 g of **I** were weighed, evaporated three times under cautious heating, then 15 ml carbontetrachloride (**CCl_4**) were added. The solution was heated with an oilbath to 85 °C and stirred for 48 h. Then the **CCl_4** was evaporated with a membrane pump. During this process white crystals formed on the vessel wall. Those crystals could be identified as hexachloroethane. The remaining colorless liquid was measured *via* NMR-spectroscopy showing in a mixture different silanes. Due to the loss of shift of the central silicon atom, the reaction destroyed the chain.

Yield: unknown

3.5.2 Synthesis of 1,1,1,3,3,5,5,5-octamethyl-2,4-bis(trimethylsilyl)-pentasilyl-2,4-dichloride J

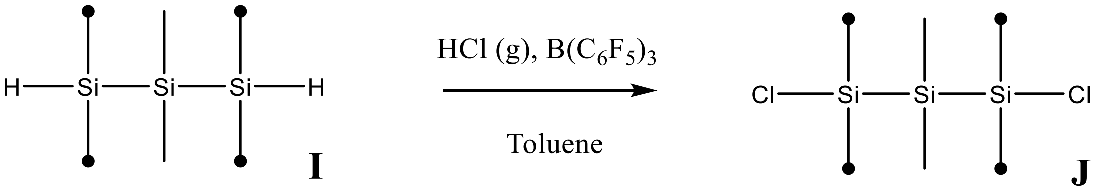

Figure 47: Synthesis of 1,1,1,3,3,5,5,5-octamethyl-2,4-bis(trimethylsilyl)-pentasilyl-2,4-dichloride J Route 2

Table 15: Synthesis of 1,1,1,3,3,5,5,5-octamethyl-2,4-bis(trimethylsilyl)-pentasilyl-2,4-dichloride J Route 2

Substance	Molar Weight [g/mol]	Density [g/cm³]	Mass [g]	Mole	Volume [ml]
$C_{14}H_{44}Si_7$ [I]	409.1	x	0.5	1.2 mmol	x
$B(C_6F_5)_3$	511.98	x	0.06	0.12 mmol	x
NaCl	58.44	x	0.7	12 mmol	x
Toluene	92.14	0.87	x	x	10

Into a 50 ml Schlenk, with a magnetic stir bar, 0.5 g of **I** were weighed, evaporated three times under cautious heating, then 9 ml toluene were added. Then 0.06 g of borane was weighed into a vial in the glovebox, dissolved in 1 ml of toluene and added to the reaction mixture. In a 50 ml Schlenk 0.7 g of sodium chloride (**NaCl**) were weighed and evaporated three times under cautious heating. The silane vessel was then cooled to -95 °C and connected to the NaCl vessel. 10 ml of concentrated sulphuric acid was then dropped slowly on the NaCl and the formed hydrogen chloride gas bubbled through the silane solution. After the gas formation finished the reaction mixture was allowed to room temperature and stirred for 20 h. The remaining colorless liquid was measured *via* NMR-spectroscopy showing just the dihydride peaks. No reaction took place.

Yield: unknown

3.5.3 Synthesis of 1,1,1,3,3,5,5,5-octamethyl-2,4-bis(trimethylsilyl)-pentasilyl-2,4-dichloride J

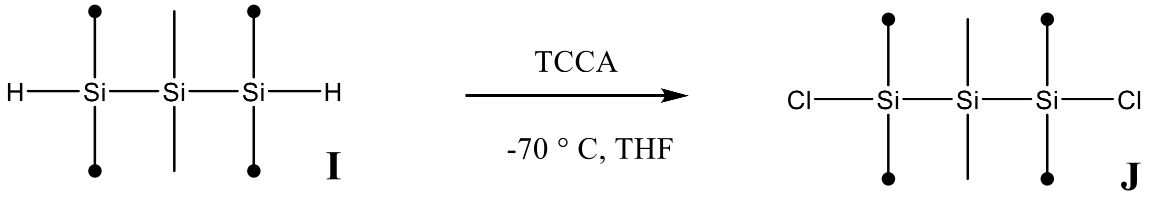

Figure 48: Synthesis of 1,1,1,3,3,5,5,5-octamethyl-2,4-bis(trimethylsilyl)-pentasilyl-2,4-dichloride J Route 3

Table 16: Synthesis of 1,1,1,3,3,5,5,5-octamethyl-2,4-bis(trimethylsilyl)-pentasilyl-2,4-dichloride J Route 3

Substance	**Molar Weight [g/mol]**	**Density [g/cm³]**	**Mass [g]**	**Mole**	**Volume [ml]**
$C_{14}H_{44}Si_7$ [I]	409.1	x	1.54	3.6 mmol	x
TCCA	232.41	x	0.6	2.68 mmol	x
THF	72.11	0.899	x	x	20

Into a 50 ml Schlenk, with a magnetic stir bar, 1.54 g of **I** were weighed, evaporated three times under cautious heating, then 20 ml tetrahydrofuran (**THF)** were added. The solution was then cooled to -70 °C with an ethanol/nitrogen bath and 0.6 g of **TCCA** were slowly added. The reaction was allowed to warm to room temperature and stirred for another 20 h. A white precipitate of **TCCA** and **TCCH** formed out of the pale yellow solution and was separated *via* filter cannula. The solvent was evaporated and a yellow waxy substance remained. This substance was diluted in 20 ml of pentane. A clear yellow solution and a white precipitate (remaining **TCCA**) formed. The solution was separated from the precipitate *via* filter cannula and the solvent was evaporated. A yellow oil remained. The NMR spectra showed a mixture of different inseparable silanes.

Yield: unknown

3.5.4 Synthesis of 1,1,1,3,3,5,5,5-octamethyl-2,4-bis(trimethylsilyl)-pentasilyl-2,4-dichloride J

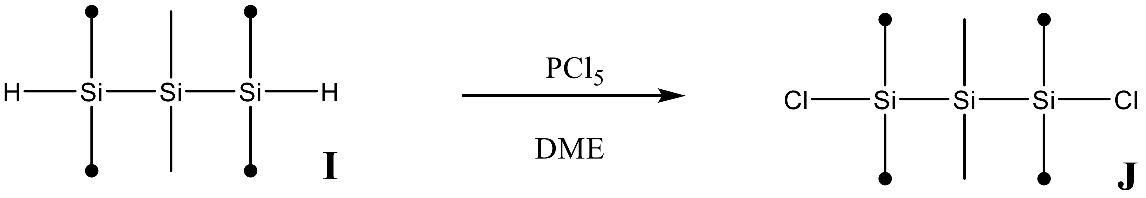

Figure 49: Synthesis of 1,1,1,3,3,5,5,5-octamethyl-2,4-bis(trimethylsilyl)-pentasilyl-2,4-dichloride J Route 4

Table 17: Synthesis of 1,1,1,3,3,5,5,5-octamethyl-2,4-bis(trimethylsilyl)-pentasilyl-2,4-dichloride J Route 4

Substance	**Molar Weight [g/mol]**	**Density [g/cm³]**	**Mass [g]**	**Mole**	**Volume [ml]**
$C_{14}H_{44}Si_7$ [I]	409.1	x	0.4	0.977 mmol	x
PCl_5	208.24	x	0.23	1.07 mmol	x
DME	90.12	0.87	x	x	5

Into a 50 ml Schlenk, with a magnetic stir bar, 0.4 g of **I** were weighed, evaporated three times under cautious heating, then 5 ml **DME** were added. Then 0.23 g of **PCl_5** were slowly added. The reaction was stirred for 20 h at room temperature. A mixture of the mono- and dichlorinated species was observed *via* NMR spectroscopy. To obtain full chlorination additional 0.5 g **PCl_5** were added to the solution and the solution was stirred for another 48 h. The NMR showed full conversion to the dichlorinated product. The side products (PCl_3, PCl_5, $OPCl_3$) were then evaporated together with the solvent under reduced pressure at 50 °C. The product remained as a high viscous grey liquid.

Yield: 0.44 g | 94 %

^{29}Si NMR (C_6D_6, 293K): δ -8.7 ppm, -10.4 ppm, -27.2 ppm

3.6 Synthesis of tris(trimethylsilyl)chlorosilane K

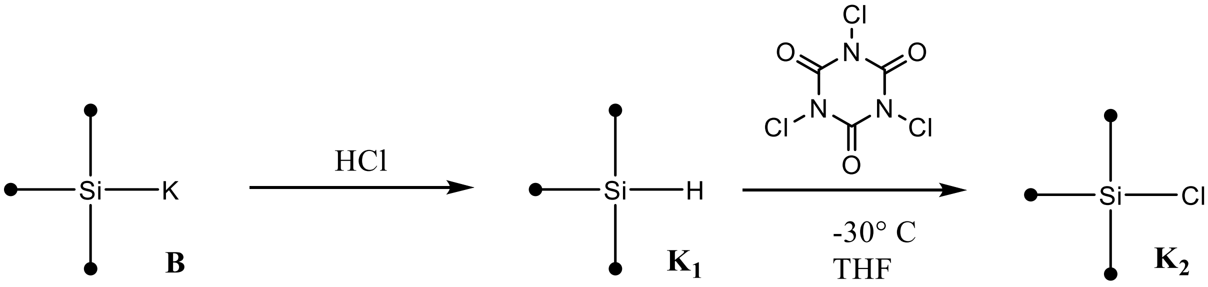

Figure 50: Synthesis of tris(trimethylsilyl)chlorosilane K

Table 18: Synthesis of tris(trimethylsilyl)chlorosilane K

Substance	**Molar Weight [g/mol]**	**Density [g/cm³]**	**Mass [g]**	**Mole**	**Volume [ml]**
Hyp-K (B)	286.66	x	4.47	15.6 mmol	x
Hyp-H (K_1)	248.66	x	2.3	9.3 mmol	x
TCCA	232.41	x	1.07	4.65 mmol	x
THF	72.11	0.899	x	x	30

In a 200 ml two-necked flask 100 ml 1 M sulphuric acid was degassed with nitrogen for at least 1 h, then the acidic solution was cooled to 0 °C with an ice bath and 4.47 g **B** dissolved in 30 ml of toluene was added *via* cannula. The mixture was extracted three times with diethylether and the combined organic phases were dried over sodium sulphate. The solvent was evaporated and a colorless oil remained.

Yield: 2.3 g | 59 % tris(trimethylsilyl)silane (**Hyp-H | K_1**)

Into a 100 ml Schlenk, with a magnetic stir bar, 2.3 g of **K$_1$** were weighted, evaporated three times under cautious heating, and 30 ml **THF** were added. The solution was then cooled to -30 °C with an ethanol/nitrogen bath and 1.07 g of **TCCA** slowly added. The reaction was allowed to warm to room temperature and was stirred for another 20 h. Then the solvent was evaporated and 30 ml of pentane were added. The remaining **TCCA** and the produced cyanuric acid (**TCCH**) precipitated as a white solid. The reaction solution was transferred *via* filter cannula into a 50 ml Schlenk and the solvent evaporated. The product remained as a yellowish oil.

Yield: 2.6 g | ~98%

^{29}Si NMR (C_6D_6, 293K): δ -13.3 ppm, -11.6 ppm

3.7 Synthesis of tris(trimethylsilyl)phenylsilane L

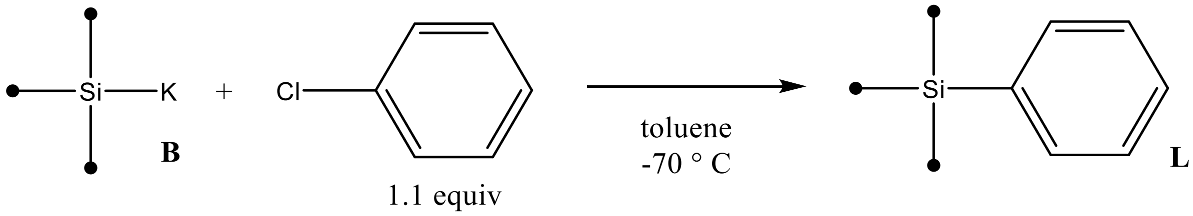

Figure 51: Synthesis of tris(trimethylsilyl)phenylsilane L

Table 19: Synthesis of tris(trimethylsilyl)phenylsilane L

Substance	Molar Weight [g/mol]	Density [g/cm³]	Mass [g]	Mole	Volume [ml]
Hyp-K (B)	286.66	x	4.47	15.6 mmol	x
Chlorobenzene	112.56	1.11	1.93	17.2	1.74
Toluene	92.14	0.87	x	x	10

A 50 ml Schlenk, with a magnetic stir bar, with 4.47 g **B** dissolved in 10 ml of toluene was cooled to -78 °C with an ethanol/nitrogen bath and 1.74 ml of chlorobenzene were added dropwise *via* syringe. The solution was then allowed to warm to room temperature and stirred for 20 h. A color change of the solution from colorless to red took place, but the NMR-measurements showed no conversion of the educts.

Yield: no reaction

3.8 Synthesis of benzyl-tris(trimethylsilyl)silane M

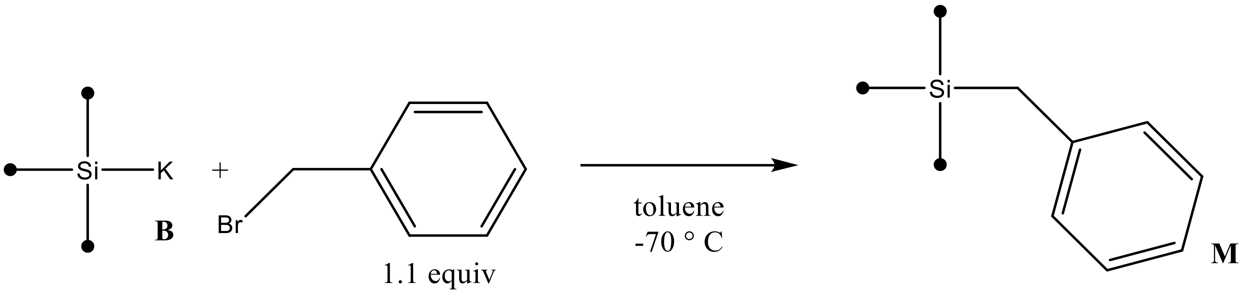

Figure 52: Synthesis of benzyl-tris(trimethylsilyl)silane M

Table 20: Synthesis of benzyl-tris(trimethylsilyl)silane M

Substance	Molar Weight [g/mol]	Density [g/cm³]	Mass [g]	Mole	Volume [ml]
Hyp-K (B)	286.66	x	2.68	9.35 mmol	x
Benzylbromide	171.04	1.44	1.75	10.28 mmol	1.22
Toluene	92.14	0.87	x	x	5

A 50 ml Schlenk, with a magnetic stir bar, with 2.68 g **B** dissolved in 5 ml of toluene was cooled to -78 °C with an ethanol/nitrogen bath and 1.22 ml of benzylbromide were added dropwise *via* a syringe. The solution was allowed to warm to room temperature and stirred for 20 h. A white precipitate (potassiumbromide) formed out of the colorless liquid and was separated from the liquid *via* celite filtration.

Yield: ~99%

^{29}Si NMR (D_2O, 293K): δ -77.4 ppm, -13.01 ppm

3.8.1 Synthesis of tris(trimethylsilyl)-trifluoromethanesulfonyl-silane N

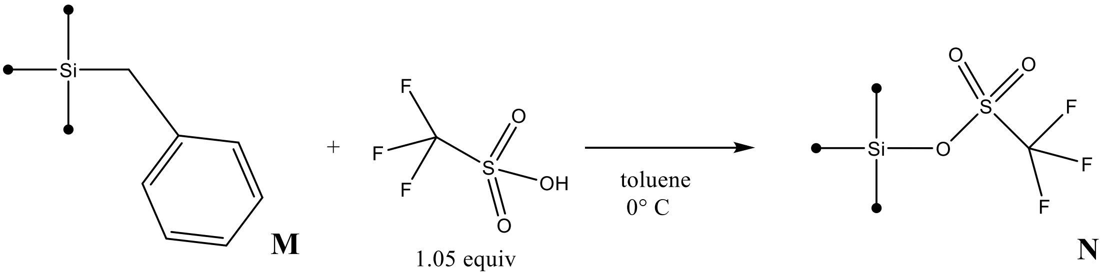

Figure 53: Synthesis of tris(trimethylsilyl)-trifluoromethanesulfonyl-silane N

Table 21: Synthesis of tris(trimethylsilyl)-trifluoromethanesulfonyl-silane N

Substance	Molar Weight [g/mol]	Density [g/cm³]	Mass [g]	Mole	Volume [ml]
$C_{16}H_{34}Si_4$ (M)	338.79	x	3.17	9.35 mmol	x
Trifluoromethanesulfonic acid	150.08	1.71	1.47	9.81 mmol	0.86
Toluene	92.14	0.867	x	x	5

Into a 50 ml Schlenk, with a magnetic stir bar, 3.17 g of **M** dissolved in 5 ml of toluene were transferred. The solution was cooled to 0 °C with an ice bath and 0.86 ml **triflate** slowly added with syringes. After the addition was finished the reaction was allowed to warm up to room temperature and stirred for another 20 h. The product formation was controlled with NMR-spectroscopy but no production formation could be detected.

Yield: 0%

3.9 Synthesis of trisodium phosphide O

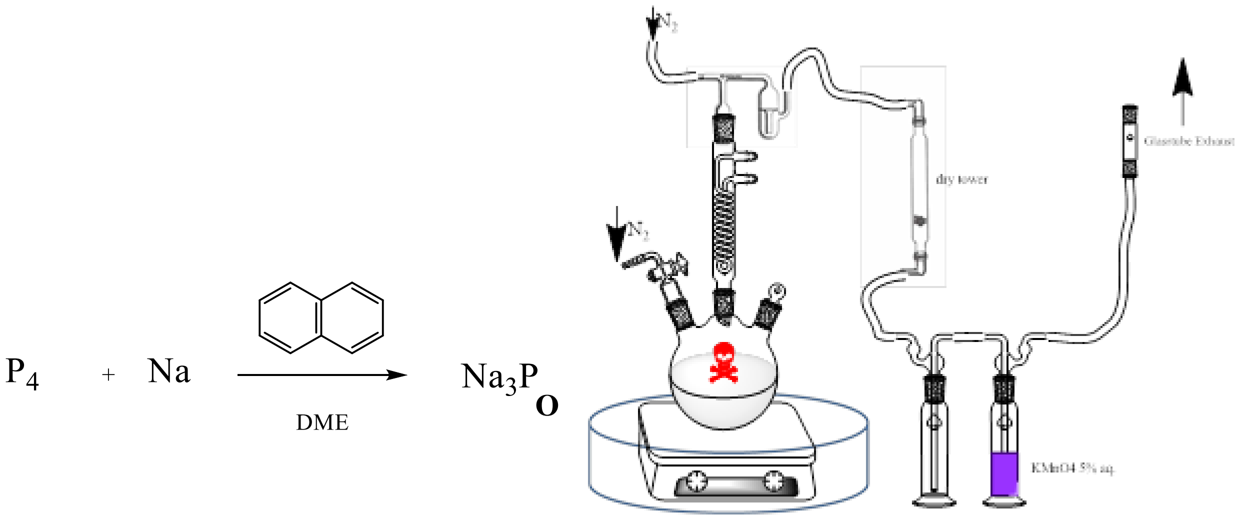

Figure 54: Synthesis of trisodium phosphide O

Table 22: Synthesis of trisodium phosphide O

Substance	Molar Weight [g/mol]	Density [g/cm^3]	Mass [g]	Mole	Volume [ml]
Sodium	22.98	x	8.642	375.9 mmol	x
Red Phosphorus	30.97	x	4.012	125.6 mmol	x
Naphthalene	128.17	x	1.612	12.56 mmol	x
DME	90.12	0.87	x	x	60

Into a 500 ml three-necked round bottom flask, with a magnetic stir bar and a reflux condenser, 4.01 g of red phosphorus were weighed and the flask evaporated three times under cautious heating. Then a bubbler, connected to two safety wash bottles filled with 5% aqueous potassium permanganate (**$KMnO_4$**) solution, was added to the reflux condenser. Afterwards 55 ml of **DME** were added and 1.61 g of naphthalene dissolved in 5 ml of **DME** were transferred to the red reaction solution. 8.64 g of sodium (**Na**) were cut into small pieces dabbed with **DME** and added to the stirring reaction mixture. The color changed from red to a black suspension. The mixture was then stirred at room temperature for another 20 h. The remaining naphthalene was dissolved in 200 ml of **DME** and separated from the product *via* filter cannula. The remaining solvent was evaporated from the black solid.

No yield was determined, but due to no residual red phosphorus, nearly 100% were assumed and the whole product was used for the next step.

3.9.1 Synthesis of alkoxy packed sodium phosphide P

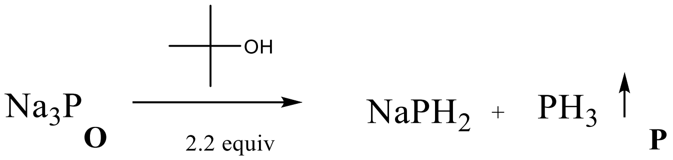

Figure 55: Synthesis of alkoxy packed sodium phosphide P

Table 23: Synthesis of alkoxy packed sodium phosphide P

Substance	Molar Weight [g/mol]	Density [g/cm³]	Mass [g]	Mole	Volume [ml]
Na_3P (O)	99.91	x	12.54	125.6 mmol	x
***tert*-butanol**	74.12	0.77	20.48	276.3 mmol	26.6
DME	90.12	0.87	x	x	60

Into a 500 ml three-necked round bottom flask with a magnetic stir bar and a reflux condenser equipped with a bubbler connected to two safety wash bottles filled with 5% aq. **$KMnO_4$** solution, 12.54 g of **O** dispensed in 60 ml of **DME** were transferred. Then 26.6 ml of *tert*-butanol were added *via* a septum and a syringe. The solution was stirred with a warm water bath for 20 h during which a color change from black to a light brown suspension took place. Afterwards the solution was transferred *via* filter cannula into a 100 ml Schlenk. The solvent of the yellow solution was then evaporated with the help of an extra cooling trap due to the dangerous phosphine gas. The product remained as a pale yellow solid.

Yield: 17.5 g | >100%

Due to the formation of sodium *tert*-butanolate, which has the same solubility as our desired product, a higher yield than 100% was obtained. The two components remained inseparable.

^{31}P NMR (D_2O, 293K): δ -292.3 ppm ($^{1}J_{PH}$ = 143.4 Hz)

3.9.2 Synthesis of sodium phosphide Q

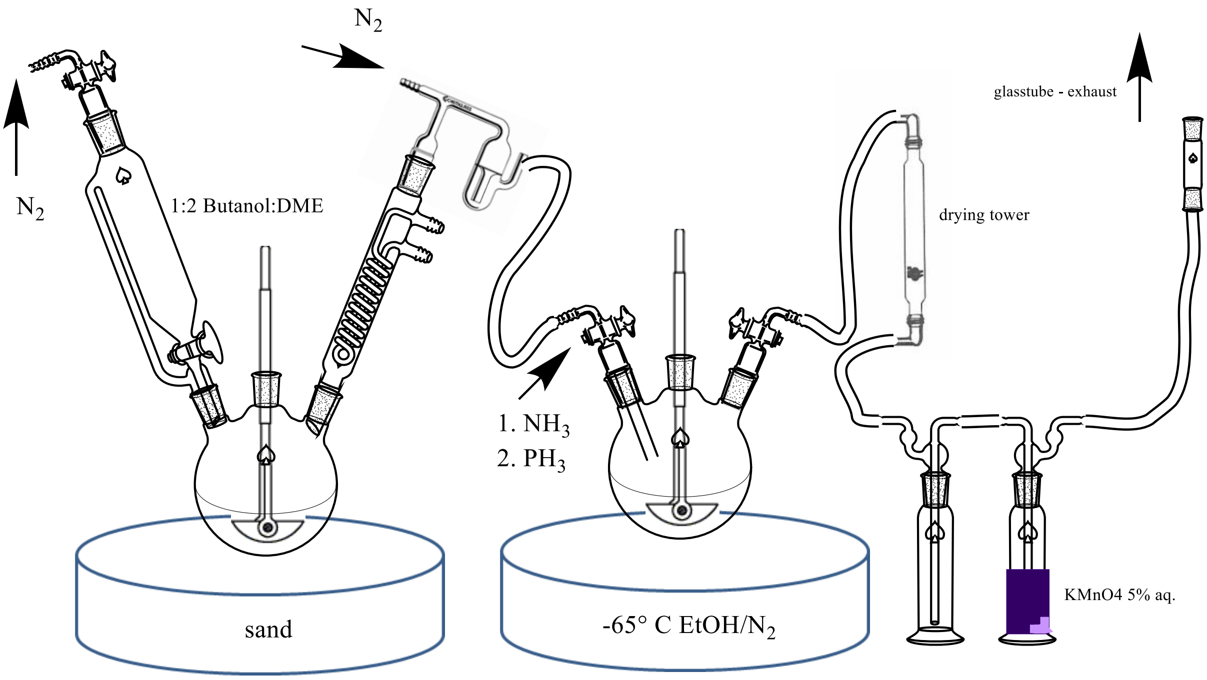

$$Na/NH_3 + PH_3 \longrightarrow \underset{\textbf{Q}}{NaPH_2}$$

Figure 56: Synthesis of alkoxy packed sodium phosphide P

Table 24: Synthesis of alkoxy packed sodium phosphide P

Substance	Molar Weight [g/mol]	Density [g/cm³]	Mass [g]	Mole	Volume [ml]
Sodium	22.98	x	11.03	0.48	x
Ammonia	17.03	0.77	x	x	550
Phosphine	34.00	1.53	x	~0.6	x
Butanol	74.12	0.81	148	1.98	183
DME	90.12	0.87	x	x	366

In a 2000 ml three-necked round bottom flask, 0.6 mol of Na_3P (**O**) were produced, and kept in **DME**. This reagent was used for *in situ* formation of phosphine (**PH_3**), and 20% excess were used.

A second 2000 ml three-necked round bottom flask, equipped with a mechanical stirrer and a bubbler, was cooled to -65 °C with an ethanol/nitrogen bath and 550 ml of ammonia (**NH_3**) condensed into it. Then 11.03 g of sodium were dissolved in the solution, which turned from colorless to dark blue.

A 1000 ml dropping funnel was equipped to the flask containing **O** and filled with 500 ml of a butanol/**DME** mixture (183/366 ml). The bubbler of the flask containing the butanol/ammonia solution was then connected to two safety wash bottles filled with 5% aq. **$KMnO_4$** solution. The alcohol solution was then slowly dripped onto the black suspension of **O**. White smears formed and the evolving **PH_3** was funnelled into the sodium/ammonia mixture. During the alcohol addition the suspension turned from black to grey to white. The reaction was finished when the blue ammonia solution turned colorless. Then the flask was allowed to warm up to room temperature and the ammonia was evaporated over 20 h. Product remained as a pale yellow solid and the remaining ammonia residue was further evaporated with a vacuum pump.

Yield: 11 g | 40 %

^{31}P NMR (D_8-THF, 293K): δ -299.6 ppm ($^{1}J_{PH}$ = 147.2 Hz)

3.10 Synthesis of 1,1,1,3,3,5,5,5-octamethyl-2,4-bis(trimethylsilyl)-pentasilyl-2,4-bis(phenylphosphine) R

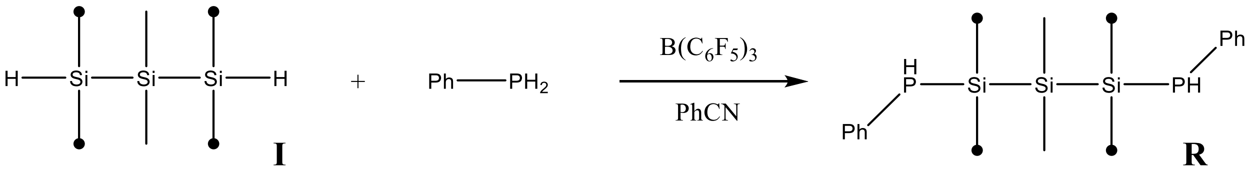

Figure 57: Synthesis of 1,1,1,3,3,5,5,5-octamethyl-2,4-bis(trimethylsilyl)-pentasilyl-2,4-bis(phenylphosphine) R

Table 25: Synthesis of 1,1,1,3,3,5,5,5-octamethyl-2,4-bis(trimethylsilyl)-pentasilyl-2,4-bis(phenylphosphine) R

Substance	Molar Weight [g/mol]	Density [g/cm³]	Mass [g]	Mole	Volume [ml]
$C_{14}H_{44}Si_7$ [I]	409.1	x	0.12	0.3 mmol	x
$B(C_6F_5)_3$	511.98	x	0.005	0.01 mmol	x
PhCN	103.12	1.0	0.02	0.2 mmol	0.02
$PhPH_2$	110.1	1.001	0.022	0.2 mmol	0.02
C_6D_6	84.14	0.95	x	x	0.5

In a sealable NMR-tube 0.12 g of **I** and 0.005 g of $B(C_6F_5)_3$ were weighed and evaporated with cautious heating three times. The tube was then transferred to the glovebox and 0.5 ml of deuterated benzene (**C_6D_6**) and 0.02 ml of phenylphosphine (**$PhPH_2$**) were added. Then 0.02 ml of benzonitrile (**PhCN**) were added. After 20 h the reaction was controlled *via* NMR, but no product formation was observed.

Yield: 0 %

3.11 Synthesis of 1,1,1,3,3,5,5,5-octamethyl-2,4-bis(trimethylsilyl)-pentasilyl-2,4-diphosphine S

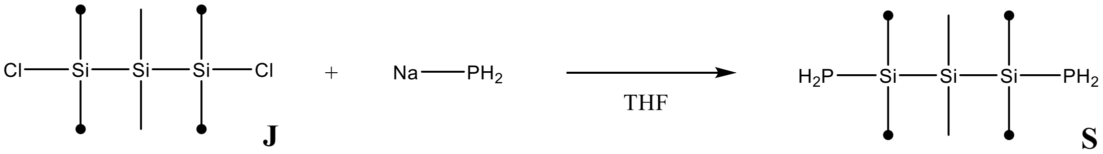

Figure 58: Synthesis of 1,1,1,3,3,5,5,5-octamethyl-2,4-bis(trimethylsilyl)-pentasilyl-2,4-diphosphine S

Table 26: Synthesis of 1,1,1,3,3,5,5,5-octamethyl-2,4-bis(trimethylsilyl)-pentasilyl-2,4-diphosphine S

Substance	**Molar Weight [g/mol]**	**Density [g/cm³]**	**Mass [g]**	**Mole**	**Volume [ml]**
$C_{14}H_{42}Cl_2Si_7$ [J]	477.9	x	0.44	0.92 mmol	x
$NaPH_2$-(0.5 DME)	101.04	x	0.204	2.02 mmol	x
THF	72.11	0.899	x	x	10

In a 50 ml Schlenk 0.204 g of $NaPH_2$ were weighed and 8 ml of **THF** were added. Then 0.44 g of **J** were dissolved in 2 ml of **THF** and added to the reaction solution. Immediately gas formation occurred, the temperature rose and a color change from yellow to orange took place. After 20 h the solvent was evaporated and 7 ml of **Et_2O** were added and the mixture stirred for another 20 h during which a white precipitate formed (**NaCl**). The liquid phase was separated *via* a syringe and the reaction was controlled *via* NMR. The product remained as a yellow oil.

Yield: 0.1 g | 23 %

^{31}P NMR (C_6D_6, 293K): δ -265.4 ppm ($^1J_{PH}$ = 179.3 Hz)

III. References

[1] V. Cappello, J. Baumgartner, A. Dransfeld and K. Hassler, *Eur. J. Inorg. Chem.,* p. 4589, 2006.

[2] C. J. H. Hendriksen, *Alkoxide Packaged Sodium Dihydrogenphosphide: Synthesis and Reactivity,* Dissertation ETH No. 20148, 2012.

[3] C. Marschner, *Eur. J. Inorg. Chem.,* p. 221, 1998.

[4] S. H. J. Lühr and A. Börner, *ChemCatChem,* vol. 3(11), p. 1708, 2011.

[5] F. Cheng, A. L. Hector, W. Levason, G. Reid, M. Webster and W. Zhang, *Inorg. Chem.,* no. 49(2), p. 752, 2010.

[6] M. Davis, W. Levason, G. Reid and M. Webster, *Dalton Trans.,* p. 2261, 2008.

[7] P. E. Goudriaan, P. W. N. van Leeuwen, M.-N. Birkholz and J. N. H. Reek, *Eur. J. Inorg. Chem.,* no. 2008(19), p. 2939, 2008.

[8] D. Lu and G. Salem, *Coord. Chem. Rev.,* no. 257(5-6), p. 1026, 2013.

[9] J. D. Andriamizaka, C. Couret, J. Escudie and J. Satge, *Phosphorus, Sulfur Silicon Relat. Elem.,* no. 12(3), p. 265, 1982.

[10] T. Gross, H. Reinke and H. Oehme, *Can. J. Chem.,* no. 78(11), p. 1399, 2000.

[11] M. Haas, J. Radebner, C. Winkler, R. Fischer, A. Torvisco and H. Stueger, *Organomet. Chem.,* no. 830, p. 131, 2017.

[12] C. Marschner, C. Kayser and G. Kickelbick, *Angew. Chem. Int. Ed.,* vol. 6, no. 41, p. 989, 2002.

[13] J. Baumgartner, D. Frank, C. Kayser and C. Marschner, *Organometallics,* vol. 24, no. 4, p. 750, 2005.

[14] A. Dzambaski, J. Baumgartner, M. Flock, G. Tekautz, K. Hassler and W. Hassler, *J. of Organomet. Chem.,* no. 691(15), p. 3362, 2006.

[15] P. C. J. Kamer and P. W. N. M. van Leeuwen, Phosphorus Ligand Effects in Homogeneous Catalysis and Rational Catalyst Design, John Wiley and Sons Ltd., 2012.

[16] C. von Hänisch, S. Traut and S. Stahl, *Z. anorg. allg. Chem.,* no. 633(13-14), p. 2199, 2007.

[17] C. von hänisch and E. Matern, *Z. anorg. allg. Chem.,* no. 631(9), p. 1655, 2005.

[18] W. S. Sheldrick and A. Borkenstein, *Acta Cryst, B,* no. B33(9), p. 2916, 1977.

[19] O. Stelzer, E. Unger and V. Wray, *Chem. Ber.,* no. 110(10), p. 3430, 1977.

[20] K. Hassler and S. Seidl, *Monatsh. Chem.,* no. 119(11), p. 1241, 1988.

[21] T. Chen, E. N. Duesler, R. T. Paine and H. Nöth, *Inorg. Chem.,* no. 38(22), p. 4993, 1999.

[22] T. Chen, J. Jackson, S. A. Jasper, E. Duesler, H. Nöth and R. T. Paine, *J. Organomet. Chem.,* no. 582(1), p. 25, 1999.

[23] S. K.-H. Thiele, V. M. Monroy, D. R. Wilson and H. Stoye, "Metal complex compositions and their use as catalysts to produce polydienes". Patent WO 2003033545 A2 20030424, 2003.

[24] S. K.-H. Thiele, V. M. Monroy and D. R. Wilson, "Random or block copolymers produced using metal complex catalysts". Patent WO 2002090394 A1 20021114, 2002.

[25] M. Kira, S. Ishida, T. Iwamoto and C. Kabuto, *J. Am. Chem. Soc.,* no. 121, p. 9722, 1999.

[26] H. Arp, J. Baumgartner, C. Marschner and T. Müller, *J. Am. Chem. Soc.,* no. 133, p. 5632, 2011.

[27] J. Hlina, J. Baumgartner, C. Marschner, L. Albers and T. Müller, *Organometallics,* no. 32(11), p. 3404, 2013.

[28] S. K. Müller, G. Weinberger, E. Schwarz, A. D. A. Torvisco, R. C. Fischer, K. Hassler and M. Flock, *Inorg. Chim. Acta,* no. 423A, p. 517, 2014.

[29] G. Leroy, D. R. Temsamani and C. Wilante, *J. Mol. Struct. (Theochem),* vol. 112(1), p. 21, 1994.

[30] G. Leroy, D. R. Temsamani, C. Wilante and J.-P. Dewispelaere, *J. Mol. Struct. (Theochem),,* no. 115(2), p. 113, 1994.

[31] G. Leroy, D. Riffi Temsamani, M. Sana and C. Wilante, *J. Mol. Struct. (Theochem),* no. 300, p. 373, 1993.

[32] B. J. Lynch and D. G. Truhlar, *J. Phys. Chem.,* vol. 105, p. 2936, 2001.

[33] Y. Zhao and D. G. Truhlar, *J. Chem. Phys.,* vol. 125, p. 1, 2006.

[34] D. Feller, *J. Comp. Chem.,* no. 17, p. 1571, EMSL/Jan 1996.

[35] M. Flock and A. Dransfeld, *Chem. Eur. J.,* no. 9, p. 3320, 2003.

[36] S. M. Whittaker, M.-C. Brun, F. Cervantes-Lee and K. H. Pannell, *J. Organomet. Chem.,* no. 499, p. 247, 1995.

[37] J. Y. Corey, D. M. Kraichely, J. L. Huhmann and A. Lindeberg, *Organometallics,* no. 14, p. 2704, 1995.

[38] W. Uhlig, *Chem. Ber.,* no. 129, p. 733, 1996.

[39] S. Varaprath and D. H. Stutts, *J. Organomet. Chem.,* no. 692, p. 1892, 2007.

[40] R. Dobrovetsky and K. Chulsky, *Angew. Chem. Int. Ed.,* no. 56, p. 4744, 2017.

[41] B. J. Albert and H. Yamamoto, *e-EROS Encyclopedia of Reagents for Organic Synthesis,* Vols. 1-2, 2011.

[42] G. Müller, M. Zaliera, G. Gscheidt, A. Rosenthal, G. Santiso-Quinones, K. Dietliker and H. Grützmacher, *Marcomol. Rapid Commun.,* no. 36(6), p. 553, 2015.

[43] D. J. Peterson and T. J. Logan, *J. Inorg. Nucl. Chem.,* no. 28, p. 53, 1966.

[44] P. Kasak, V. B. Arion and M. Widhalm, *Tetrahedron Letters,* no. 48(32), p. 5665, 2007.

[45] E. C. Evers, *J. Am. Chem. Soc.,* no. 73, p. 2038, 1951.

[46] L. Brandsma, N. K. Gusarova, A. V. Gusarov, H. D. Verkruijsse and B. A. Trofimov, *Synthetic Commun,* no. 24, p. 3219, 1994.

[47] R. Appel and W. Paulen, *Angew. Chem.,* no. 93, p. 902, 1981.

[48] L. Wu, S. S. Chitnis, H. Jiao, V. T. Annibale and I. Manners, *J. Am. Chem. Soc.,* no. 139, p. 16780, 2017.

[49] M. J. Frisch, G. W. Trucks, H. B. Schlegel, G. E. Scuseria, M. A. Robb, J. R. Cheeseman, G. Scalmani, V. Barone, B. Mennucci, G. A. Petersson, H. Nakatsuji, M. Caricato, X. Li, H. P. Hratchian, A. F. Izmaylov, J. Bloino, G. Zheng, J. L. Sonnenberg, M. Hada, M. Ehara, K. Toyota, R. Fukuda, J. Hasegawa, M. Ishida, T. Nakajima, Y. Honda, O. Kitao, H. Nakai, T. Vreven, J. A. J. Montgomery, J. E. Peralta, F. Ogliarao, M. Bearpark, J. J. Heyd, E. Brothers, K. N. Kudin, V. N. Staroverov, T. Keith, R. Kobayashi, J. Normand, K. Raghavachari, A. Rendell, J. C. Burant, S. S. Iyengar, J. Tomasi, M. Cossi, N. Rega, J. M. Millam, M. Klene, J. E. Knox, J. B. Cross, V. Bakken, C. Adamo, J. Jaramillo, R. Gomperts, R. E. Stratmann, O. Yazyev, A. J. Austin, R. Cammi, C. Pomelli, J. W. Ochterski, R. L. Martin, K. Morokuma, V. G. Zakrzewski, G. A. Voth, P. Salvador, J. J. Dannenberg, S. Dapprich, A. D. Daniels, O. Farkas, J. B. Foresman, J. V. Ortiz, J. Cioslowski and D. J. Fox, *Gaussian 09, Revision D.01,* Gaussian, Inc., 2013.

[50] R. Fischer, D. Frank, W. Gaderbauer, C. Kayser, C. Mechtler, J. Baumgartner and C. Marschner, *Organometallics,* no. 22(18), p. 3723, 2003.

[51] W. Gaderbauer, M. Zirngast, J. Baumgartner, C. Marschner and T. D. Tilley, *Organometallics,* no. 25(10), p. 2599, 2006.

[52] K. Hassler, A. Dzambaski and J. Baumgartner, *Silicon Chemistry,* no. 3(6), p. 271, 2008.

[53] T. Iwamoto, Y. Furiya, H. Kobayashi, H. Isobe and M. Kira, *Organometallics,* no. 29(8), p. 1869, 2010.

[54] H. Wagner, J. Baumgartner and C. Marschner, *Organometallics,* vol. 24(19) , p. 4649, 2005.

[55] M. Zirngast, J. Baumgartner and C. Marschner, *Organometallics,* no. 27(24), p. 6472, 2008.

[56] H. Kobayashi, T. Iwamoto and M. Kira, *J. Am. Chem. Soc.,* no. 127(44), p. 15376, 2005.

IV. Appendix A

IV.1.1 Calculated structure of H_1

$C_{14}H_{44}Si_7$

Energy: -2586.4964528

Si	-1.907926	-0.01997	-0.496344
Si	0.076756	-1.04165	0.308347
Si	2.107756	-0.191641	-0.577061
H	-1.738803	0.228869	-1.967769
H	2.044192	-0.566004	-2.033263
Si	3.956926	-1.446181	0.232526
Si	2.43051	2.146844	-0.637282
Si	-3.672988	-1.607898	-0.574575
Si	-2.736117	1.931262	0.571506
C	0.044571	-0.870724	2.204873
H	0.87909	-1.405139	2.66929
H	0.106787	0.176121	2.518171
H	-0.884133	-1.285972	2.612971
C	0.070359	-2.901404	-0.088841
H	-0.822032	-3.390202	0.315542
H	0.105737	-3.089474	-1.16601
H	0.944316	-3.382423	0.364276
C	4.129284	-3.015711	-0.813819
H	3.231873	-3.640704	-0.769825
H	4.309389	-2.77046	-1.865662
H	4.974777	-3.618137	-0.460011
C	5.580861	-0.479254	0.092198
H	5.58251	0.413476	0.726263
H	6.415691	-1.114153	0.413555
H	5.781285	-0.162809	-0.936187
C	3.757863	-1.951456	2.048448
H	3.616799	-1.085296	2.703506
H	2.90831	-2.626241	2.19661
H	4.658491	-2.47866	2.385848
C	1.049146	2.927425	-1.672049
H	1.149997	2.623996	-2.719818
H	0.0507	2.62727	-1.343425
H	1.106545	4.021991	-1.635871
C	4.061581	2.56421	-1.506851
H	4.935033	2.255612	-0.925556
H	4.126311	2.087809	-2.490704
H	4.129723	3.6485	-1.659149
C	2.485056	2.894333	1.101582
H	2.61079	3.982476	1.050279
H	1.572386	2.691923	1.669094
H	3.328798	2.49187	1.673064
C	-3.998275	-2.441642	1.096671
H	-4.825274	-3.156312	1.0067
H	-3.122492	-2.99537	1.45113
H	-4.268898	-1.717541	1.871612
C	-5.272065	-0.767631	-1.15588
H	-6.07135	-1.512873	-1.251497
H	-5.622936	0.005321	-0.465293
H	-5.136396	-0.301718	-2.13783
C	-3.277529	-2.95007	-1.853423
H	-3.091653	-2.513067	-2.840254
H	-2.399536	-3.542265	-1.580528
H	-4.127536	-3.636976	-1.948504
C	-3.948293	1.434717	1.94211
H	-3.449695	0.851547	2.723914
H	-4.357709	2.335861	2.414738
H	-4.791648	0.845006	1.571691
C	-3.644675	2.96564	-0.727243
H	-2.96027	3.302858	-1.51264
H	-4.447296	2.397745	-1.208126
H	-4.091058	3.854317	-0.265107
C	-1.436278	3.022208	1.410593
H	-0.902406	2.478163	2.196326
H	-0.697675	3.423132	0.712427
H	-1.93919	3.873368	1.886167

IV.1.2 Calculated structure of H_2

$C_{14}H_{44}Si_7$

Energy: -2586.49377814

Si	-2.142995	-0.54752	0.682684
Si	0.099507	-0.349654	1.422493
Si	1.700088	-0.071243	-0.305489
H	-2.764208	-1.199853	1.891691
H	1.197433	-0.808471	-1.514756
Si	3.748791	-1.13728	0.227292
Si	1.988899	2.170877	-0.998563
Si	-2.379073	-2.130037	-1.060151
Si	-3.475996	1.399703	0.468259
C	0.246514	1.079774	2.670559
H	1.249683	1.093913	3.110484
H	0.061726	2.0593	2.217367
H	-0.476103	0.95368	3.484801
C	0.368407	-1.967669	2.391131

H	-0.388536	-2.055706	3.179399
H	0.280954	-2.854918	1.755969
H	1.352219	-1.982726	2.868897
C	4.395196	-0.618068	1.931892
H	4.56953	0.46135	1.99155
H	3.702336	-0.887103	2.734443
H	5.349131	-1.11753	2.140488
C	3.522055	-3.017284	0.196414
H	3.177224	-3.357565	-0.785806
H	4.47475	-3.518896	0.406229
H	2.796307	-3.355566	0.941124
C	5.084401	-0.70571	-1.046194
H	4.762088	-0.937343	-2.066485
H	5.356527	0.35418	-1.01149
H	5.993239	-1.285687	-0.844089
C	0.313903	3.022431	-1.234462
H	-0.26917	2.532922	-2.022197
H	-0.286849	3.01047	-0.318575
H	0.455468	4.070052	-1.526416
C	2.910912	2.217841	-2.652711
H	3.913898	1.786101	-2.582841
H	2.3648	1.666764	-3.425621
H	3.018234	3.254464	-2.994342
C	2.985329	3.144607	0.28531
H	3.093142	4.189017	-0.030759
H	2.498063	3.14325	1.265842
H	3.992587	2.734503	0.412796
C	-1.348517	-3.674837	-0.687209
H	-1.502925	-4.426844	-1.470563
H	-0.277443	-3.447708	-0.652368
H	-1.626918	-4.126959	0.270417
C	-4.199831	-2.637931	-1.200558
H	-4.311679	-3.431149	-1.949258
H	-4.590549	-3.016437	-0.250071
H	-4.833412	-1.800542	-1.510078
C	-1.802434	-1.417113	-2.716742
H	-2.392776	-0.545659	-3.014797
H	-0.750757	-1.111132	-2.682391
H	-1.903929	-2.174108	-3.503379
C	-5.237355	0.886911	0.94676
H	-5.279328	0.520428	1.977791
H	-5.91481	1.745373	0.866195
H	-5.626007	0.093129	0.301394
C	-3.496248	2.105771	-1.288828
H	-2.496262	2.386974	-1.638662
H	-3.912577	1.390982	-2.005445
H	-4.124392	3.003997	-1.317034
C	-2.917254	2.768508	1.653024
H	-2.878929	2.4144	2.688434
H	-1.926159	3.160286	1.397764
H	-3.625186	3.605138	1.612666

IV.1.3 Calculated structure of H_3

$C_{14}H_{44}Si_7$

Energy: -2586.49308384

Si	-2.073665	0.339921	0.738832
Si	0.131032	1.245117	0.57825
Si	1.905594	-0.287661	0.223556
H	-2.415596	0.80941	2.126546
H	1.630896	-1.461947	1.118475
Si	4.037744	0.502935	0.951821
Si	1.894753	-1.100723	-1.999389
Si	-2.375237	-1.939723	1.235172
Si	-3.680651	1.31183	-0.709546
C	0.269469	2.676121	-0.67028
H	1.182989	3.253279	-0.489138
H	0.309026	2.310051	-1.704092
H	-0.579485	3.356822	-0.592201
C	0.39618	1.988367	2.314318
H	-0.477471	2.569487	2.63176
H	0.558662	1.210214	3.06062
H	1.265835	2.654737	2.330035
C	4.231852	2.382502	0.885463
H	4.099408	2.763829	-0.131914
H	3.503286	2.883578	1.5274
H	5.232148	2.676677	1.224187
C	4.289027	-0.092903	2.729956
H	4.273796	-1.184591	2.790786
H	5.249343	0.256677	3.124105
H	3.500222	0.288533	3.387752
C	5.421182	-0.23925	-0.109701
H	5.299552	-1.320965	-0.226902
H	5.411453	0.203298	-1.111049
H	6.408239	-0.050816	0.325969
C	0.130244	-1.069241	-2.705607
H	-0.607102	-1.487123	-2.028267
H	-0.148387	-0.028519	-2.922626
H	0.050139	-1.626091	-3.645722
C	2.571175	-2.868825	-2.06876
H	3.601996	-2.908008	-1.700731

H	1.98342	-3.540901	-1.43615
H	2.566648	-3.260407	-3.091594
C	2.936662	0.006516	-3.138402
H	2.664288	-0.193697	-4.182748
H	2.775268	1.07386	-2.955291
H	4.008	-0.189601	-3.030347
C	-4.113895	-2.108656	1.979638
H	-4.364156	-3.170434	2.096015
H	-4.167274	-1.640642	2.968417
H	-4.886673	-1.655699	1.351842
C	-2.271899	-3.096709	-0.265078
H	-2.751723	-4.056233	-0.038678
H	-2.768844	-2.683165	-1.14881
H	-1.230259	-3.304637	-0.535045
C	-1.132212	-2.525362	2.544545
H	-1.027982	-3.616651	2.516734
H	-0.136734	-2.095525	2.403944
H	-1.478497	-2.249597	3.547821
C	-4.22021	2.969245	0.03756
H	-3.417447	3.708007	-0.060584
H	-5.100643	3.364586	-0.482833
H	-4.462344	2.884816	1.102339
C	-5.218377	0.223642	-0.927296
H	-4.973931	-0.823435	-1.127504
H	-5.869383	0.255209	-0.048373
H	-5.795774	0.596774	-1.782372
C	-2.977516	1.636846	-2.439956
H	-1.933723	1.95799	-2.425439
H	-3.044645	0.743635	-3.070642
H	-3.560616	2.429716	-2.925821

IV.1.4 Calculated structure of H_4

$C_{14}H_{44}Si_7$

Energy: -2586.492161

Si	-1.973328	0.34904	-0.618385
Si	-0.20926	-1.204331	-0.977718
Si	2.058338	-0.798913	-0.405553
H	-2.165918	0.972506	-1.97342
H	2.65316	-2.039694	-1.025107
Si	2.755376	-1.067478	1.841771
Si	3.227601	0.925594	-1.547086
Si	-4.029857	-0.798352	-0.325276
Si	-1.771365	2.135462	0.910159
C	-0.61277	-2.852431	-0.115073
H	-1.539535	-3.280309	-0.511324
H	0.189323	-3.579679	-0.28218
H	-0.733155	-2.733279	0.965477
C	-0.212482	-1.541925	-2.850152
H	-1.187948	-1.924467	-3.170994
H	-0.009001	-0.631441	-3.420758
H	0.547636	-2.286505	-3.111812
C	1.984601	-2.612694	2.620064
H	0.904242	-2.508291	2.759954
H	2.157619	-3.503854	2.008532
H	2.430478	-2.792888	3.605932
C	4.636627	-1.306444	1.817142
H	5.156037	-0.433414	1.40838
H	5.012339	-1.468336	2.834978
H	4.920017	-2.175092	1.213957
C	2.374955	0.40819	2.965127
H	2.831662	1.332495	2.597782
H	1.300298	0.583758	3.069458
H	2.776409	0.218546	3.967897
C	2.171684	1.729314	-2.897962
H	1.902004	1.012148	-3.679158
H	1.244105	2.150869	-2.498194
H	2.730647	2.5435	-3.375431
C	4.743156	0.135561	-2.362553
H	5.403672	-0.326403	-1.621217
H	4.451816	-0.643178	-3.074923
H	5.324321	0.890335	-2.906371
C	3.853275	2.288902	-0.388469
H	4.419803	3.031075	-0.964215
H	3.037008	2.814748	0.113578
H	4.522832	1.891931	0.381848
C	-4.096031	-1.820186	1.26841
H	-3.331382	-2.602373	1.284424
H	-3.956999	-1.199178	2.159438
H	-5.073332	-2.310058	1.3561
C	-5.458289	0.447281	-0.276519
H	-6.417544	-0.085009	-0.273846
H	-5.425653	1.069512	0.623785
H	-5.449431	1.112869	-1.145616
C	-4.322887	-1.947902	-1.803763
H	-4.291612	-1.397478	-2.749859
H	-3.577574	-2.747609	-1.859457
H	-5.309648	-2.420247	-1.724853
C	-2.08375	1.517808	2.674699
H	-1.420007	0.69014	2.944572
H	-1.921472	2.323879	3.40014
H	-3.113923	1.166734	2.79684

C	-3.046205	3.476761	0.506941
H	-4.070493	3.093131	0.484904
H	-3.002727	4.270562	1.262747
H	-2.841034	3.934032	-0.46681
C	-0.059518	2.929675	0.821708
H	0.727778	2.205942	1.046516
H	0.13708	3.34838	-0.170367
H	0.018834	3.745944	1.550301

IV.1.5 Calculated structure of H_5

$C_{14}H_{44}Si_7$

Energy: -2586.49203

Si	-1.91061	-0.357782	-0.502358
Si	-0.249367	-1.118521	1.005037
Si	2.076183	-0.583372	0.658903
H	-1.855491	-1.298547	-1.661243
H	2.664956	-1.47039	1.74033
Si	2.943541	1.537446	1.25963
Si	3.085038	-1.527826	-1.275004
Si	-4.059316	-0.738228	0.434714
Si	-1.689496	1.811841	-1.40584
C	-0.756239	-0.479595	2.717217
H	-0.031989	-0.825021	3.466171
H	-0.784759	0.612162	2.733619
H	-1.751467	-0.861122	2.981701
C	-0.397794	-3.009758	1.001883
H	-1.399732	-3.313987	1.348292
H	-0.263169	-3.416055	-0.02282
H	0.352217	-3.445398	1.666892
C	1.98124	2.329749	2.692706
H	0.945716	2.560735	2.402977
H	1.972255	1.652421	3.560063
H	2.475548	3.265054	2.973602
C	4.726191	1.253271	1.841885
H	5.347637	0.94075	0.995009
H	5.114532	2.185652	2.210503
H	4.777648	0.507093	2.622434
C	2.943324	2.699443	-0.22046
H	3.486416	2.308166	-1.084714
H	1.91047	2.91537	-0.572323
H	3.354527	3.654587	0.009311
C	2.274577	-0.977188	-2.892575
H	1.176881	-1.328817	-2.948475
H	2.283023	0.130329	-3.008274
H	2.866788	-1.310223	-3.758336
C	2.784689	-3.389189	-1.258495
H	3.16601	-3.826872	-0.334363
H	1.71712	-3.616613	-1.310623
H	3.296396	-3.897149	-2.047437
C	4.968935	-1.332679	-1.172971
H	5.43147	-1.899709	-1.979423
H	5.278102	-0.291596	-1.307088
H	5.357537	-1.650224	-0.197829
C	-4.540941	0.67346	1.584721
H	-5.519626	0.45918	2.022065
H	-3.801077	0.848537	2.366233
H	-4.625867	1.64973	1.04048
C	-5.321312	-0.831491	-0.973645
H	-6.318494	-1.02634	-0.570646
H	-5.369896	0.084099	-1.569319
H	-5.060622	-1.634334	-1.668854
C	-4.129099	-2.377231	1.394267
H	-3.978175	-3.221149	0.71273
H	-3.36432	-2.404115	2.190886
H	-5.112562	-2.489468	1.908028
C	-1.465729	3.078318	-0.009575
H	-0.564604	2.850393	0.584633
H	-1.341747	4.079981	-0.433573
H	-2.320668	3.159141	0.591902
C	-3.22058	2.218747	-2.451569
H	-3.346369	1.524495	-3.285296
H	-4.136708	2.24925	-1.847783
H	-3.099774	3.291904	-2.876356
C	-0.192439	1.870674	-2.548421
H	0.725301	1.569911	-2.040693
H	-0.284069	1.15694	-3.363593
H	-0.041937	2.882242	-2.919764

IV.1.6 Calculated structure of H_6

$C_{14}H_{44}Si_7$

Energy: -2586.4902737

Si	-2.081064	0.184857	-0.680429
Si	0.042799	0.440997	-1.718506
Si	2.137017	-0.141489	-0.748553
H	-2.923395	0.223705	-1.931657
H	2.958579	-0.346165	-1.993834
Si	2.479755	-2.139831	0.46308
Si	3.169619	1.691416	0.347705

Si	-2.796422	-1.933165	0.103825
Si	-2.866175	1.959206	0.67991
C	-0.076603	-0.668596	-3.264285
H	0.848601	-0.610037	-3.84912
H	-0.245305	-1.718778	-3.005363
H	-0.905481	-0.345675	-3.903318
C	0.164007	2.221701	-2.373916
H	-0.746398	2.474076	-2.92911
H	0.295237	2.969025	-1.58734
H	1.008908	2.303321	-3.066824
C	1.537194	-3.597073	-0.292768
H	0.45541	-3.441667	-0.309711
H	1.865446	-3.772828	-1.32319
H	1.732433	-4.5128	0.277971
C	4.325085	-2.557984	0.346634
H	4.937273	-1.897297	0.968078
H	4.496712	-3.58851	0.683637
H	4.690969	-2.479504	-0.681795
C	2.027079	-1.951071	2.29243
H	2.590323	-1.135552	2.758293
H	0.963786	-1.748817	2.446015
H	2.270082	-2.871528	2.836258
C	3.698212	2.998333	-0.917068
H	4.440087	2.590267	-1.611988
H	2.857793	3.366309	-1.510917
H	4.153405	3.858284	-0.410566
C	4.726684	1.168259	1.295049
H	4.517878	0.414979	2.061141
H	5.492307	0.763766	0.625314
H	5.156746	2.041558	1.801293
C	1.977648	2.479895	1.592112
H	2.451938	3.337772	2.083105
H	1.064522	2.842076	1.107777
H	1.682599	1.772569	2.374396
C	-1.953931	-2.539168	1.685598
H	-2.446113	-3.453255	2.039992
H	-0.899789	-2.777003	1.528017
H	-2.014401	-1.797552	2.489502
C	-4.652552	-1.813108	0.470113
H	-5.057063	-2.817674	0.646286
H	-4.856644	-1.216155	1.364628
H	-5.207521	-1.371897	-0.363938
C	-2.581931	-3.230188	-1.260762
H	-3.164718	-2.960758	-2.14693
H	-1.540554	-3.351176	-1.573297
H	-2.939199	-4.207029	-0.910163
C	-2.359127	1.69882	2.487099
H	-1.274508	1.592017	2.590955
H	-2.665779	2.558629	3.095542
H	-2.827012	0.80756	2.916934
C	-4.755237	2.049636	0.571196
H	-5.091693	2.125311	-0.467986
H	-5.2401	1.175592	1.014006
H	-5.117192	2.937887	1.103708
C	-2.201633	3.640782	0.116072
H	-1.12529	3.737855	0.283432
H	-2.393306	3.820903	-0.946424
H	-2.696353	4.438878	0.683703

IV.2.1 Calculated structure of Cl_1

$C_{14}H_{42}Si_7Cl_2$

Energy: -3505.8123744

Si	-1.91061	-0.357782	-0.502358
Si	-0.249367	-1.118521	1.005037
Si	2.076183	-0.583372	0.658903
Si	2.943541	1.537446	1.25963
Si	3.085038	-1.527826	-1.275004
Si	-4.059316	-0.738228	0.434714
Si	-1.689496	1.811841	-1.40584
C	-0.756239	-0.479595	2.717217
H	-0.031989	-0.825021	3.466171
H	-0.784759	0.612162	2.733619
H	-1.751467	-0.861122	2.981701
C	-0.397794	-3.009758	1.001883
H	-1.399732	-3.313987	1.348292
H	-0.263169	-3.416055	-0.02282
H	0.352217	-3.445398	1.666892
C	1.98124	2.329749	2.692706
H	0.945716	2.560735	2.402977
H	1.972255	1.652421	3.560063
H	2.475548	3.265054	2.973602
C	4.726191	1.253271	1.841885
H	5.347637	0.94075	0.995009
H	5.114532	2.185652	2.210503
H	4.777648	0.507093	2.622434
C	2.943324	2.699443	-0.22046
H	3.486416	2.308166	-1.084714
H	1.91047	2.91537	-0.572323
H	3.354527	3.654587	0.009311
C	2.274577	-0.977188	-2.892575
H	1.176881	-1.328817	-2.948475

H	2.283023	0.130329	-3.008274
H	2.866788	-1.310223	-3.758336
C	2.784689	-3.389189	-1.258495
H	3.16601	-3.826872	-0.334363
H	1.71712	-3.616613	-1.310623
H	3.296396	-3.897149	-2.047437
C	4.968935	-1.332679	-1.172971
H	5.43147	-1.899709	-1.979423
H	5.278102	-0.291596	-1.307088
H	5.357537	-1.650224	-0.197829
C	-4.540941	0.67346	1.584721
H	-5.519626	0.45918	2.022065
H	-3.801077	0.848537	2.366233
H	-4.625867	1.64973	1.04048
C	-5.321312	-0.831491	-0.973645
H	-6.318494	-1.02634	-0.570646
H	-5.369896	0.084099	-1.569319
H	-5.060622	-1.634334	-1.668854
C	-4.129099	-2.377231	1.394267
H	-3.978175	-3.221149	0.71273
H	-3.36432	-2.404115	2.190886
H	-5.112562	-2.489468	1.908028
C	-1.465729	3.078318	-0.009575
H	-0.564604	2.850393	0.584633
H	-1.341747	4.079981	-0.433573
H	-2.320668	3.159141	0.591902
C	-3.22058	2.218747	-2.451569
H	-3.346369	1.524495	-3.285296
H	-4.136708	2.24925	-1.847783
H	-3.099774	3.291904	-2.876356
C	-0.192439	1.870674	-2.548421
H	0.725301	1.569911	-2.040693
H	-0.284069	1.15694	-3.363593
H	-0.041937	2.882242	-2.919764
Cl	-1.62984684	-1.47725429	-2.16017398
Cl	2.73995002	-1.63742614	2.24911783

IV.2.2 Calculated structure of Cl_2

$C_{14}H_{42}Si_7Cl_2$

Energy: -3505.8123132

Si	-2.017725	0.113341	-0.168176
Si	-0.000046	-0.000226	1.079127
Si	2.017657	-0.11337	-0.168205
Si	3.668649	-1.338471	1.022271
Si	2.853915	1.977022	-0.926738
Si	-2.854165	-1.976939	-0.926783
Si	-3.668583	1.338624	1.02229
C	0.188522	1.516554	2.213659
H	1.114175	1.447563	2.796482
H	0.217878	2.451791	1.647111
H	-0.641989	1.578827	2.924833
C	-0.188431	-1.517221	2.213391
H	-1.114088	-1.448494	2.796235
H	-0.217656	-2.452352	1.646657
H	0.642105	-1.57951	2.924533
C	3.155108	-3.153091	1.155968
H	2.25723	-3.286994	1.766272
H	2.956822	-3.579083	0.167284
H	3.962047	-3.736245	1.615985
C	5.313753	-1.262311	0.090059
H	5.733895	-0.251667	0.073469
H	6.047505	-1.917802	0.574855
H	5.200796	-1.598285	-0.945699
C	3.918619	-0.618031	2.757167
H	4.210801	0.436503	2.724535
H	3.01708	-0.695619	3.373424
H	4.716515	-1.164796	3.27401
C	1.499982	3.110038	-1.591729
H	0.959084	2.644934	-2.420416
H	0.761518	3.374899	-0.82933
H	1.950322	4.040427	-1.959302
C	4.087485	1.638782	-2.318334
H	4.942107	1.044101	-1.982479
H	3.609567	1.099278	-3.141949
H	4.470904	2.586815	-2.714549
C	3.73618	2.853748	0.503589
H	4.110134	3.826847	0.163013
H	3.066619	3.038299	1.350147
H	4.595265	2.283346	0.871215
C	-3.736253	-2.853829	0.503546
H	-4.109747	-3.827133	0.163057
H	-3.066703	-3.037975	1.350201
H	-4.59562	-2.28374	0.870994
C	-4.087834	-1.63863	-2.318278
H	-4.471312	-2.586647	-2.714476
H	-4.942413	-1.043914	-1.982378
H	-3.609938	-1.099154	-3.141925
C	-1.500204	-3.109786	-1.592016
H	-0.959297	-2.644463	-2.420578
H	-0.761733	-3.374794	-0.829674
H	-1.950483	-4.040112	-1.959821

C	-3.918676	0.617964	2.757084
H	-3.017078	0.695099	3.373312
H	-4.716369	1.16485	3.27411
H	-4.211201	-0.436469	2.724202
C	-5.313727	1.262779	0.090129
H	-5.200837	1.598862	-0.9456
H	-5.733999	0.25219	0.073465
H	-6.047346	1.918305	0.575081
C	-3.154756	3.153151	1.156131
H	-2.257126	3.286886	1.766838
H	-2.955921	3.579046	0.167513
H	-3.961775	3.736515	1.615737
Cl	1.704132	-1.273243	-1.925145
Cl	-1.703791	1.273209	-1.924949

IV.2.3 Calculated structure of Cl_3

$C_{14}H_{42}Si_7Cl_2$

Energy: -3505.8120302

Si	-2.142995	-0.54752	0.682684
Si	0.099507	-0.349654	1.422493
Si	1.700088	-0.071243	-0.305489
Si	3.748791	-1.13728	0.227292
Si	1.988899	2.170877	-0.998563
Si	-2.379073	-2.130037	-1.060151
Si	-3.475996	1.399703	0.468259
C	0.246514	1.079774	2.670559
H	1.249683	1.093913	3.110484
H	0.061726	2.0593	2.217367
H	-0.476103	0.95368	3.484801
C	0.368407	-1.967669	2.391131
H	-0.388536	-2.055706	3.179399
H	0.280954	-2.854918	1.755969
H	1.352219	-1.982726	2.868897
C	4.395196	-0.618068	1.931892
H	4.56953	0.46135	1.99155
H	3.702336	-0.887103	2.734443
H	5.349131	-1.11753	2.140488
C	3.522055	-3.017284	0.196414
H	3.177224	-3.357565	-0.785806
H	4.47475	-3.518896	0.406229
H	2.796307	-3.355566	0.941124
C	5.084401	-0.70571	-1.046194
H	4.762088	-0.937343	-2.066485
H	5.356527	0.35418	-1.01149
H	5.993239	-1.285687	-0.844089
C	0.313903	3.022431	-1.234462
H	-0.26917	2.532922	-2.022197
H	-0.286849	3.01047	-0.318575
H	0.455468	4.070052	-1.526416
C	2.910912	2.217841	-2.652711
H	3.913898	1.786101	-2.582841
H	2.3648	1.666764	-3.425621
H	3.018234	3.254464	-2.994342
C	2.985329	3.144607	0.28531
H	3.093142	4.189017	-0.030759
H	2.498063	3.14325	1.265842
H	3.992587	2.734503	0.412796
C	-1.348517	-3.674837	-0.687209
H	-1.502925	-4.426844	-1.470563
H	-0.277443	-3.447708	-0.652368
H	-1.626918	-4.126959	0.270417
C	-4.199831	-2.637931	-1.200558
H	-4.311679	-3.431149	-1.949258
H	-4.590549	-3.016437	-0.250071
H	-4.833412	-1.800542	-1.510078
C	-1.802434	-1.417113	-2.716742
H	-2.392776	-0.545659	-3.014797
H	-0.750757	-1.111132	-2.682391
H	-1.903929	-2.174108	-3.503379
C	-5.237355	0.886911	0.94676
H	-5.279328	0.520428	1.977791
H	-5.91481	1.745373	0.866195
H	-5.626007	0.093129	0.301394
C	-3.496248	2.105771	-1.288828
H	-2.496262	2.386974	-1.638662
H	-3.912577	1.390982	-2.005445
H	-4.124392	3.003997	-1.317034
C	-2.917254	2.768508	1.653024
H	-2.878929	2.4144	2.688434
H	-1.926159	3.160286	1.397764
H	-3.625186	3.605138	1.612666
Cl	0.93561185	-1.00591292	-1.92486183
Cl	-3.04811746	-1.30097549	2.32385984

IV.2.4 Calculated structure of Cl_4

$C_{14}H_{42}Si_7Cl_2$

Energy: -3505.8113447

Si	-2.171184	-0.575444	0.614903

Si	0.047581	-0.176583	1.382012
Si	1.764781	-0.177351	-0.262081
Si	3.791766	-1.043415	0.60962
Si	2.194738	1.875597	-1.355027
Si	-2.359146	-1.924728	-1.316667
Si	-3.717985	1.217078	0.712376
C	0.16973	1.437017	2.382665
H	1.187632	1.579773	2.762359
H	-0.088994	2.316927	1.78583
H	-0.503821	1.404789	3.245626
C	0.392618	-1.611767	2.583181
H	-0.358425	-1.61134	3.380535
H	0.33649	-2.57996	2.076919
H	1.380956	-1.531096	3.048054
C	3.591815	-2.908538	0.876033
H	2.798954	-3.143108	1.594082
H	3.344317	-3.419531	-0.061294
H	4.527292	-3.33426	1.256426
C	5.213074	-0.741628	-0.610001
H	5.427117	0.325401	-0.740879
H	6.124128	-1.22191	-0.234207
H	5.001172	-1.157157	-1.601294
C	4.22737	-0.20301	2.252924
H	4.39332	0.872839	2.125713
H	3.445673	-0.324479	3.009667
H	5.148497	-0.637616	2.656438
C	0.591842	2.714542	-1.90484
H	0.027311	2.087652	-2.603478
H	-0.064672	2.940261	-1.061518
H	0.820614	3.658679	-2.41238
C	3.250649	1.543667	-2.893064
H	4.162429	0.979138	-2.666415
H	2.688215	0.973445	-3.6401
H	3.547633	2.493227	-3.353304
C	3.134719	3.035788	-0.187729
H	3.319204	3.996921	-0.68145
H	2.570294	3.235313	0.729319
H	4.104991	2.621445	0.107937
C	-1.210444	-3.42068	-1.137417
H	-1.479572	-4.022995	-0.263118
H	-1.288397	-4.061062	-2.023979
H	-0.161066	-3.127838	-1.031354
C	-4.142893	-2.545199	-1.472361
H	-4.228667	-3.211088	-2.33937
H	-4.446448	-3.110053	-0.584794
H	-4.86044	-1.727742	-1.605832
C	-1.917195	-0.967921	-2.889098
H	-2.548399	-0.081648	-3.015657
H	-0.873684	-0.639101	-2.876681
H	-2.056022	-1.604059	-3.771367
C	-5.360921	0.685947	-0.069934
H	-5.733992	-0.252188	0.353844
H	-6.121408	1.456866	0.103702
H	-5.268868	0.546776	-1.15306
C	-3.144912	2.801599	-0.148463
H	-2.262447	3.231128	0.335161
H	-2.905619	2.639156	-1.203534
H	-3.941647	3.553306	-0.098938
C	-4.011397	1.619159	2.540378
H	-4.382104	0.74504	3.085502
H	-3.094853	1.95454	3.036083
H	-4.754065	2.419702	2.638553
Cl	1.00981793	-1.38425421	-1.69519489
Cl	-2.83316014	-1.74723171	2.12125659

IV.2.5 Calculated structure of Cl_5

$C_{14}H_{42}Si_7Cl_2$

Energy: -3505.81017443

Si	-2.081064	0.184857	-0.680429
Si	0.042799	0.440997	-1.718506
Si	2.137017	-0.141489	-0.748553
Si	2.479755	-2.139831	0.46308
Si	3.169619	1.691416	0.347705
Si	-2.796422	-1.933165	0.103825
Si	-2.866175	1.959206	0.67991
C	-0.076603	-0.668596	-3.264285
H	0.848601	-0.610037	-3.84912
H	-0.245305	-1.718778	-3.005363
H	-0.905481	-0.345675	-3.903318
C	0.164007	2.221701	-2.373916
H	-0.746398	2.474076	-2.92911
H	0.295237	2.969025	-1.58734
H	1.008908	2.303321	-3.066824
C	1.537194	-3.597073	-0.292768
H	0.45541	-3.441667	-0.309711
H	1.865446	-3.772828	-1.32319
H	1.732433	-4.5128	0.277971
C	4.325085	-2.557984	0.346634
H	4.937273	-1.897297	0.968078
H	4.496712	-3.58851	0.683637
H	4.690969	-2.479504	-0.681795

C	2.027079	-1.951071	2.29243
H	2.590323	-1.135552	2.758293
H	0.963786	-1.748817	2.446015
H	2.270082	-2.871528	2.836258
C	3.698212	2.998333	-0.917068
H	4.440087	2.590267	-1.611988
H	2.857793	3.366309	-1.510917
H	4.153405	3.858284	-0.410566
C	4.726684	1.168259	1.295049
H	4.517878	0.414979	2.061141
H	5.492307	0.763766	0.625314
H	5.156746	2.041558	1.801293
C	1.977648	2.479895	1.592112
H	2.451938	3.337772	2.083105
H	1.064522	2.842076	1.107777
H	1.682599	1.772569	2.374396
C	-1.953931	-2.539168	1.685598
H	-2.446113	-3.453255	2.039992
H	-0.899789	-2.777003	1.528017
H	-2.014401	-1.797552	2.489502
C	-4.652552	-1.813108	0.470113
H	-5.057063	-2.817674	0.646286
H	-4.856644	-1.216155	1.364628
H	-5.207521	-1.371897	-0.363938
C	-2.581931	-3.230188	-1.260762
H	-3.164718	-2.960758	-2.14693
H	-1.540554	-3.351176	-1.573297
H	-2.939199	-4.207029	-0.910163
C	-2.359127	1.69882	2.487099
H	-1.274508	1.592017	2.590955
H	-2.665779	2.558629	3.095542
H	-2.827012	0.80756	2.916934
C	-4.755237	2.049636	0.571196
H	-5.091693	2.125311	-0.467986
H	-5.2401	1.175592	1.014006
H	-5.117192	2.937887	1.103708
C	-2.201633	3.640782	0.116072
H	-1.12529	3.737855	0.283432
H	-2.393306	3.820903	-0.946424
H	-2.696353	4.438878	0.683703
Cl	3.04762419	-0.6624635	-2.47475696
Cl	-3.05862417	0.32590264	-2.4424966

IV.2.6 Calculated structure of Cl$_6$

$C_{14}H_{42}Si_7Cl_2$

Energy: -3505.81017443

Si	-1.873392	-0.026073	-0.395324
Si	0.093513	-0.953723	0.565262
Si	2.055949	-0.21894	-0.544072
Si	3.968045	-1.380916	0.249644
Si	2.363671	2.111102	-0.800639
Si	-3.547919	-1.66187	-0.777049
Si	-2.833964	1.845771	0.704172
C	0.141594	-0.552141	2.423802
H	0.97102	-1.072459	2.913641
H	0.265613	0.518347	2.610184
H	-0.785464	-0.872298	2.912837
C	0.07195	-2.850447	0.409822
H	-0.834609	-3.279958	0.848965
H	0.128153	-3.170446	-0.634656
H	0.929575	-3.282004	0.937767
C	4.015181	-3.102514	-0.539874
H	3.128001	-3.693855	-0.292932
H	4.073512	-3.034141	-1.631215
H	4.894756	-3.657613	-0.191631
C	5.576961	-0.492206	-0.210712
H	5.661549	0.480905	0.283929
H	6.435155	-1.098518	0.104324
H	5.66238	-0.330934	-1.289926
C	3.947103	-1.575613	2.134854
H	3.846517	-0.61227	2.645736
H	3.127031	-2.218312	2.46935
H	4.883526	-2.03489	2.473822
C	0.875229	2.868952	-1.691299
H	0.773396	2.451481	-2.698506
H	-0.066067	2.684656	-1.166665
H	1.003402	3.954051	-1.78991
C	3.87915	2.447887	-1.887437
H	4.81434	2.1414	-1.410512
H	3.805639	1.926334	-2.847603
H	3.949585	3.522047	-2.098984
C	2.618711	2.968833	0.869011
H	2.783009	4.043317	0.724136
H	1.752339	2.852559	1.527719
H	3.492906	2.570171	1.395275
C	-4.050322	-2.555975	0.816427
H	-4.822288	-3.304643	0.60135
H	-3.206393	-3.077293	1.279129

H	-4.459491	-1.862882	1.558285
C	-5.09644	-0.84525	-1.507284
H	-5.84025	-1.611918	-1.75699
H	-5.566213	-0.146683	-0.807501
H	-4.866373	-0.295448	-2.425899
C	-2.936252	-2.939567	-2.034474
H	-2.607342	-2.458289	-2.961489
H	-2.098991	-3.528639	-1.648724
H	-3.744601	-3.635997	-2.288973
C	-4.085794	1.274599	2.007578
H	-3.611829	0.662437	2.782282
H	-4.532272	2.145448	2.502712
H	-4.901769	0.690274	1.571102
C	-3.731065	2.888117	-0.597784
H	-3.029565	3.281956	-1.340703
H	-4.488223	2.306455	-1.132728
H	-4.233626	3.740512	-0.124869
C	-1.589571	2.96145	1.595762
H	-1.105698	2.440764	2.427608
H	-0.808333	3.339101	0.930294
H	-2.115719	3.828891	2.013167
Cl	1.75590587	-0.7367889	-2.47337411
Cl	-1.17107601	0.69621495	-2.14616733

IV.3.1 Calculated structure of $[PH_2]_1$

$C_{14}H_{46}Si_7P_2$

Energy: -3270.420987

Si	-1.51322883	-1.43902666	-0.74901465
Si	0.54307688	-2.51327358	-0.74841171
Si	2.24068529	-0.93382523	-0.82501835
Si	4.29734248	-2.00467283	-0.74855496
Si	2.04672774	0.49858144	0.98964184
Si	-3.09514802	-2.7976364	-1.76592727
Si	-2.15848321	-1.00280413	1.43633583
C	0.7112545	-3.52961686	0.80025308
H	1.64858	-4.06568633	0.77902979
H	0.68797712	-2.87908664	1.6620353
H	-0.10514211	-4.23421242	0.85891887
C	0.66251965	-3.62445723	-2.23522182
H	-0.14150958	-4.34513463	-2.2115342
H	0.58807142	-3.03143288	-3.13476592
H	1.61035095	-4.1420076	-2.22267445
C	4.85266794	-2.40476783	-2.47804553
H	4.11938153	-3.03899634	-2.95390815
H	4.95847706	-1.49029053	-3.04278945
H	5.80259227	-2.91732984	-2.44165931
C	5.54683573	-0.89028988	0.06170257
H	5.24341559	-0.68846513	1.07836524
H	6.51266473	-1.37358196	0.06346547
H	5.60993908	0.03823851	-0.48625089
C	4.14140342	-3.57752446	0.23196571
H	3.74920623	-3.35288283	1.2128416
H	3.47136041	-4.25429916	-0.27736559
H	5.11309837	-4.03866006	0.3297557
C	0.46111192	1.46125537	0.85296202
H	0.52578068	2.14496283	0.01943814
H	-0.36165729	0.77941274	0.69630487
H	0.29853164	2.01836973	1.76378101
C	3.48700003	1.67540211	1.00721572
H	4.39718962	1.12747567	1.20146173
H	3.56093796	2.16821114	0.04905476
H	3.33915963	2.41383475	1.78133487
C	2.03661943	-0.4925173	2.56356087
H	1.91484458	0.17164636	3.40644729
H	1.21891313	-1.1976342	2.53975809
H	2.97026554	-1.02703527	2.65840533
C	-3.0175772	-4.50167634	-1.02442161
H	-3.76174378	-5.13100233	-1.48978694
H	-2.0364551	-4.92180572	-1.18962069
H	-3.2094916	-4.44166352	0.03669446
C	-4.79096492	-2.08180574	-1.49873539
H	-5.52513343	-2.70158607	-1.99195841
H	-5.0034691	-2.04487094	-0.4404926
H	-4.8289489	-1.08332212	-1.90859837
C	-2.74516472	-2.89865732	-3.58990821
H	-2.74677534	-1.90471634	-4.01237564
H	-1.77878044	-3.35477246	-3.74630647
H	-3.50673535	-3.49513367	-4.07014371
C	-3.0311329	-2.4899868	2.1337383
H	-2.36480639	-3.33973739	2.11549218
H	-3.32910727	-2.28790216	3.15195885
H	-3.90618845	-2.70586466	1.53869668
C	-3.3075691	0.45954734	1.46335055
H	-2.79645598	1.32630911	1.07106571
H	-4.17472783	0.24722549	0.85560457
H	-3.61873467	0.65421472	2.47906735
C	-0.65406363	-0.62824279	2.46396685
H	0.02025198	-1.47139065	2.43568011
H	-0.15598466	0.24452903	2.06825647
H	-0.95292676	-0.44037511	3.48464632
P	2.08055696	0.24731598	-2.73335909

P	-1.34751649	0.49736419	-1.88278265
H	0.85216963	-0.0895004	-3.40508769
H	3.19648206	-0.06684798	-3.58753247
H	-0.03264818	0.60400611	-2.46014634
H	-2.33449431	0.52585605	-2.93095392

IV.3.2 Calculated structure of $[PH_2]_2$

$C_{14}H_{46}Si_7P_2$

Energy: -3270.420694

Si	-1.900713	0.037303	-0.362025
Si	0.064385	-0.516503	0.861881
Si	1.988047	-0.185821	-0.478003
Si	3.827347	-1.452067	0.313293
Si	2.578373	2.060538	-0.914887
Si	-3.214703	-1.857686	-0.923231
Si	-3.245818	1.73274	0.60487
C	0.222183	0.569926	2.417967
H	1.162057	0.3535	2.937917
H	0.212994	1.638317	2.181313
H	-0.595448	0.373263	3.119715
C	-0.005161	-2.312466	1.485794
H	-0.944807	-2.506583	2.014941
H	0.080289	-3.037705	0.67247
H	0.813384	-2.499366	2.189991
C	3.520927	-3.295445	0.002391
H	2.646916	-3.664971	0.547459
H	3.358639	-3.495827	-1.061902
H	4.388565	-3.884011	0.324663
C	5.422837	-0.973962	-0.592777
H	5.718381	0.060057	-0.386894
H	6.245421	-1.623034	-0.268122
H	5.321944	-1.084661	-1.67744
C	4.108383	-1.18438	2.168935
H	4.306388	-0.133447	2.404753
H	3.245478	-1.502043	2.763393
H	4.97357	-1.767635	2.506646
C	1.059203	3.114732	-1.308636
H	0.488724	2.699507	-2.145636
H	0.383464	3.188853	-0.451843
H	1.364421	4.132526	-1.581009
C	3.725202	2.100304	-2.421797
H	4.646007	1.533493	-2.254051
H	3.231707	1.680201	-3.304483
H	4.006242	3.134286	-2.656378
C	3.483098	2.828827	0.562659
H	3.743656	3.871821	0.345906
H	2.866973	2.823252	1.467912
H	4.41343	2.297764	0.789792
C	-4.233124	-2.492721	0.543011
H	-4.809469	-3.378609	0.250637
H	-3.598947	-2.776138	1.389655
H	-4.944109	-1.73823	0.895669
C	-4.396072	-1.385029	-2.328132
H	-4.962229	-2.26608	-2.654708
H	-5.117283	-0.617829	-2.032266
H	-3.844014	-1.005783	-3.194692
C	-2.134024	-3.273083	-1.571042
H	-1.452499	-2.933351	-2.357806
H	-1.533099	-3.729542	-0.779541
H	-2.769955	-4.058319	-1.997997
C	-3.72109	1.261353	2.378182
H	-2.853453	1.265526	3.04538
H	-4.444457	1.984436	2.774144
H	-4.180973	0.269455	2.433179
C	-4.843876	1.950058	-0.390367
H	-4.645904	2.139601	-1.450201
H	-5.489699	1.06903	-0.320664
H	-5.408856	2.804796	0.001351
C	-2.373081	3.411896	0.657142
H	-1.467492	3.383897	1.271077
H	-2.093213	3.756576	-0.343125
H	-3.043653	4.162567	1.093172
P	1.38406127	-0.9670605	-2.49972654
P	-1.0803218	0.9139626	-2.26489815
H	1.5051689	-1.41865334	-3.86882627
H	0.0778746	-0.34279267	-3.73758907
H	-0.55527142	1.47502475	-3.48273696
H	-1.8447504	1.2911236	-3.5864632

IV.3.3 Calculated structure of $[PH_2]_3$

$C_{14}H_{46}Si_7P_2$

Energy: -3270.420003

Si	-3.17465247	0.08943843	0.80185402
Si	-1.04741713	0.88728434	1.27165366
Si	-0.4620082	2.49667965	-0.29344797
Si	1.8455154	2.54273881	-0.52927288
Si	-1.20829288	4.57495737	0.41804405
Si	-3.40538715	-0.19524897	-1.48902236

Si	-4.75527956	1.61151686	1.55504407
C	-1.02938937	1.64062539	2.97216895
H	-0.03412336	1.99322096	3.19915338
H	-1.72135046	2.46913587	3.0062313
H	-1.32222657	0.89694319	3.69851815
C	0.17064548	-0.51669351	1.20259065
H	-0.11222042	-1.27423117	1.91849817
H	0.17336554	-0.94244221	0.21005318
H	1.15805415	-0.14862045	1.43912043
C	2.64035449	2.56017638	1.15225225
H	2.30515416	3.42857723	1.69990242
H	2.36326329	1.66590299	1.69067178
H	3.71416547	2.59617395	1.04255199
C	2.40357348	1.03412713	-1.46322255
H	1.92816483	1.01466531	-2.43276257
H	3.47584572	1.06451679	-1.58855694
H	2.1307274	0.14721158	-0.91065055
C	2.3426439	4.07087349	-1.46589855
H	1.81443901	4.10385994	-2.40733972
H	2.09562178	4.94627433	-0.88361558
H	3.40652617	4.04979022	-1.6505875
C	-2.99842519	4.4561896	0.90888058
H	-3.58945951	4.17557374	0.04961742
H	-3.11092688	3.71076342	1.68223895
H	-3.33432086	5.41326973	1.27978723
C	-1.02469927	5.80613871	-0.96401453
H	0.01807238	5.89510378	-1.23068381
H	-1.58841427	5.47088098	-1.82205163
H	-1.39715318	6.76731084	-0.64179379
C	-0.20006861	5.12874923	1.87968641
H	-0.56878076	6.08101921	2.23130158
H	-0.28039609	4.39740185	2.67030548
H	0.83439157	5.22938318	1.58614775
C	-1.99918232	-1.23036303	-2.12990212
H	-2.12903849	-1.39800342	-3.18887996
H	-1.06566473	-0.71493873	-1.95878016
H	-1.98633769	-2.1791809	-1.61416995
C	-5.01807811	-1.0495121	-1.84827486
H	-5.0924065	-1.24764742	-2.90733939
H	-5.06098329	-1.98122929	-1.3037914
H	-5.83724574	-0.41568336	-1.542292
C	-3.38388657	1.46588748	-2.32554101
H	-4.21326744	2.0590008	-1.96952983
H	-2.4565756	1.97103255	-2.09899561
H	-3.46933247	1.33215992	-3.3938181
C	-6.36608013	0.73288427	1.85988222
H	-6.22621602	-0.02211907	2.61936099
H	-7.10722188	1.4447407	2.19210101
H	-6.70011179	0.26582117	0.94518288
C	-5.0036904	2.93398629	0.27092309
H	-4.0584475	3.41100854	0.057931
H	-5.39438342	2.48962798	-0.6325727
H	-5.70247883	3.66920783	0.64179236
C	-4.16328795	2.38796776	3.13816438
H	-3.96010186	1.61480948	3.86434733
H	-3.26059821	2.94958738	2.94807327
H	-4.92542673	3.05034888	3.5213037
P	-1.40834932	1.99725902	-2.27271993
P	-3.48099926	-1.88440695	1.83751132
H	-4.82073491	-1.94730598	2.36167934
H	-2.53668614	-2.01110845	2.91724252
H	-2.41493966	2.97875946	-2.58422076
H	-0.40062776	2.00183817	-3.30134829

IV.3.4 Calculated structure of $[PH_2]_4$

$C_{14}H_{46}Si_7P_2$

Energy: -3270.419094

Si	-2.08394	-0.177727	-0.3664
Si	-0.207578	-1.121267	0.759554
Si	2.058345	-0.474407	0.338891
Si	2.853535	1.497108	1.399439
Si	2.998117	-0.730849	-1.841287
Si	-4.079453	-0.661407	0.824608
Si	-1.887054	2.11257	-0.9029
C	-0.492978	-0.872314	2.626557
H	-1.378267	-1.433179	2.945644
H	0.361024	-1.242724	3.203333
H	-0.648123	0.178054	2.889918
C	-0.28189	-2.996532	0.438586
H	-1.291322	-3.373829	0.634712
H	-0.026517	-3.250513	-0.594424
H	0.404933	-3.532692	1.101833
C	2.47694	1.447393	3.254309
H	1.406703	1.546841	3.459941
H	2.819891	0.518456	3.720094
H	2.988994	2.281485	3.749573
C	4.73929	1.536155	1.194928
H	5.037871	1.614354	0.144872
H	5.146637	2.408811	1.720529
H	5.218223	0.646592	1.616026
C	2.174248	3.120378	0.706324

H	2.542076	3.328504	-0.303918
H	1.082472	3.145459	0.688202
H	2.511704	3.944164	1.348071
C	1.976325	-1.869636	-2.953359
H	1.796898	-2.841928	-2.483054
H	1.004457	-1.437249	-3.210017
H	2.518368	-2.050821	-3.889397
C	4.713052	-1.515793	-1.653874
H	5.353663	-0.954483	-0.966381
H	4.648699	-2.543922	-1.28282
H	5.212921	-1.544738	-2.629476
C	3.281149	0.91613	-2.741639
H	3.755675	0.688714	-3.704848
H	2.382497	1.502222	-2.955093
H	3.975128	1.557789	-2.189254
C	-4.200236	0.322831	2.439045
H	-3.392017	0.078263	3.134596
H	-4.176001	1.403	2.265253
H	-5.148864	0.089081	2.937452
C	-5.571922	-0.219787	-0.253162
H	-6.495168	-0.527762	0.252484
H	-5.637305	0.856978	-0.438075
H	-5.537912	-0.720821	-1.225508
C	-4.199665	-2.5057	1.245982
H	-4.158922	-3.134072	0.349983
H	-3.405086	-2.832067	1.92383
H	-5.157491	-2.703345	1.742842
C	-1.972666	3.215644	0.637491
H	-1.502414	2.764933	1.516964
H	-1.479567	4.17714	0.452494
H	-3.018804	3.407666	0.895403
C	-3.262798	2.665028	-2.080395
H	-4.248778	2.623028	-1.607336
H	-3.088338	3.70191	-2.392989
H	-3.299335	2.045513	-2.981761
C	-0.234687	2.28336	-1.804284
H	0.560391	1.774119	-1.250852
H	-0.286711	1.832332	-2.800249
H	0.071131	3.331926	-1.924723
P	-2.470514	-1.167937	-2.399653
P	3.042556	-2.054204	1.706818
H	-1.177497	-0.965722	-2.95446
H	-2.191611	-2.505514	-2.006818
H	4.394067	-1.754276	1.38675
H	2.978421	-3.144801	0.797485

IV.3.5 Calculated structure of [PH$_2$]$_5$

$C_{14}H_{46}Si_7P_2$

Energy: -3270.418481

Si	2.017785	0.15109	0.312002
Si	0.077765	-1.238534	0.382587
Si	-2.171304	-0.436246	0.184878
Si	-3.081327	-0.460184	-2.014838
Si	-2.882315	1.381417	1.545198
Si	3.950925	-1.228183	0.114033
Si	2.289339	1.954209	-1.221237
C	0.245647	-2.599622	-0.939923
H	-0.600464	-3.291614	-0.878446
H	0.278371	-2.195485	-1.957552
H	1.15971	-3.181972	-0.77881
C	0.173275	-2.096175	2.079171
H	1.144813	-2.5845	2.215074
H	0.037833	-1.387686	2.902043
H	-0.601955	-2.863992	2.176696
C	-3.281885	-2.24613	-2.615352
H	-2.331062	-2.786638	-2.652978
H	-3.966289	-2.81471	-1.978734
H	-3.700881	-2.240066	-3.629358
C	-4.807085	0.319817	-2.008477
H	-4.775309	1.396362	-1.810948
H	-5.264976	0.179481	-2.996049
H	-5.467853	-0.142137	-1.268187
C	-2.045519	0.465799	-3.294471
H	-1.723536	1.441394	-2.922814
H	-1.145454	-0.095558	-3.568693
H	-2.626147	0.629186	-4.209385
C	-2.274007	1.156983	3.316694
H	-2.613621	0.19891	3.717551
H	-1.186113	1.194703	3.41071
H	-2.688901	1.946031	3.950518
C	-4.77588	1.36096	1.630878
H	-5.2484	1.573847	0.668247
H	-5.159749	0.400891	1.990303
H	-5.106664	2.129348	2.339638
C	-2.344569	3.082314	0.917584
H	-2.847641	3.861206	1.502595
H	-1.267174	3.232556	1.031129
H	-2.597984	3.241244	-0.135087
C	4.063613	-2.12054	-1.554263
H	5.051571	-2.590424	-1.643604
H	3.313331	-2.91241	-1.647091

H	3.940701	-1.447107	-2.406441
C	5.496275	-0.146796	0.310343
H	6.388724	-0.784258	0.336341
H	5.614729	0.552106	-0.524355
H	5.47926	0.437467	1.235835
C	4.012518	-2.555778	1.463126
H	3.987034	-2.128644	2.471383
H	3.188539	-3.270853	1.378227
H	4.948403	-3.120539	1.367374
C	0.681747	2.88546	-1.573031
H	0.238289	3.329649	-0.678298
H	0.876361	3.694719	-2.28753
H	-0.049937	2.213129	-2.026991
C	2.941652	1.340611	-2.891561
H	3.943007	0.906001	-2.813023
H	2.281421	0.59088	-3.340247
H	3.005515	2.184134	-3.590198
C	3.535341	3.186085	-0.503244
H	3.183629	3.610346	0.441874
H	4.513535	2.735161	-0.313625
H	3.679999	4.013432	-1.209504
P	-3.287313	-2.143806	1.281723
P	2.352124	1.102015	2.383283
H	0.991128	1.137668	2.778487
H	2.605655	-0.103996	3.082622
H	-4.527875	-1.983514	0.603201
H	-2.864619	-3.204766	0.431443

IV.3.6 Calculated structure of $[PH_2]_6$

$C_{14}H_{46}Si_7P_2$

Energy: -3270.418445

Si	-2.11443	-0.320245	0.488013
Si	0.133585	-0.993364	0.955527
Si	1.973442	-0.263092	-0.376956
Si	3.987059	-0.717953	0.796781
Si	1.880606	2.015258	-1.01462
Si	-2.993034	-1.344763	-1.460613
Si	-2.689344	1.9606	0.747555
C	0.448779	-0.496178	2.769331
H	1.383271	-0.936386	3.134237
H	0.514237	0.587637	2.90155
H	-0.357171	-0.864073	3.413632
C	0.152348	-2.892457	0.883434
H	-0.6984	-3.310974	1.431011
H	0.115845	-3.262509	-0.145194
H	1.070551	-3.276239	1.341036
C	3.982709	-2.427331	1.61491
H	3.228487	-2.510582	2.403301
H	3.803202	-3.230626	0.893181
H	4.961728	-2.607925	2.074784
C	5.471493	-0.662435	-0.382503
H	5.572423	0.308435	-0.876558
H	6.388412	-0.8393	0.193377
H	5.422444	-1.430042	-1.160871
C	4.304789	0.577713	2.144669
H	4.432464	1.579117	1.721634
H	3.499547	0.623319	2.884306
H	5.231205	0.328012	2.676026
C	0.59525	2.27605	-2.399641
H	0.977672	1.745158	-3.283645
H	-0.428086	1.895216	-2.231003
H	0.484938	3.342683	-2.632042
C	3.519533	2.592691	-1.779386
H	4.365921	2.502037	-1.091704
H	3.768028	2.042813	-2.693203
H	3.427347	3.652154	-2.051476
C	1.677654	3.095347	0.531708
H	1.717327	4.157832	0.26416
H	0.796036	2.932448	1.163218
H	2.550933	2.90227	1.16527
C	-3.23522	-3.198469	-1.154049
H	-3.666868	-3.661099	-2.050311
H	-2.29552	-3.712621	-0.934276
H	-3.921808	-3.390218	-0.323023
C	-4.676586	-0.621938	-1.946971
H	-5.070031	-1.174779	-2.808789
H	-5.412547	-0.700598	-1.140734
H	-4.604829	0.430888	-2.237424
C	-1.787253	-1.11629	-2.899987
H	-1.717424	-0.071086	-3.217131
H	-0.789015	-1.44466	-2.592403
H	-2.090384	-1.714734	-3.765909
C	-2.035191	2.607003	2.40368
H	-0.938268	2.611996	2.405515
H	-2.378313	3.632741	2.579179
H	-2.370828	1.995718	3.247044
C	-4.57363	2.149491	0.730064
H	-5.011969	1.858496	-0.228334
H	-5.050222	1.54917	1.512566
H	-4.837834	3.197724	0.914076
C	-1.994891	3.077956	-0.612606

H	-0.906523	3.144672	-0.617995
H	-2.27754	2.730369	-1.608416
H	-2.366222	4.105082	-0.503474
P	1.994928	-1.629745	-2.260576
P	-3.193267	-1.457036	2.197064
H	-4.516311	-1.085906	1.822321
H	-3.093113	-0.436215	3.182881
H	3.40721	-1.790546	-2.27116
H	2.06602	-0.580263	-3.222095

IV.3.7 Calculated structure of $[PH_2]_7$

$C_{14}H_{46}Si_7P_2$

Energy: -3270.418427

Si	-1.59700168	-0.50947234	-1.55187382
Si	0.31260414	-0.62997609	-0.23989651
Si	1.94452548	0.76477906	-1.11960714
Si	3.86093515	0.62912162	0.18092006
Si	1.16980425	2.95158312	-1.12935558
Si	-2.47594766	-2.63770913	-1.83553231
Si	-3.16738272	0.84311353	-0.50936969
C	-0.0919281	-0.09393015	1.49463756
H	0.7734068	-0.23350949	2.12559962
H	-0.37184719	0.94916271	1.49303367
H	-0.91223358	-0.6861912	1.8724282
C	0.93985977	-2.3808734	-0.21733568
H	0.15366488	-3.04062681	0.11885331
H	1.2479363	-2.66571576	-1.21250083
H	1.78219108	-2.45292767	0.45474033
C	4.88717723	-0.81857731	-0.37639044
H	4.31369056	-1.7277668	-0.27204717
H	5.1656122	-0.68531187	-1.41133695
H	5.77811142	-0.88325265	0.23061316
C	4.84707584	2.19545313	-0.00274309
H	4.27295196	3.02864922	0.3748361
H	5.76704559	2.10934584	0.55640018
H	5.07382779	2.35784715	-1.04610867
C	3.3849843	0.40172921	1.96455777
H	2.70265622	1.18582298	2.25785856
H	2.90576566	-0.55800278	2.08971369
H	4.27017244	0.44533312	2.58176166
C	-0.34220154	3.0689282	-2.2062347
H	-0.07810616	2.82717842	-3.22516094
H	-1.09010065	2.37414037	-1.85364884
H	-0.7363369	4.07360322	-2.16518098
C	2.49388272	4.07546113	-1.7951742
H	3.33679818	4.078171	-1.11998076
H	2.81096945	3.7228404	-2.76549097
H	2.10270927	5.07796634	-1.88664362
C	0.73661886	3.46357363	0.60552659
H	0.39038015	4.48656576	0.60310613
H	-0.04292294	2.82054327	0.9866126
H	1.61087237	3.38089667	1.23421198
C	-2.67375356	-3.45314248	-0.17555
H	-3.07591652	-4.4466601	-0.30816855
H	-1.71187216	-3.51614821	0.31149666
H	-3.34832703	-2.87009655	0.43388259
C	-4.13449363	-2.51754192	-2.66883003
H	-4.51675829	-3.5103721	-2.85473851
H	-4.8204998	-1.98147328	-2.02974791
H	-4.02926191	-1.99102674	-3.60590423
C	-1.32426799	-3.6487018	-2.88963276
H	-1.14900462	-3.13681763	-3.82432915
H	-0.38635399	-3.78296359	-2.37127854
H	-1.76872813	-4.61335219	-3.08534892
C	-4.10776793	-0.15425179	0.74782484
H	-3.41801668	-0.56587484	1.46977338
H	-4.81996585	0.48182714	1.25238179
H	-4.63135137	-0.95782301	0.25130328
C	-4.34959428	1.51304003	-1.77947767
H	-3.80710292	2.11284534	-2.49525467
H	-4.8326187	0.69279819	-2.28966463
H	-5.09550664	2.12246614	-1.29099578
C	-2.30380191	2.25497242	0.3394428
H	-1.66079011	1.86876481	1.11647531
H	-1.71117898	2.79964311	-0.38064879
H	-3.03800102	2.91629358	0.77533957
P	2.42003118	0.12817134	-3.22463088
P	-1.07355142	0.35969312	-3.56011963
H	1.55926719	-0.96284785	-3.60194042
H	2.21084612	1.23639254	-4.12000085
H	-0.05380496	-0.44568446	-4.18067107
H	-2.24644889	0.37555745	-4.39537998

IV.3.8 Calculated structure of $[PH_2]_8$

$C_{14}H_{46}Si_7P_2$

Energy: -3270.417442

Si	-2.1243663	-0.21739119	0.42981286
Si	0.13591991	0.09899647	0.84623223

Si	1.38149361	-0.97631684	-0.78920271
Si	3.44268003	-1.58557156	0.08413527
Si	1.69617673	0.45510223	-2.58765037
Si	-2.40907618	-2.08903651	-0.91118829
Si	-2.97959173	1.64743091	-0.65343597
C	0.52183084	1.91837889	0.8234204
H	1.58395943	2.06276923	0.95545934
H	0.21617735	2.33936136	-0.12302014
H	-0.01057425	2.40941293	1.62456358
C	0.5635285	-0.60462568	2.51406518
H	-0.01461432	-0.10245521	3.27562653
H	0.3372952	-1.66057239	2.52803136
H	1.61619348	-0.45940426	2.70695679
C	3.23597495	-3.07336489	1.18110564
H	2.57155808	-2.82961405	1.99690939
H	2.81856113	-3.88800909	0.60793853
H	4.19778333	-3.36635155	1.57541954
C	4.60783472	-1.99731742	-1.30600138
H	4.78513652	-1.11350306	-1.90084274
H	5.54354668	-2.35083159	-0.89872891
H	4.17135646	-2.76669324	-1.92563642
C	4.13673334	-0.17448656	1.07747769
H	4.28402042	0.68042146	0.43417466
H	3.44654383	0.0837171	1.86701509
H	5.08263445	-0.46825858	1.50802278
C	0.05896219	1.17068439	-3.10443922
H	-0.60648609	0.37217467	-3.39762996
H	-0.37340625	1.71432258	-2.27744765
H	0.20613821	1.84105524	-3.938311
C	2.43665018	-0.4887197	-4.00909303
H	3.33528817	-0.98911275	-3.67976559
H	1.72641084	-1.22082407	-4.36403424
H	2.678179	0.19574806	-4.8088228
C	2.84520688	1.83094523	-2.09127776
H	2.96267738	2.51731395	-2.91680708
H	2.43260458	2.35597566	-1.24245364
H	3.80751748	1.41842265	-1.8263562
C	-1.60115718	-3.5578508	-0.10530278
H	-2.06772825	-3.74598427	0.85037355
H	-1.71626991	-4.42475587	-0.73904142
H	-0.55034693	-3.35567189	0.04071607
C	-4.22545875	-2.42367405	-1.13112482
H	-4.35781828	-3.30826175	-1.73642272
H	-4.68288614	-2.5768466	-0.16484414
H	-4.69036431	-1.58022075	-1.61984699
C	-1.6288714	-1.7861279	-2.57225026
H	-2.06891078	-0.90834274	-3.02198192
H	-0.5668911	-1.63339951	-2.44867081
H	-1.79779019	-2.64075903	-3.21058565
C	-4.6127037	1.21712789	-1.43278479
H	-5.27185005	0.80495029	-0.68309439
H	-5.05699918	2.10751517	-1.85256096
H	-4.45753048	0.48904212	-2.21522481
C	-1.78934678	2.19856426	-1.97221154
H	-0.86630608	2.51976991	-1.51262173
H	-1.5901725	1.3764872	-2.6437165
H	-2.2204598	3.01943001	-2.5260355
C	-3.22240131	3.02168441	0.57622693
H	-3.90729989	2.6987878	1.34632543
H	-2.27282796	3.27704384	1.02288342
H	-3.62806228	3.88717524	0.07346973
P	0.28528238	-2.81649148	-1.4780991
P	-3.21091351	-0.51761532	2.37706236
H	-2.59667054	-1.59491435	3.10899977
H	-4.58939124	-0.83949983	2.11288531
H	1.22013617	-3.89979788	-1.63964058
H	-0.3600445	-2.54766803	-2.73702212

IV.3.9 Calculated structure of $[PH_2]_9$

$C_{14}H_{46}Si_7P_2$

Energy: -3270.382284

Si	-1.60405101	1.5393794	-1.92294025
Si	0.69119839	1.36964956	-2.21521066
Si	1.76098472	1.79974659	-0.20201079
Si	0.48885162	0.95661124	1.54533009
Si	2.01774472	4.0901667	0.06341348
Si	-2.22880642	0.37677853	-0.01494657
Si	-2.19159768	3.77215	-1.69507108
C	1.11777947	-0.34723044	-2.78962484
H	2.19132862	-0.45332526	-2.84096789
H	0.71749231	-1.06953303	-2.09360102
H	0.69220971	-0.5157311	-3.76783643
C	1.24710062	2.60563388	-3.48914766
H	0.70298602	2.44490125	-4.40811683
H	1.05638045	3.60543667	-3.12801029
H	2.30472739	2.48422649	-3.67104281
C	-0.05936397	-0.77273083	1.13492091
H	-0.6214311	-0.76288091	0.21275849
H	0.80690419	-1.40769675	1.02179374
H	-0.68190308	-1.15175495	1.93190633
C	1.51015329	0.93084725	3.09963994

H	1.63699792	1.93966218	3.46378672
H	1.00881026	0.33757572	3.85002921
H	2.47768584	0.50035482	2.8876092
C	-1.00413428	2.03575533	1.80231478
H	-0.68602156	3.04574468	2.01474314
H	-1.61073043	2.02976582	0.90877953
H	-1.58254115	1.65834373	2.63261953
C	3.44933204	4.67728634	-0.96879206
H	4.35620758	4.1961482	-0.63340744
H	3.27193142	4.42892791	-2.00476847
H	3.55111809	5.74770087	-0.86753819
C	2.34555129	4.47395292	1.85362324
H	1.52628052	4.10975863	2.45575106
H	3.26153544	3.99268633	2.16306712
H	2.43917723	5.54225743	1.98152817
C	0.46420228	4.95553693	-0.48178395
H	0.58728646	6.02237157	-0.36726698
H	0.26858661	4.72493229	-1.5185848
H	-0.36532315	4.62177997	0.1239337
C	-1.27960904	1.02757092	1.44624938
H	-1.64794868	0.56480884	2.34989598
H	-0.23120137	0.79795816	1.32575319
H	-1.40855349	2.09785366	1.51158071
C	-4.05148259	0.60214388	0.27943762
H	-4.37305541	-0.05985828	1.06984514
H	-4.24621275	1.62527646	0.56523455
H	-4.59354446	0.37183278	-0.62583899
C	-1.85620912	-1.43146439	-0.2408421
H	-2.44081327	-1.81966123	-1.06178133
H	-0.80539388	-1.55841144	-0.45548548
H	-2.10606374	-1.96625733	0.66357439
C	-1.75351985	4.3570273	0.01536931
H	-0.70697436	4.16790188	0.20344935
H	-1.94780118	5.41647016	0.09433509
H	-2.35140899	3.82630439	0.74149724
C	-4.02196943	3.96237989	-1.96553702
H	-4.29362012	3.52106027	-2.91308275
H	-4.55702833	3.46496765	-1.17011699
H	-4.27805635	5.01156781	-1.97045607
C	-1.27035409	4.78710889	-2.95235733
H	-0.21527286	4.77443537	-2.72204673
H	-1.42903234	4.37168619	-3.93655507
H	-1.63184144	5.80453607	-2.92850737
P	3.78321219	0.81329035	-0.20162719
P	-2.6543232	0.66610794	-3.71090706
H	-3.57306149	-0.35437543	-3.2771633
H	-3.37906995	1.70451217	-4.39651542
H	4.45964538	1.10169274	-1.43971532
H	3.62303445	-0.61100787	-0.06263914